THE UNIVERSITY OF ALBERTA

AN OPERATIONAL MIXING DEPTH MODEL FOR NORTHERN ALBERTA

by

© RONALD BRUCE THOMSON

A THESIS

SUBMITTED TO THE FACULTY OF GRADUATE STUDIES AND RESEARCH

IN PARTIAL FULFILMENT OF THE REQUIREMENTS FOR THE DEGREE

OF MASTER OF SCIENCE

IN

METEOROLOGY

DEPARTMENT OF GEOGRAPHY

EDMONTON, ALBERTA

FALL, 1977

DEDICATION

To my wife, Lynda, and daughter, Elisa,

for their love, understanding and encouragement.

ABSTRACT

A time-dependent mixing height model capable of being used on a minicomputer system is developed. The main source of energy considered in the model is the net surface radiation which is calculated as a function of time by a radiation model. A relationship is derived to transform energy to an equivalent area on a thermodynamic diagram. This area is analyzed using basic geometry to produce a value of the mixing height.

It is assumed that thermal turbulence driven by the surface radiation excess is the predominant process in the development of the mixed layer. It is assumed also that the morning lapse rate of temperature is linear and that the vertical temperature gradient in the mixed layers remains constant with time.

The model requires input data from the surface and the 850 and 700 hectopascal levels. Required surface data include the location's latitude, longitude, elevation above mean sea level as well as the surface albedo and a forecast of the minimum and maximum surface temperatures for the day. The heights and temperatures of the 850 and 700 hectopascal levels at 1200(GMT) and 0000(GMT) are used as input. Finally, the cloud albedoes are required at three-hourly intervals from 1300(GMT) to 0300(GMT) the following day.

The model presented in this study adequately describes the variations in height of the mixed layer for the period from

sunrise to late afternoon. A comparison with Holzworth's technique (1964), based on test samples of minisonde data in Central Alberta, demonstrates a marked improvement in the prediction of mixing heights by means of the new model. Because the input data are readily available, the new model is very attractive for operational use where a good first approximation of the mixing depth is required. This method can also be coupled with a pollution concentration model to provide pollution potentials over areas where observed data are scarce.

TABLE OF CONTENTS

LIST OF TABLES

LIST OF FIGURES

Figure		Page

CHAPTER 1

INTRODUCTION

1.1 The Concept of Mixing Depth

The mixing layer of the atmosphere comprises the lower few kilometers and contains that region where surface effects predominate. As will be seen later, the mixing layer is synonymous with what is called the Planetary Boundary Layer (PBL). The actual definition of the layer varies from person to person depending on which meteorological parameters are being considered. Summers (1965) considered the mixing depth to be the distance from the ground to the top of the adiabatic layer which formed over an urban area. A similar and very widely accepted definition based on the same principle, was stated by Holzworth (1967). He contended that the mixing layer is that region where surface convection coupled with turbulence causes strong vertical mixing. Others consider mixing depth or height to be the level at which parcels of air from the surface reach equilibrium with their surroundings. Workers in the field of large-scale air pollution studies prefer to consider the mixed layer and the PBL as one and the same (Laikhtman 1961, Hanna 1969, Agnew and Jarvis 1972, Munn 1975).

From the previous section, the mixing depth has been generally defined as the height to which surface air parcels will rise. This creates a layer containing most of the surface emissions from a wide variety of man-made and natural sources. The extent to which the air is mixed becomes critical when air pollution concentrations are being determined. As the depth of this layer varies, the efficiency of diffusion-dispersion processes also varies. Therefore, the purpose of forecasting or in some manner determining the height of the mixed layer is to aid in the prediction of pollution episodes.

1.2 Structure of the Mixing Layer

The growth of a mixed layer depends on processes which are time dependent, and, therefore, the development of this layer is also a time-dependent phenomenon. The strength of the mixing in the lower layers and the degree of contrast between the upper more stable airmass with that below, will determine the intensity of the inversion which delineates the top of the mixed layer. In theoretical models, Carson (1973) and others, describe the lower atmosphere by using three distinct regions (see Fig. 1.1). A superadiabatic layer dominated by forced convection develops close to the ground. Next is an adiabatic or free-convection layer which is capped by a deep non-turbulent zone. Carson's model contains a fourth layer which is not as distinct as the others. This is the interfacial entrainment layer which separates the free-convection region from the more stable layer aloft. This region of entrainment varies both in depth and character in the real atmosphere but does

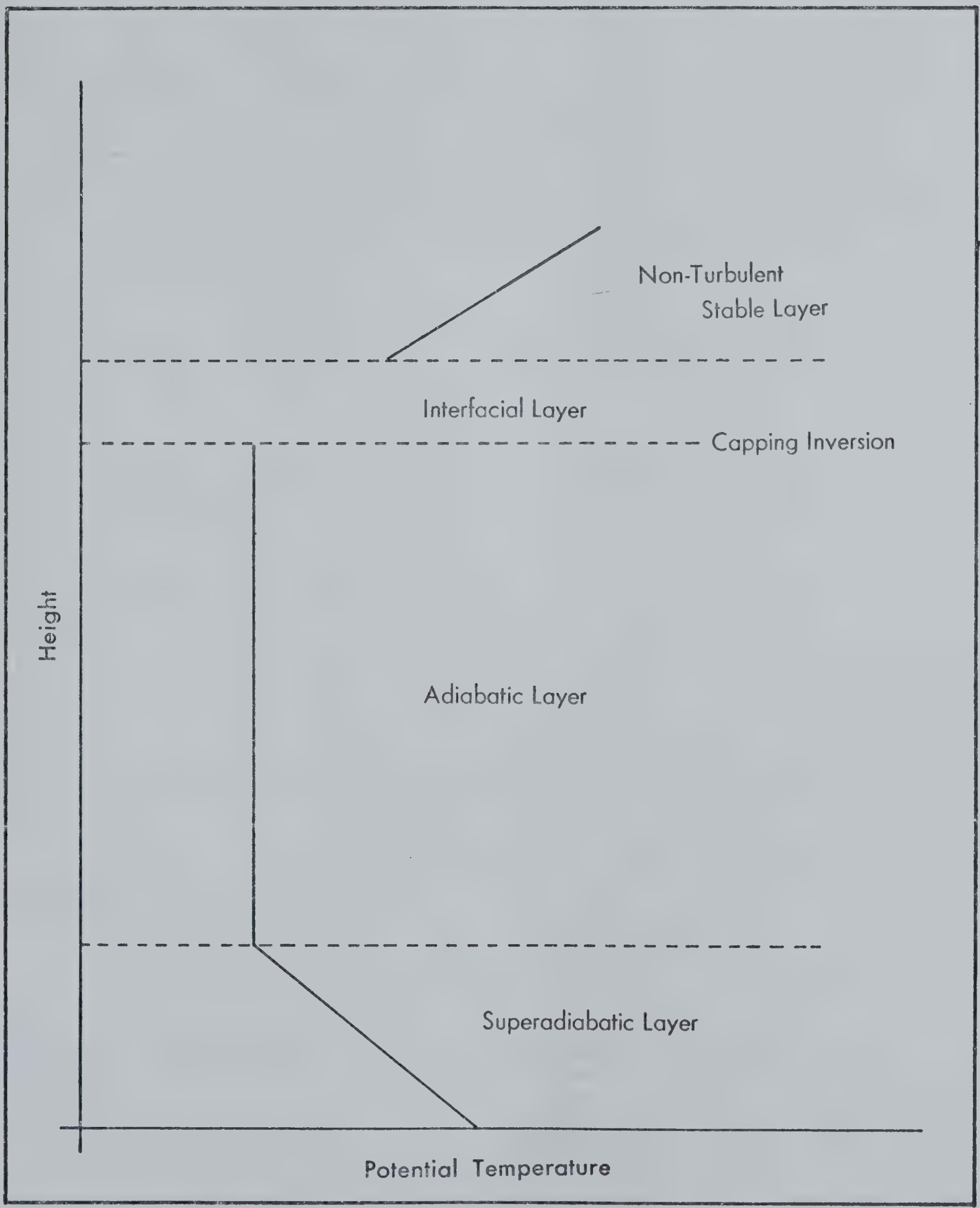

Fig. 1.1 Structure of Carson's Model Atmosphere

act as a boundary to the free-convection layer.

Carson's model accurately depicts all but the lowest layer of the atmosphere as observed by Holmgren et al (1973) who studied acoustic sounding and balloon ascent records over Fairbanks, Alaska. The proximity of forest vegetation appeared to hamper the development of a superadiabatic layer next to the ground. This discrepancy was attributed by Holmgren et al, to a warming of the air by the nearby forested areas. Carson's model atmosphere describes the real atmosphere well, with some modification to the lowest layer needed under particular conditions. It will be used as a basis for the rest of this study.

1.3 Review of Mixing Height Models

The first attempts to predict the height of the PBL relied totally on the theory provided by classical fluid dynamics (Hanna, 1969). When this theory was applied to atmospheric problems, such as calculating the height of the Ekman Layer, estimates were found to be proportional to;

$$H_D = \pi(2K/f)^{\frac{1}{2}} \qquad (1.3.1)$$

where H_D is the height at which the wind direction in the PBL first coincides with that of the geostrophic wind. The eddy viscosity is given by K, π = 3.1416 radians and f is the coriolis parameter. This led Blackadar (1962) and others to propose that H_D could be calculated under adiabatic, steady-state, barotropic conditions using the formula;

$$H_D = H(U_o^*/f) = 0.2\ U_o^*/f \qquad (1.3.2)$$

which incorporates the friction velocity near the ground, U_o*, with the coriolis parameter f. Equation (1.3.2) has a similar form to one proposed by Rossby and Montgomery (1935);

$$H(U_g/f,\alpha_o) = 0.021\ (U_g/f)\sin(\alpha_o) \qquad (1.3.3)$$

where U_g is the geostrophic wind at the top of the PBL and α_o is the angle between the direction of the surface wind and that of U_g. Equation (1.3.3) was also applied in the following form to stable conditions;

$$H(U_g,\Delta\Theta,\alpha_o) = 0.38\ U_g\sin(\alpha_o)/\ \frac{g}{T}\left[\frac{\Delta\Theta}{\Delta Z}\right]^{\frac{1}{2}} \qquad (1.3.4)$$

The lapse rate of potential temperature, $\Delta\Theta/\Delta Z$, and the mean temperature of the layer, T, are combined with the acceleration of gravity, g, to represent the influence of buoyancy forces. Equations (1.3.2) and (1.3.4) were tested by Hanna (1969). The results exhibited a large degree of scatter when compared with measurements of the mixing height. In a later study by Carson (1971), the formulae were again tested on the same data with similarily poor results. Carson attributed the wide scatter to the use of equations based on steady-state similarity theory and indicated that time-dependent models were absolutely necessary. A similar conclusion was reached by Deardorff (1972). The time-dependent equation for the height of the mixed layer, as derived by Carson (1973), is given by;

$$h^2(t) = h^2(t_o)\exp\{2\beta(t_o - t)\} +$$

$$+ 2\exp(-2\beta t)\int_{t_o}^{t}\exp(2\beta\tau)\{(H(0,\tau) - 2H(h,\tau))/\rho c_p\gamma(\tau)\}d\tau \quad (1.3.5)$$

In this formulation, the height of the PBL, $h(t)$ is related to the initial height $h(t_o)$ by integration of the change in heat flux at the surface, $H(0,\tau)$ to that at the height h, $H(h,\tau)$ for a given time, τ. Also included is a constant convergence parameter, β, describing large scale convergence which leads to subsidence. The β- term is related to stability by;

$$\gamma(t) = \gamma(0)\exp(\beta t) \quad (1.3.6)$$

where γ (t) is the lapse rate of potential temperature and $\gamma(0)$ is the same quantity at $t = 0$. The net effect of β is to increase stability due to large-scale subsidence. Deardorff, Willis and Lilly (1969) assumed no subsidence ($\beta = 0$) and a constant surface heat flux (H_o), which reduces (1.3.4) to;

$$h^2(t) = \frac{2\,H_o t}{\rho c_p\gamma(0)} \quad (1.3.7)$$

where $\gamma(0)$ is the lapse rate of potential temperature at $t = 0$. The simplification of (1.3.5) to (1.3.7) produced a model which demonstrated success in calculating the height of the convectively-unstable boundary layer (Carson, 1973). This formulation (1.3.7) should be restricted to days with a dry convectively-unstable

boundary layer under almost clear-sky, non-advective situations.

A similar approach was presented by Summers (1965). He considered the advection of a column of air across an urban area. A method was proposed which would slowly alter the rural lapse rate by adding heat to the air column from below. The amount of heat added dictates the height to which the dry-adiabatic layer will extend. The level at which the dry-adiabatic lapse rate changed to the rural lapse rate defined the height of the mixing layer. Using the amount of heat available from an urban area, H, the mixing height, h, is given by;

$$h = (2\ HL/U_o \alpha \rho c_p)^{\frac{1}{2}} \qquad (1.3.8)$$

where L is length of trajectory of the city, U_o is the surface wind in the rural area and α is the difference between the rural and the dry-adiabatic lapse rates. This method is widely accepted for urban heat island situations and has been used by Leahey and Friend (1971) and by Hage (1972) with minor modifications. The major problem with this model is the assumption that all available heat comes from the urban heating rate, H, hence ignoring any other sources of energy.

A similar technique to that of Summers (1965), uses the morning temperature sounding (1200 GMT) and replaces the urban heat rate by the rate of increase of surface temperature. In this method the intersection of a dry adiabat through the surface temperature and the morning vertical temperature profile defines the height of the mixed layer. Hosler (1961), Holzworth (1964 and 1967) and Miller

(1967) used this technique both in calculating mixing heights and as a forecast tool (Miller 1967). The use of a dry-adiabatic lapse rate requires that certain implicit assumptions be made (see Section 2.3). A practical problem in using this technique results from the requirement for a morning sounding which may not be available for the area of interest.

1.4 Outline of Method Used in this Study

The main parameter appearing in most of the previously mentioned models is the surface heat flux. To properly describe the energy available to the lower atmosphere, the present model uses a surface energy balance. In determining this balance, consideration is given to the effect of changing cloud cover, varying sun-angle and surface albedo. The surface heat flux is assumed to be equal to the net radiation, neglecting losses to the ground. Once the surface heating rate is determined, a technique similar to that of Summers and Holzworth is used.

Assuming that the morning lapse rate is linear with height and that a constant lapse rate for the remainder of the day can be predicted, the effect of the surface heat flux can be represented by a triangular area on a temperature-height graph (see Section 2.2). By using a thermodynamic diagram, area and energy are easily transformed into an equivalent area, the altitude of the triangular area is calculated giving the mixing height. This eliminates the need for an observed temperature profile and allows mixing layer depths to be calculated for areas where such profiles are not available.

Most of the data required for the model are used in the radiation component. The site location, cloud amount and surface albedo are required together with the minimum and maximum temperatures for the day of interest. If predicted or observed heights and temperatures are available for the 850 and 700 hectopascal surfaces at 00 and 12 G.M.T. a more detailed form of the model can be used. The final piece of information is the date (day and month) which gives the correct solar declination.

The resulting model is time-dependent and produces hourly values of the mixing height from sunrise to late afternoon. The required input data for this model are available from forecast weather offices in the area of interest.

CHAPTER 2

ENERGY APPROACH TO MIXING DEPTH

2.1 Development of a Mixed Layer

For the development of a mixed layer to proceed, processes which destroy stability and therefore produce instability must be present. The primary forcing agent is thermal or convective turbulence generated by the surface heat flux. An upward surface heat flux is created by solar insolation or by cold air advection over a warm surface. Once the basic turbulent state is established, it can be enhanced by the advection of cold air, radiational cooling aloft or by forced convection. Wind over rough terrain will add to the turbulence through enhanced mixing. In the present model, an upward surface heat flux produced by solar heating is considered to be the fundamental energy source with mixing enhanced by advection being considered only indirectly.

The strength of the convective turbulence depends on the time of year, the time of day, cloud amount and the type of surface covering. This process is therefore highly variable even over very short time intervals. For convective turbulence to be effective, the

air next to the ground must become warm enough so that buoyancy forces will overcome gravity. This leads to an unstable layer in the lower levels of the atmosphere and usually results in an inversion-capped mixing layer as described in Section 1.2. Surface heating is the primary forcing agent which will develop a mixed layer and must be the basic parameter in mixing height models.

A strong correlation exists between mixing and instability, hence a process which alters the ambient stability will be important in the development of a mixed layer. Such a process is advection, both frontal and non-frontal. Cooling or warming in the lower levels associated with frontal passages can very quickly alter the stability of the lower layers. The passing of a cold front can cause very stable conditions to break down becoming unstable in minutes. Warm-air advection usually has a stabilizing effect but can lead to mixing if the warm air reaches the surface and combines with the sensible heat flux resulting in a warmer but unstable airmass. The advection of cold or warm air over the location of interest will usually alter the stability and, therefore, will be of great importance when the depth of the mixing must be determined.

Another process involved in the erosion of the stable air above an inversion is caused by a combination of wind shear and convective turbulence (Carson and Smith, 1974). This process draws heat downward into the lower layers from the warmer, more stable air aloft. The effects of this 'entrainment' of air through the inversion is discussed by Barnum and Rao (1975). However, the exact role of this process in the break down of an inversion is not

well understood (Turner, 1973).

In the high arctic, for at least two of the winter months, no incoming solar energy is available. This implies that thermally-driven processes resulting from surface heating will not occur. With no convective turbulence, mixing of the air must result from either advection or radiational cooling aloft, or from a combination of the two. In figures 2.1 and 2.2, radiosonde ascents from Resolute Bay in the N.W.T. show how the combination of the two processes act to provide a mixing depth without surface heating. It will be necessary to include both advection and radiational processes in any model which is to be used in the arctic in winter.

The processes of mixing as described above create a homogeneous layer based at the ground. It has been calculated (R. Portelli, 1967; C.L. Norton and C.B. Hoidale, 1976) that this mixing layer may extend to several kilometers. Portelli (1976), using Holzworth's technique, determined monthly mean maximum mixing heights for many areas in Canada. A great seasonal variation can be seen in values for the northern locations (Table 2.1). An equally dramatic range in mixing heights due to latitudinal variations is demonstrated by Portelli's work (Table 2.1 and Figures 2.3-2.7).

2.2 Energy and Mixing Depth

Once the sources of energy have been defined it remains to devise a method by which the amount of energy can be translated into a workable mathematical form for prediction of mixed-layer depths. The first step in this manipulation was provided by Godson (1958), who derived a relation between the energy provided to the lower

Table 2.1

Mean Maximum Afternoon Mixing Heights (Meters Above Surface)
- Portelli (1976)

Station Name	Jan	Feb	Mar	Apr	May	Jun	Jul	Aug	Sept	Oct	Nov	Dec
Alert	96	62	78	127	231	358	347	221	148	109	100	88
Edmonton	227	295	696	1578	2396	2185	1954	1563	1322	998	420	208
Fort Smith	208	324	547	1025	1499	1779	1610	1537	1009	578	283	231
Norman Wells	155	247	474	812	1327	1555	1448	1117	758	355	180	135
Albany	560	872	1036	1599	1637	1581	1733	1498	1305	1257	849	669

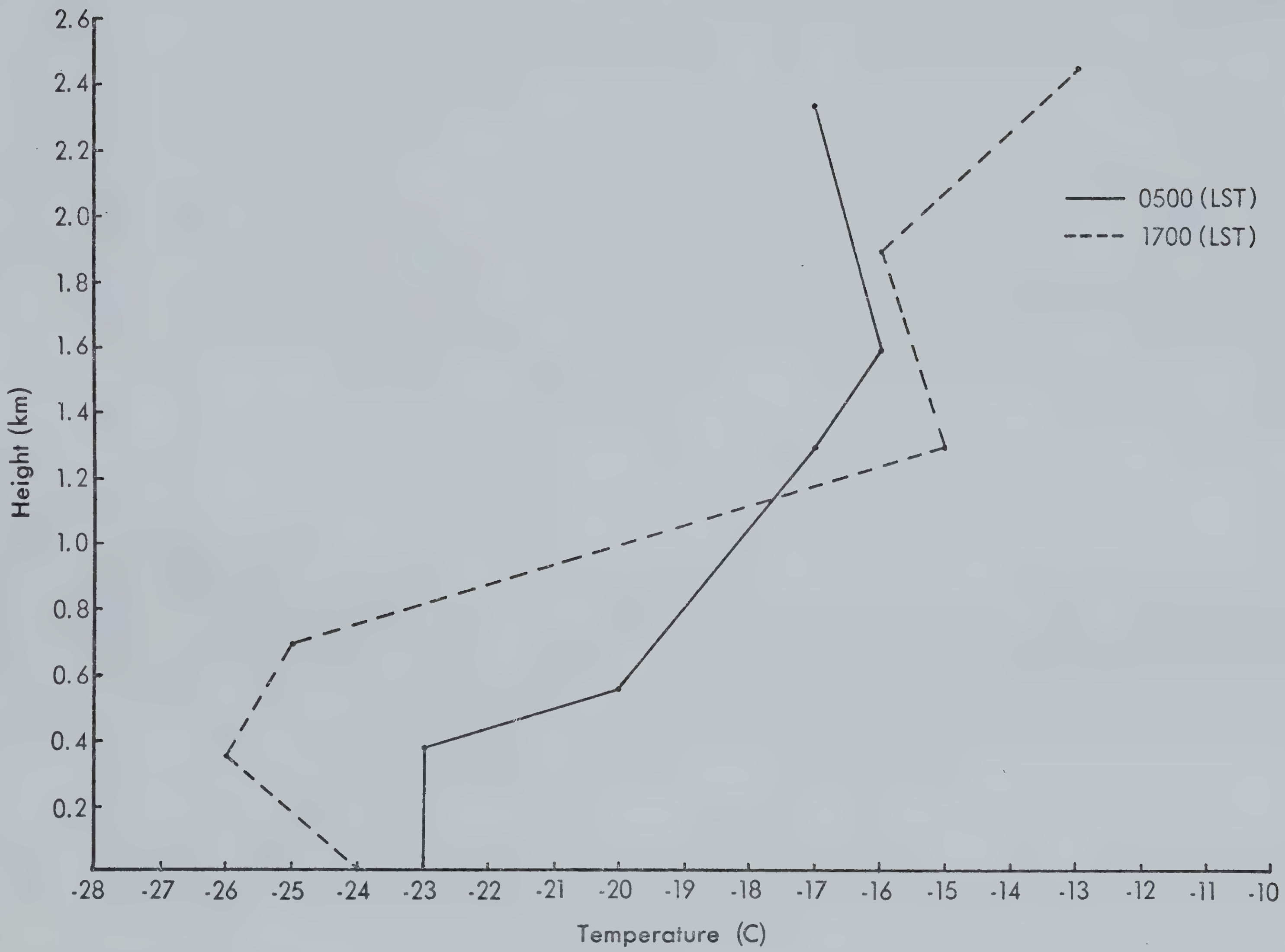

Fig. 2.1 Radiosonde Ascent for Resolute Bay Jan. 14, 1965

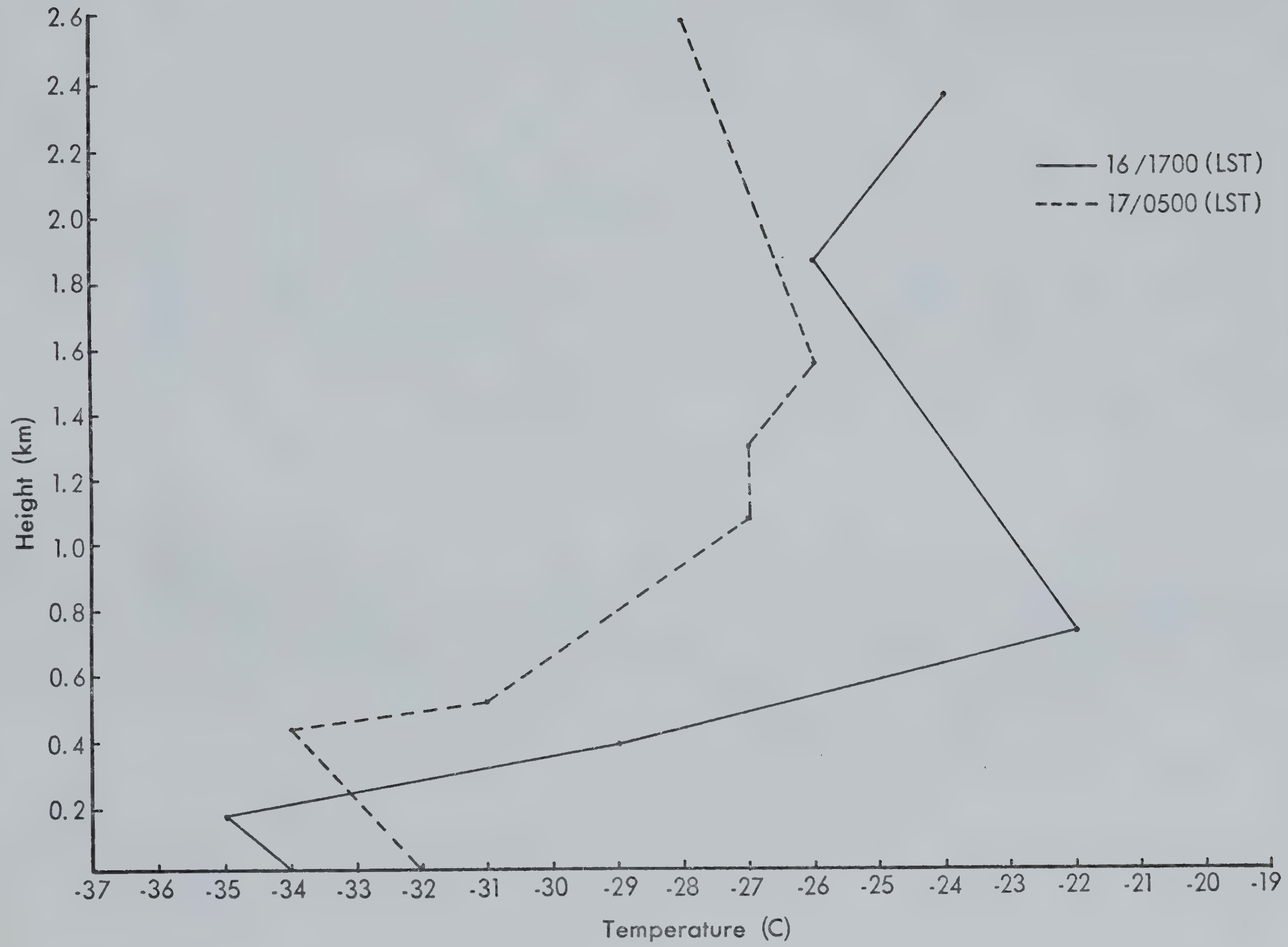

Fig. 2.2 Radiosonde Ascent for Resolute Bay Jan. 17, 1965

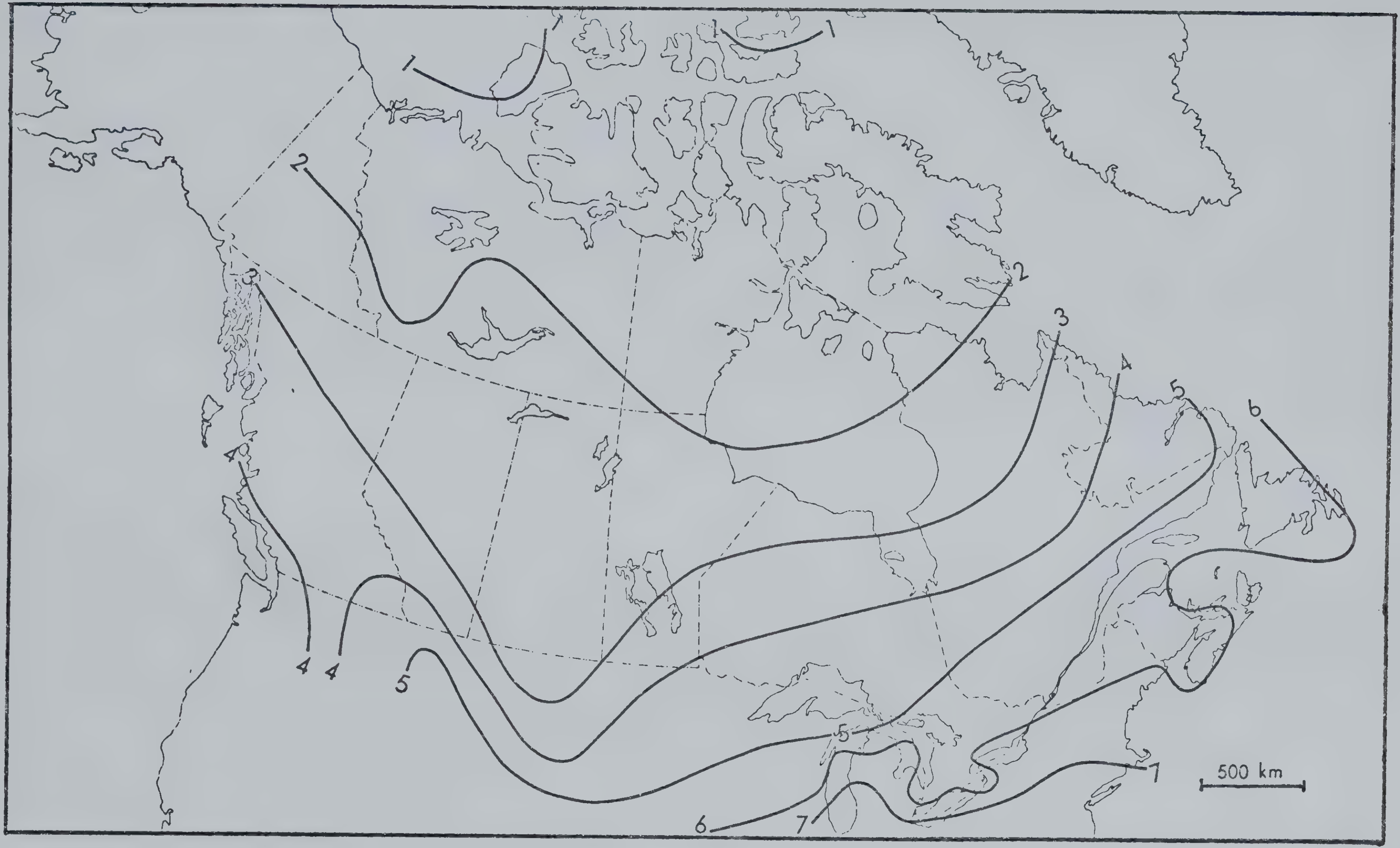

Fig. 2.3 Mean Winter Maximum Mixing Heights (m x 10^{-2}) - Portelli (1976)

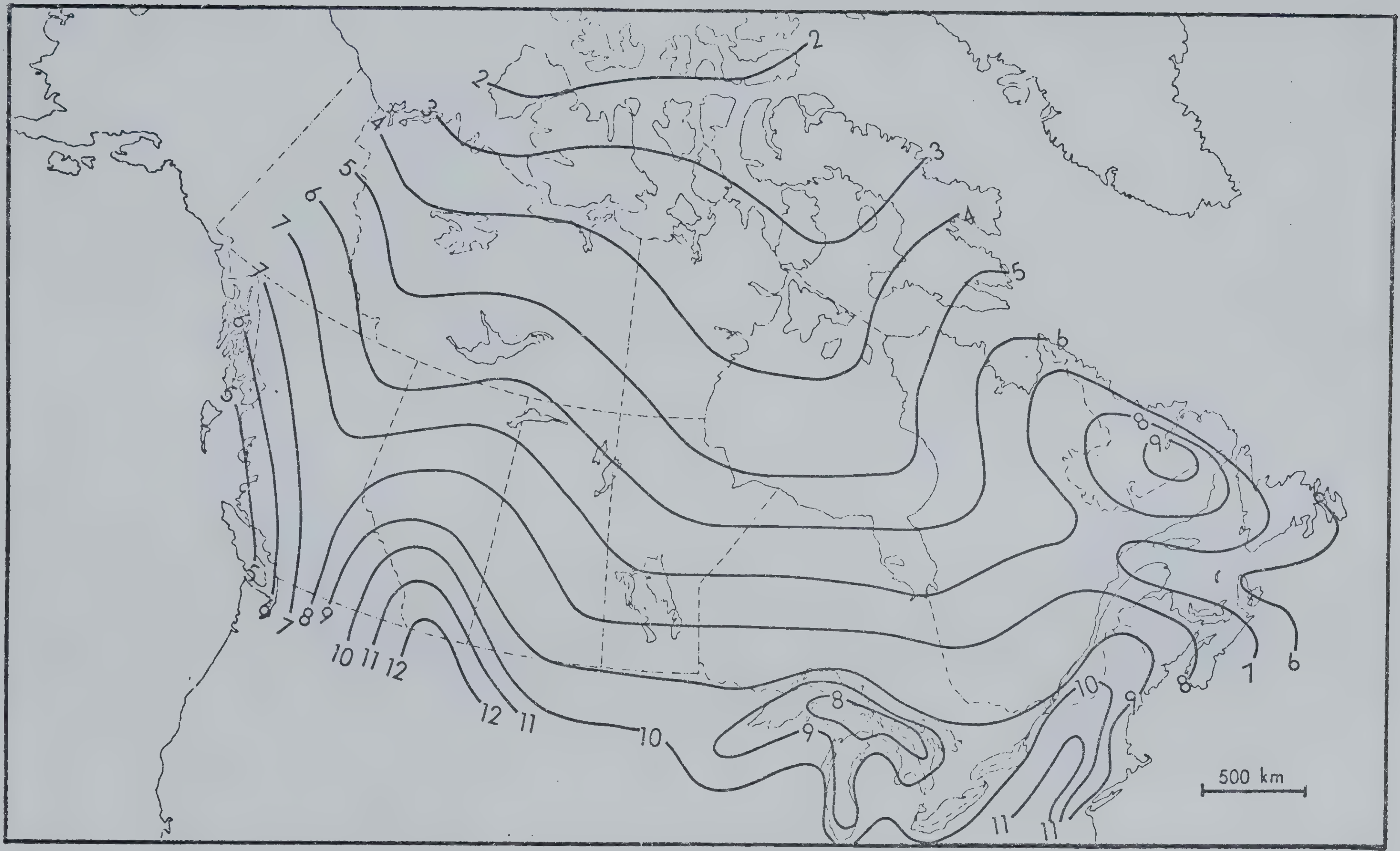

Fig. 2.4 Mean Autumn Maximum Mixing Heights (m x 10^{-2}) - Portelli (1976)

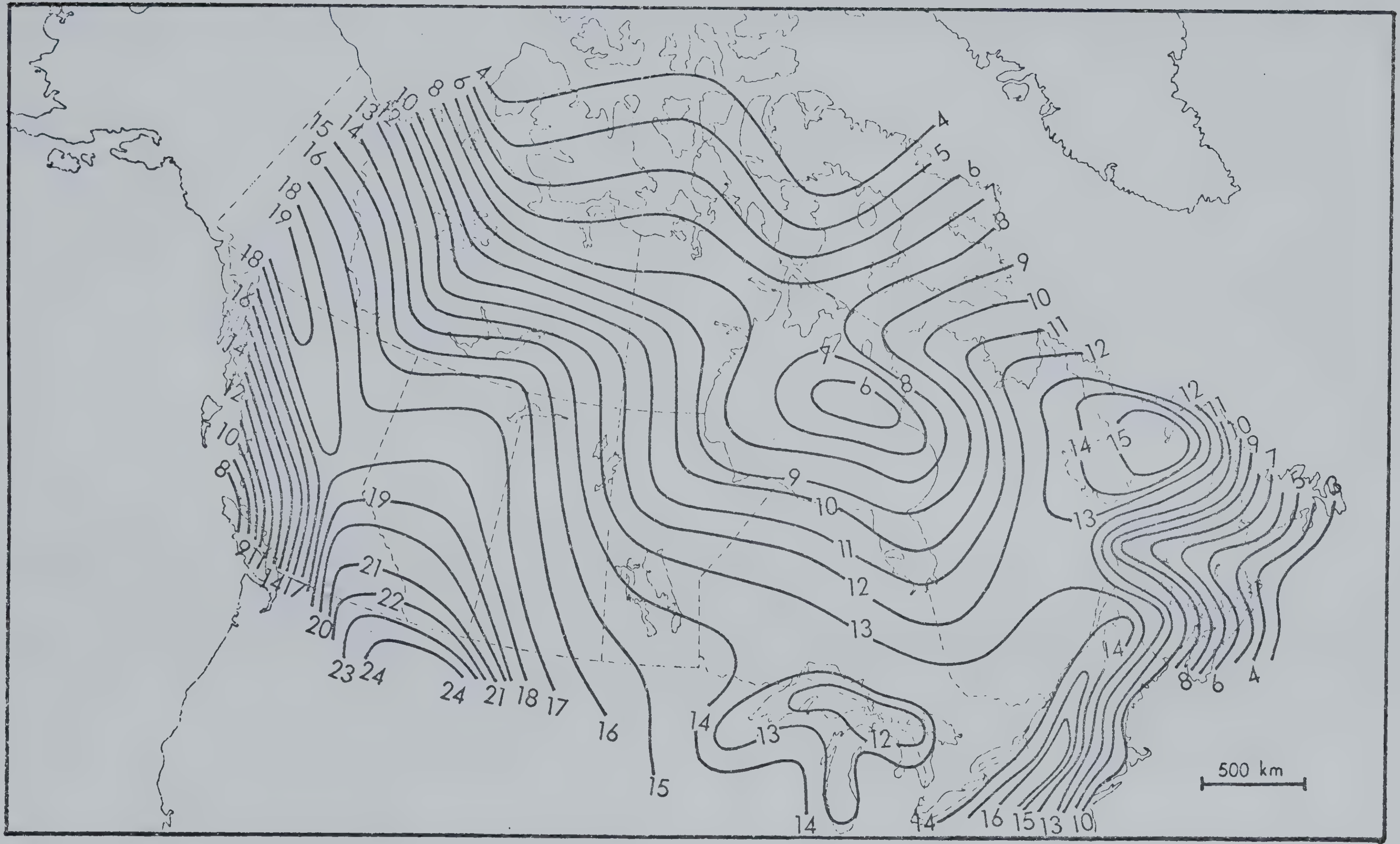

Fig. 2.5 Mean Summer Maximum Mixing Heights (m x 10^{-2}) - Portelli (1976)

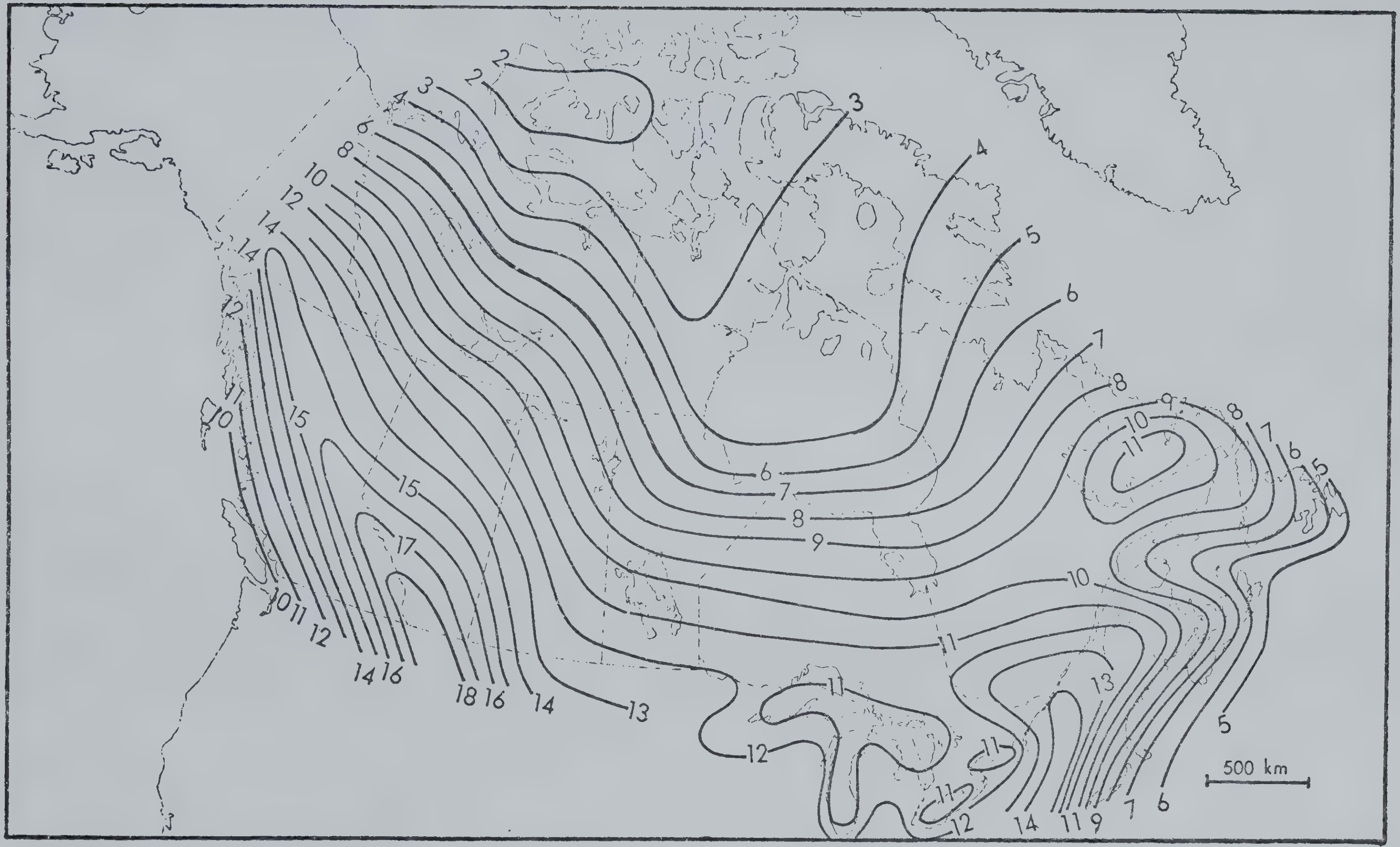

Fig. 2.6 Mean Spring Maximum Mixing Heights (m x 10^{-2}) - Portelli (1976)

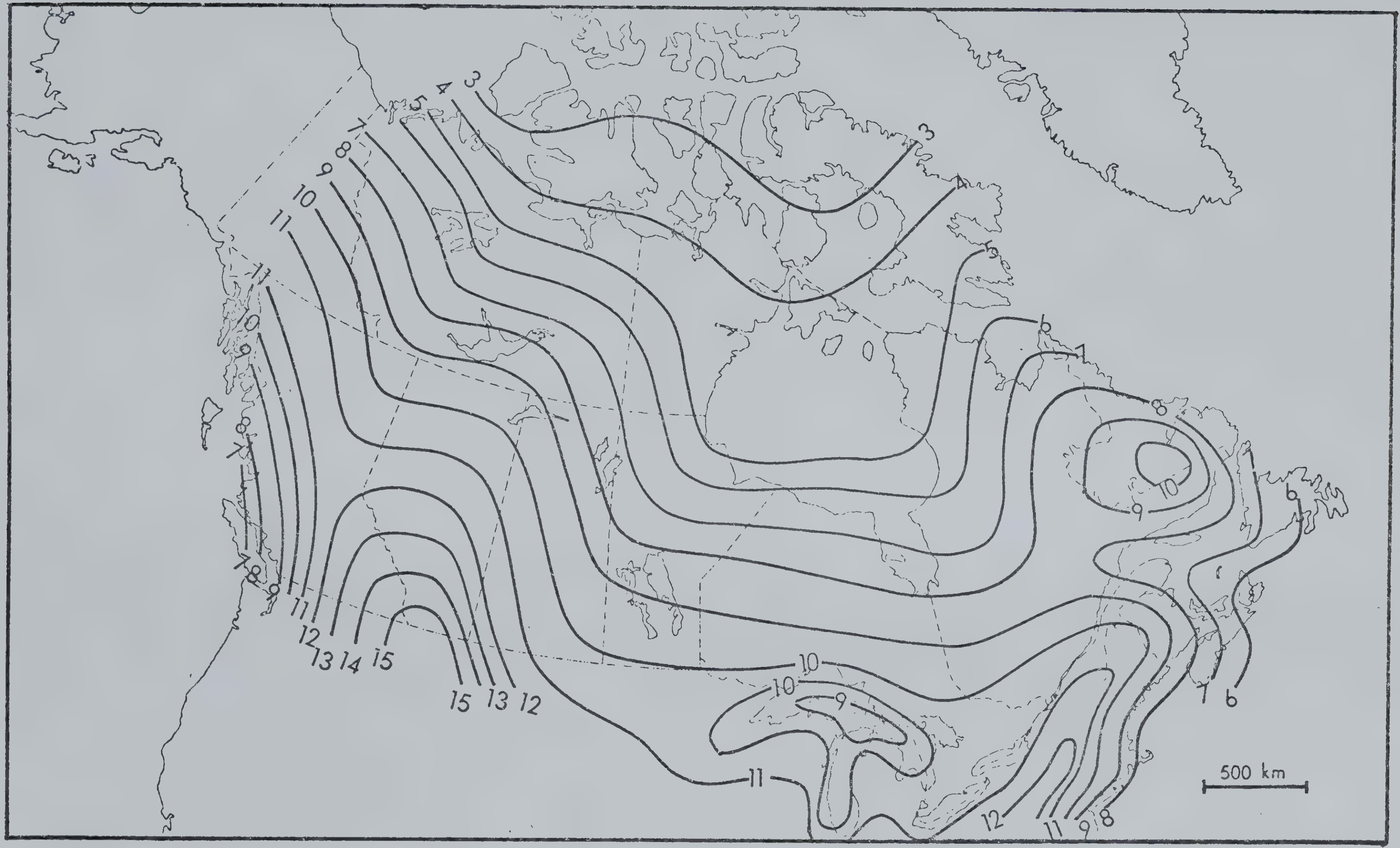

Fig. 2.7 Mean Annual Maximum Mixing Heights (m x 10^{-2}) - Portelli (1976)

atmosphere and area on a thermodynamic diagram (the Canadian Tephigram).

$$Q_a = \frac{c_p}{Rg} \overline{P} A \qquad (2.2.1)$$

where Q_a is the available energy, A is the energy per unit mass and $\overline{P}$ is the mean pressure of the layer of air immediately above the earth's surface which is affected by the surface heating. Rewriting (2.2.1) and solving for A in terms of the available energy, Q_a;

$$A = 0.28 \frac{Q_a}{\overline{P}} \qquad (2.2.2)$$

when A = joule g^{-1}
Q_a = joule m^{-2}
$\overline{P}$ = hectopascal

The form of A in (2.2.2) does not lend itself well to calculation. Transforming to area in metric units on the tephigram as published by the Atmospheric Environment Service (A.E.S.) yields;

$$A = 394.9 \frac{Q_a}{\overline{P}} \qquad (2.2.3)$$

when A = m^{-2}
Q_a = joule m^{-2}
$\overline{P}$ = hectopascal

Equation (2.2.3) permits one to calculate an area in square meters on a standard tephigram given the available energy in joules per square meter. However, the area itself is not very useful unless the geometric shape which the area occupies can be approximated.

The growth of a mixed layer (see Fig. 2.8) is frequently observed to be accompanied by the formation of a shallow superadiabatic

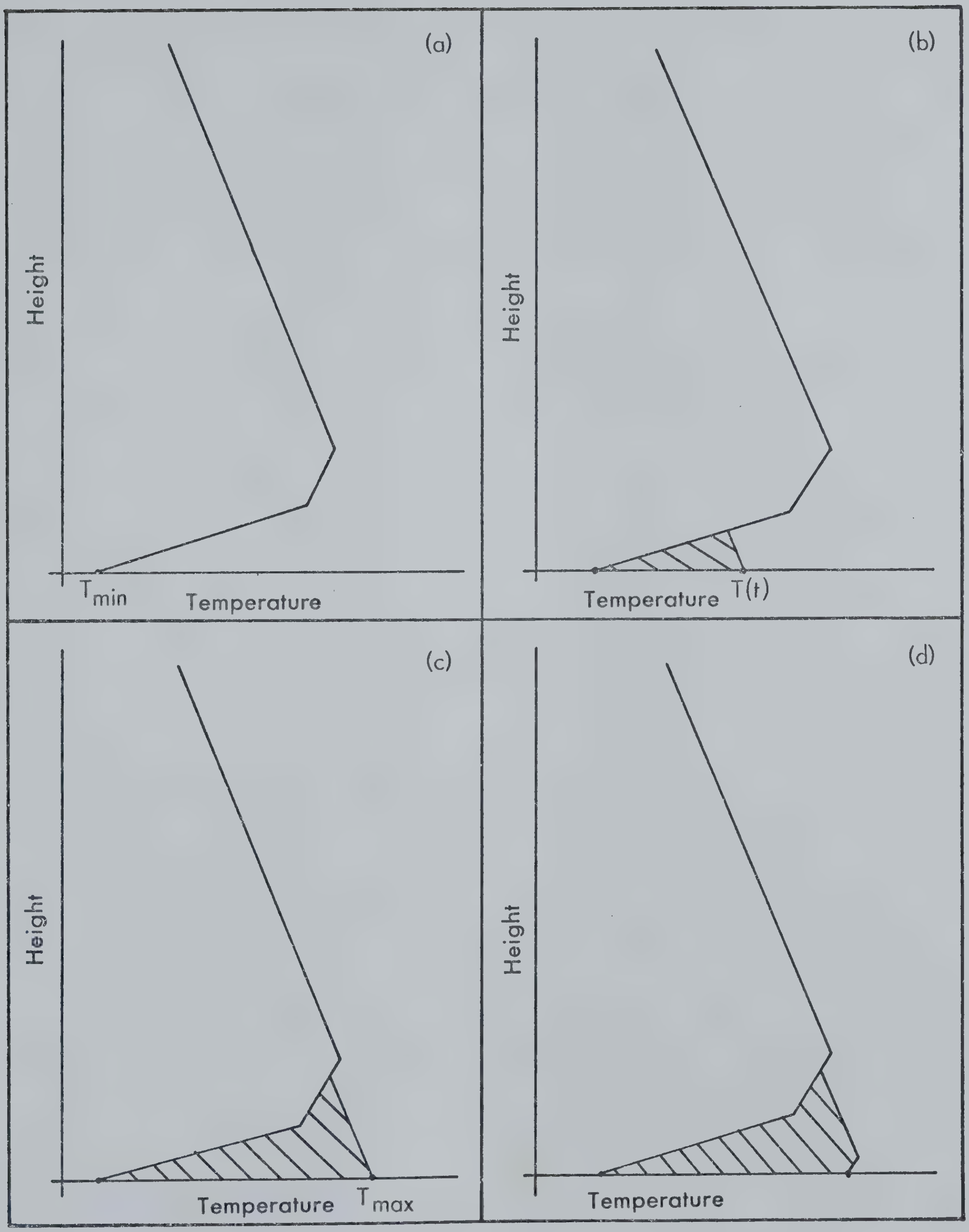

Fig. 2.8 Development of the Mixed Layer
(a) Morning Sounding
(b) Early Stages of Modification
(c) Maximum Mixing at Maximum Temperature
(d) Surface Heat Flux Negative - Mixing Reduces

layer which becomes more nearly dry-adiabatic with increasing height. Assuming that the lapse rate in the mixing layer can be adequately described, usually by a dry-adiabat, an energy-area technique can then be employed. The technique amounts to approximating the deformation of the lower atmospheric sounding by equating the energy to the area of a triangle, Kagawa (1968). From Neiburger (1941) and Holzworth (1967 and 1972), assuming that the sounding is affected by surface heating only, the depth of the mixed layer can be determined by the intersection of the dry-adiabat through the maximum surface temperature with the temperature profile aloft from the morning sounding (see Fig. 2.9).

Alternatively, given the area and surface temperature excess above the minimum temperature, and assuming a constant temperature gradient in the mixed layer one can compute the height of the mixed layer without knowledge of the initial temperature profile. The only new assumption needed is that the initial temperature profile is linear. This technique must be abandoned when surface heat flux becomes negative. Businger (1973) describes the collapse of the dry-adiabat next to the ground near sunset leaving an elevated mixing layer with a stable layer developing beneath. For this reason, the present model is terminated when the heat flux becomes negative.

2.3 Adiabatic Assumption

Minisonde data from Edmonton and Fort McMurray, Alberta, appear to support the assumption that a dry-adiabatic lapse rate will develop and persist. In numerical models of the PBL, constant potent-

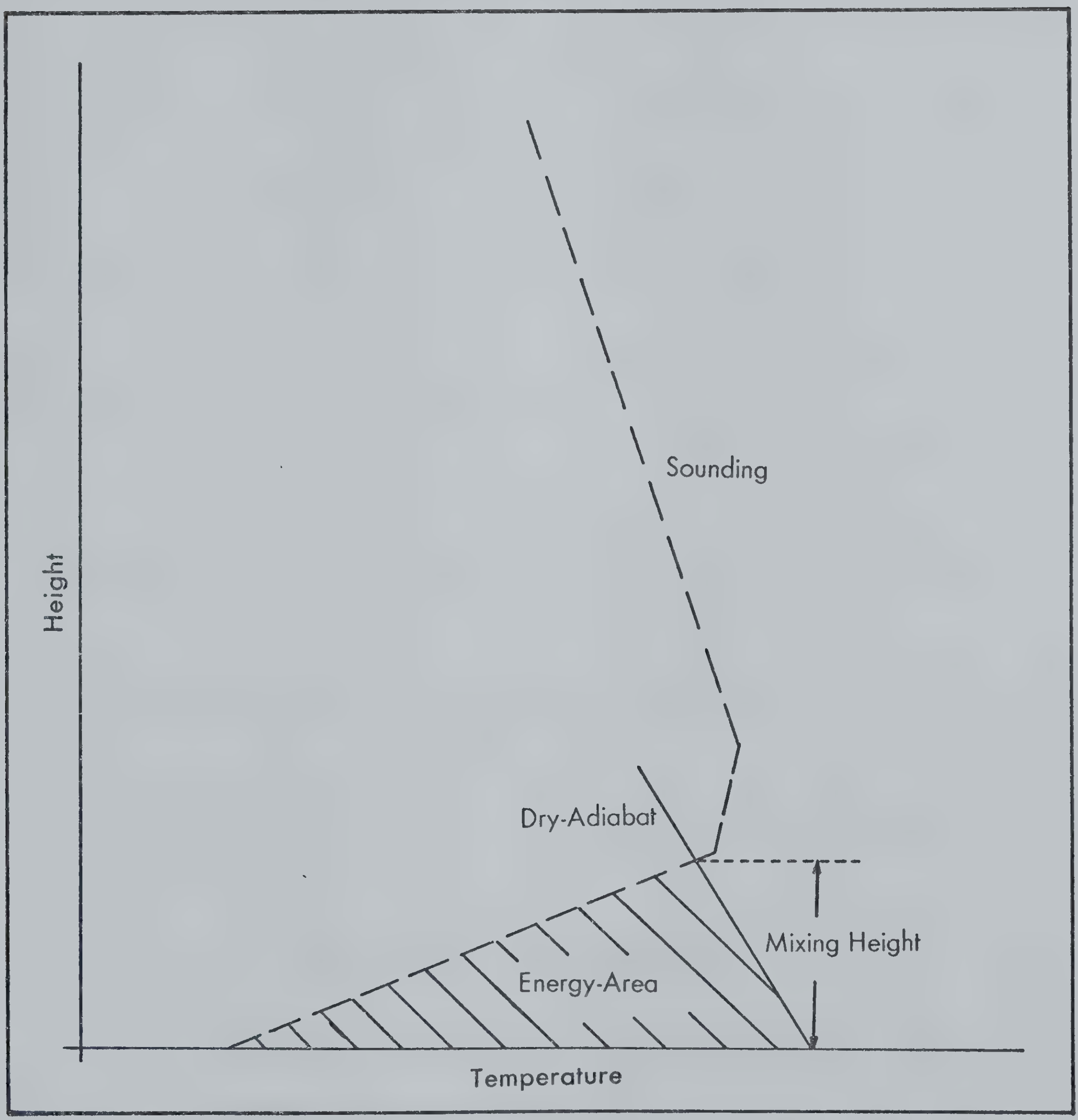

Fig. 2.9 Mixing Height and Energy Area Relationship

ial temperature layers are developed and maintained for the duration of the forecast period (Carson, 1973) in order to describe the lower layers of the atmosphere. Most studies, however, have been performed in areas that exhibit strong surface heating consequently developing dry-adiabatic layers reasonably easily. The present study includes periods in late fall and early spring when the surface heat flux is weak. Therefore the development of the adiabatic layer is retarded and only extends a few hundred meters in many cases. This is the critical time of the year for pollution problems when mixing layers may extend just above the stack heights.

For many locations in the arctic, solar insolation disappears for one or two months in the winter. Unstable layers are still able to develop (see Fig. 2.1 and 2.2) even when heat fluxes at the surface are negative. These mixing layers must be developed by advection-entrainment processes as discussed earlier. Unfortunately the present model is not capable of calculating entrainment or low level advection effects. These situations will not be considered in the present study.

2.4 Difficulties with a Surface Heat Flux Model

The main difficulty with this type of approach is that the surface heat flux is a parameter dependent on many other meteorological processes. Calculation of the heating rate therefore depends on the model's ability to correctly depict properties such as cloud cover, surface temperature and albedo as well as atmospheric stability. It is very difficult to obtain an accurate measure of the upward sur-

face heat flux when the sun angle is low and the albedo and cloud amount are large. Care must be taken to recognize when calculated values of the flux are nearing the same order of magnitude as the model errors. This problem will occur in late fall and early spring and must be considered when results are being analyzed.

CHAPTER 3

MODEL DEVELOPMENT

3.1 Shortwave Component

This component of the model calculates the contribution of the shortwave radiation to the total energy balance. Incoming solar energy passes through layers of cloud and then reflects at the earth's surface. The available energy is determined by the equation;

$$R_n = (1 - \alpha)(Q + q) - L\uparrow + L\downarrow \qquad (3.1.1)$$

where R_n is the net radiation, $L\uparrow$ and $L\downarrow$ are the upward and downward longwave radiation components, respectively. The shortwave radiation is divided into the direct radiation, Q, and the diffuse part, q. As will be seen later in Section 3.3, the albedo of the earth's surface, α, is a very important parameter in the calculation of the radiation balance.

In this model, direct and diffuse solar radiation are combined into the available shortwave radiation, Q_a. The available surface energy on clear days, Q_a', can be calculated by (Goddard, 1973);

$$Q_a' = Q_o T^m \cos(Z) \qquad (3.1.2)$$

Hence, the available energy is related to the solar constant Q_o, the atmospheric transmission coefficient T, the optical airmass m ($m = \sec Z$) and the zenith angle of the sun Z. Equation (3.1.2) represents the entire shortwave model required to calculate the average attenuated intensity of the solar radiation received at the ground (Goddard, 1973).

The formulation shown above contains implicit assumptions with respect to the transmission coefficient, T. Equation (3.1.2) contains the simplest and crudest measure of atmospheric transmissivity (Stagg, 1950). No attempt is made to isolate particular wavelengths or to distinguish T from the true monochromatic transmissivity q'. It should be noted that q' is independent of m whereas T is not, as observed by Stagg (1950) and Latimer (1974). These characterisitics demand the calculation of local values of transmissivity in order to improve the simulation of atmospheric conditions over the area of operation of the model. To this end, values of T were obtained by rewriting (3.1.2) in terms of T;

$$T = \exp \frac{1}{m} \log \left[\frac{Q_a' \sec(Z)}{Q_o} \right] \qquad (3.1.3)$$

The values for Q_a' were obtained from the Monthly Radiation Summary for Stony Plain, Alberta with care being taken to insure that clear days only were chosen. After the analysis was performed, a

diurnal dependence of T on m was observed. However, such dependence was considered small enough to ignore when compared with the hourly fluctuations. This implies that T is independent of m in this model. The main variation of the transmission coefficient was seasonal. Three values of T were obtained from the data by averaging over three monthly periods. Further adjustment was made by running the radiation model and comparing shortwave radiation value (actual and observed). The characteristic values and standard deviations are given in Table 3.1. Similar trends were observed by Stagg (1950) and Latimer (1974).

Table 3.1

Seasonal Transmission Coefficients for Northern Alberta

Season	Transmission Coefficient
Winter (Nov-Feb)	0.910 ± 0.050
Spring & Fall (Mar-Apr) - (Sept-Oct)	0.875 ± 0.049
Summer (May-Aug)	0.760 ± 0.023

It should be noted that Q_a', calculated by (3.1.2), is the sum of the direct plus diffuse radiation for clear days only. Modification is required for days with cloud cover. In order to simulate multi-layered cloud cover, a model proposed by Pandolfo, Cooley and Newburg (1963) was incorporated. The original formulation accepted four cloud layers of different height and amount. In the

present model only three layers are used. The heights of the various layers are incorporated by the use of transmission coefficients which take on values indicative of the respective cloud layers. Values used by Pandolfo et al. (1963), for transmission of shortwave radiation, are extrapolated from Fritz (1951) (see Table 3.2). These transmissivities are in good agreement with those presented by Reynolds et al (1975) and Liou (1976) where absorption of shortwave radiation by the cloud is also considered. The available shortwave radiation reaching the earth's surface, is, therefore, described by;

$$Q_a = (1 - N_1(1-\psi_1))(1 - N_2(1-\psi_2))(1 - N_3(1-\psi_3))Q_a'$$

or

$$Q_a = \left[\prod_{i=1}^{3} (1 - N_i(1-\psi_i))\right] Q_a' \qquad (3.1.4)$$

N_i is the cloud amount in the i^{th} layer and ψ_i is the transmissivity for the i^{th} layer.

Table 3.2

Cloud Transmissivities

Cloud	Transmissivities(%)
Stratus	25
Stratocumulus	45
Altocumulus	55
Cirrus	75

The values in Table 3.2 are taken from Fritz (1951) and from the Smithsonian Meteorological Tables.

The final modification needed to complete the shortwave component is the depletion of radiation due to reflection at the earth's surface. Values of surface albedo used in the model are those obtained from the Smithsonian Meteorological Tables. Further discussion of surface albedo is deferred to Section 3.3. The available shortwave radiation in the model is calculated by;

$$Q_a = (1 - \alpha) \left[\prod_{i=1}^{3} (1 - N_i(1-\psi_i)) \right] T^m \cos(Z) Q_o \qquad (3.1.5)$$

3.2 Net Longwave Component

To complete the surface energy balance, the emission of longwave radiation must be studied. The surface of the earth emits energy as a grey body following the Stefan-Boltzman law;

$$L\uparrow = \varepsilon\sigma T^4 \qquad (3.2.1)$$

where ε is the surface emissivity, σ is the Stefan-Boltzman constant and T is the absolute temperature. The value of the emissivity is usually between 1.0 and .85 (Petzold, 1974) with temperature measured at the ground level. Considering the operational nature of this model, ground temperature was replaced by screen temperature. This assumption was also made by Petzold (1974). However, such a crude approximation would not be appropriate for microscale modelling.

Longwave radiation emitted downward from the clouds acts as a partial balance to the surface emission. Brunt (1932) and

others, modelled downward longwave radiation using both temperature and vapour pressure in their prediction equations. Swinbank (1963) was able to show that a more general and equally acceptable formulation could be obtained by using a modification of the Stefan-Boltzman law. Swinbank (1963) then performed a regression analysis for clear nights which gave the following relation;

$$L\downarrow = 5.31 \times 10^{-14} T^6 \qquad (3.2.2)$$

where T is temperature in degrees Kelvin. Temperature in (3.2.2) should be the temperature of the emitting body. This, however, is often difficult to ascertain. Using the theory of longwave transmission and emission it is possible to show that effectively all of the downward flux originates at a level very close to screen height (Swinbank, 1963). Hence screen temperature can be used in (3.2.2).

Combining (3.2.1) and (3.2.2) results in a relationship for the net longwave radiation (L_n). It must be noted that the downward flux calculated, as in (3.2.2), is for clear skies only and must therefore be modified for cloud cover. The complete longwave radiation balance can then be written in the following form;

$$L_n = -\varepsilon\sigma T_s^4 + nk5.31 \times 10^{-14} T_s^6 \qquad (3.2.3)$$

The Swinbank formulation (3.2.2) is, therefore, modified by the cloud amount n and by a factor k which depends both on cloud amount and type (Reuter, 1951). In a similar formulation by Goddard (1973), the upward flux rather than the downward flux is modified by cloud amount. Comments

by Goddard (1973) indicate good results for clear sky situations. Cloudy occasions were not tested adequately.

The method used to calculate the net longwave radiation in the present model differs from both of the above methods. An analysis of the above techniques indicated that the combination of upward and downward fluxes did not correlate as well with L_n as did the screen temperature. This led to a regression equation for the longwave net radiation in the form;

$$L_n = c_1 T_s + c_2 \qquad (3.2.4)$$

A similar technique used by Petzold (1974) gave very good results over snow-covered surfaces. This approach follows logically after a careful analysis of the variables in (3.2.3). For any given time period less than a day, the only variables are cloud amount and type, and screen temperature. Since screen temperature also reflects variability in cloud cover, the only truly independent meteorological parameter is temperature.

The use of temperature in (3.2.4) must be investigated carefully. For each month of the year, screen temperatures will exhibit different relationships with cloud cover due to sun angle as well as ground cover. As an example, a temperature of -15C could be observed in January under a heavy overcast deck of stratus cloud. The same deck of cloud may be accompanied by a 0 C temperature in March, with snow-covered ground in both cases. To help reduce this type of error the constants in (3.2.4) were derived separately each month.

The method consisted of determining the constants C_1 and

C_2 for the months used in the model verification are presented in Table 3.3. The 95 percent confidence limits shown in Table 3.3, indicate that the largest variation occurs in March. This is due to the difficulty in determining a representative albedo value under ablation conditions (see Sections 3.3 and 4.2.4). The error analysis presented in Section 4.2.2 confirms that these values are acceptable for use in the net longwave component of the model.

Table 3.3

Monthly Regression Coefficients for
Net Longwave Radiation Component

Month	Regression Coefficients and 95% Confidence Limits	
	C_1	C_2
March	0.067 ± 0.031	-2.308 ± 0.504
August	-0.113 ± 0.084	-4.724 ± 1.124
September	-0.294 ± 0.077	-3.698 ± 0.881
November	-0.143 ± 0.032	-5.479 ± 0.337

The final form of the equation used in the model consists of the sum of (3.1.5) and (3.2.4) which equals the net radiation (R_n) available to heat the lower atmosphere.

$$R_n = (1 - \alpha)\left[\prod_{i=1}^{3} (1 - N_i\psi_i)\right] T^m \cos(Z)Q_o + c_1T_s + c_2 \qquad (3.2.5)$$

3.3 Surface Albedo

Perhaps one of the most important parameters in the radiation model is the value given to the albedo of the earth's surface. The albedo value controls the extent to which the shortwave radiation influences the overall energy balance. If this value is in error, by more than 10 percent, especially over snow cover, it will drastically affect the model output (see Section 4.2).

The most representative albedo values for various surface types were obtained by a verification procedure using published values as a guide. A complete list of albedo values is available from the Smithsonian Meteorological Tables. However, most of the values are reported as ranges requiring the user to extract the particular value which best describes the situation being studied. Several trials were needed using different albedoes to determine the value that gave the best reproduction of the observed net radiation under the same meteorological conditions. The albedo values in Table 3.4 were selected by this method.

In Table 3.4, several different values are given for snow surfaces. Snow has the peculiar property of changing its albedo sharply from day to day especially during an ablation period (Arai, 1966). Values can vary by as much as 50 percent over the space of two or three days. A trial-and-error process similar to that described above was used to obtain the values for snow cover. Some further discussion on their use in particular meteorological situations is worthwhile. The value of 87 percent is reserved for days where measureable amounts of snow are falling, whereas 81 percent is used

Table 3.4

Surface Albedo Values

Surface	Albedo (%)
Grass	20
Frozen Ground	20
Wet Grass	25
Grass (Trace-Snow)	25
Snow (Melting)	46
Snow (Old)	70
Snow (New)	81
Tops of Pine	14
Tops of Fir	10

for days where only trace amounts have fallen or days immediately following a significant snowfall. When more than two days have passed with no new snow and with temperatures remaining below $0^{o}C$, a value of 70 percent is recommended. A value of 46 percent is used to describe melting snow with temperatures well above freezing during the peak insolation period. Often these periods are accompanied by light rain and snow or rain showers. For surfaces with trace amounts of snow and bare ground visible, 25 percent is the best value for the albedo. These were the values used in the longwave radiation regression analysis described in Section 3.2. For other surfaces, the albedo values in the Smithsonian Meteorological Tables would be more than sufficient for this model.

The preceding discussion of albedo values is primarily concerned with nearly flat surfaces of homogeneous cover. In a woodland area, the albedo of the treed and open sections must be considered separately. For the present radiation model, the value of albedo at the top of the forest canopy is used. This requires the calculation of a weighted albedo taking the percentages of treed to open areas in the region of interest. A procedure similar to this was used in the Fort McMurray study and will be discussed further in Section 4.3.

3.4 Diurnal Temperature-Wave

An integral part of the radiation model, particularly the net longwave radiation component, is an hourly predicted temperature. This requires a forecast equation which will correctly describe the diurnal temperature-wave. From studies of the diurnal temperature trend of Edmonton and Calgary, by Hage and Longley (1967), it is apparent that a modified sinusoidal wave would be appropriate.

Before the diurnal temperature-wave model can be formulated, two further assumptions are required in order to specify the times of maximum and minimum temperatures. It was found that sunrise correlated very well with the occurrence of minimum temperatures except in winter. From a study of daily temperature trends for Edmonton, Alberta, the months from November through to February require that the time of minimum temperature occurrence be predicted. Using a similar study, the average time of occurrence of maximum temperature was determined to be 1500 local standard time except for the winter months where the

average was 1400 local standard time. The only remaining problem was to correctly describe the behaviour of the diurnal cycle immediately after the maximum temperature was reached. From Businger (1973) (see Section 2.1), the mixing layer continues to receive energy until the surface heat flux becomes negative. Therefore, the diurnal wave is modelled in such a way that the value of maximum temperature is maintained until the net radiation becomes negative. Due to other factors which will be discussed in Section 4.3, the temperature cycle is terminated at this point.

The general form of the temperature-wave model can be written in the following manner;

$$T = aM + .5P\sin(C) \qquad (3.4.1)$$

The values of a, M and P are calculated for each day. M is the average value of temperature calculated from the morning minimum and maximum temperatures for the day and P is the difference between these values. Therefore, M gives the appropriate ordinate value for each day and P is an adjustment to the amplitude of the wave (see Fig. 3.1). The distance in time units from the minimum to maximum temperature is varied from day to day by C, which is given by;

$$C = 4.7 + (\pi/(TMAX - TSR))t \qquad (3.4.2)$$

The difference (TMAX-TSR) is the time in hours between maximum and minimum temperature which is exactly one half the period of oscillation. The value of 4.7 is the phase angle in radians when the sine function is at its minimum, $\pi = 3.1416$ radians and t is the time in hours.

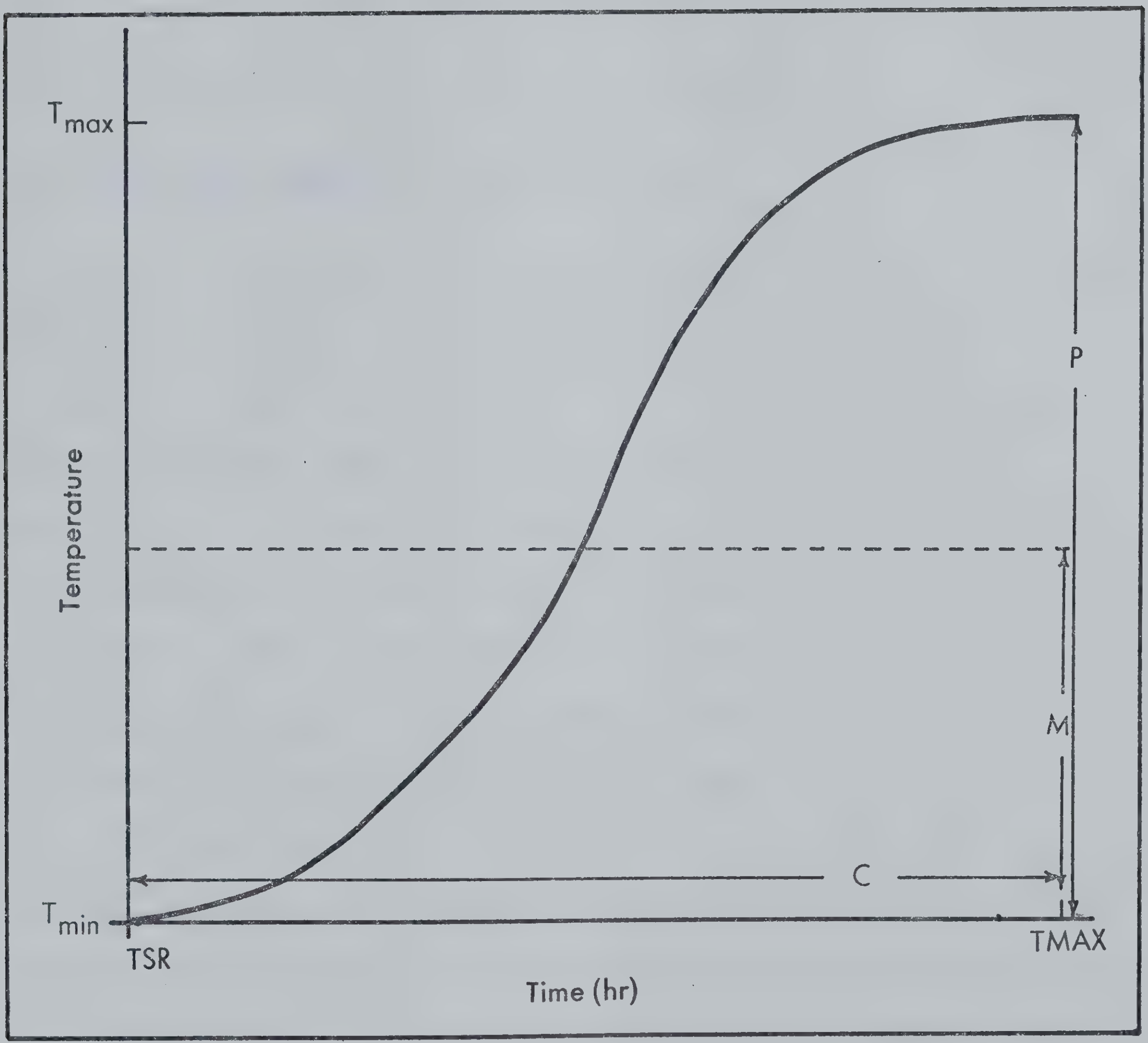

Fig. 3.1 Diagram of Diurnal Temperature-Wave Component

With all the variables defined, the values of a and b can be obtained by solving (3.4.1) for the maximum temperature simultaneously with a similar equation for the minimum temperature. This completes the diurnal temperature-wave model which enables hourly values of temperature to be provided internally to the main model.

3.5 Upper-Air Stability Component

On many occasions in the spring and fall the surface heating will be sufficiently strong to destroy the low level inversion and increase the mixing depth dramatically. This process is dependent both on the energy input to the lower atmosphere and the overall stability of the atmosphere. Therefore a technique is required which will monitor the relationship between the stability in the PBL with the stability aloft. The critical point will be reached when the lapse rate is unstable from the ground to some point above the inversion level hence allowing increased mixing.

This component is incorporated into the model by the use of forecast heights and temperatures at both 850 and 700 hectopascals. By interpolating values for each hour between 1200 (GMT) and 0000 (GMT), a complete set of upper-air data is generated for each hour. As the heat flux from the surface increases the mixing depth, the temperature at the top of the mixed layer is compared with the upper-air temperatures at the two levels previously mentioned. When the lapse rate between the top of the inversion and either the 850 or 700 hectopascal level becomes unstable, the mixing height is increased to the top of the entire unstable layer. Instability occurs when the lapse rate

exceeds 8.5 C km^{-1} (mean value of the wet and dry-adiabatic lapse rates). It is reasonable to expect that the hourly progression of mixing heights may exhibit a sudden increase due to the presence of unstable air aloft. An example illustrating the model prediction in an observed situation of this type is shown in Fig. 3.2.

By adopting this component some of the problems of advection are eliminated. In Fig. 3.2, cold-air advection has created an unstable lapse rate to nearly 850 hectopascals. The model is able to correctly detect this change by using the upper-air stability component. A problem that remains unsolved is the case where advection occurs below the 850 hectopascal level but does not actually effect the level itself. Warm-air advection, as shown in Fig. 3.3, is not handled well by the model and the addition of the above component is of no real help. As can be seen by the actual calculation of mixing heights (Appendix D), the depth of the mixed layer resulting from surface heating alone will not be sufficient to produce mixing heights of the magnitude of those observed.

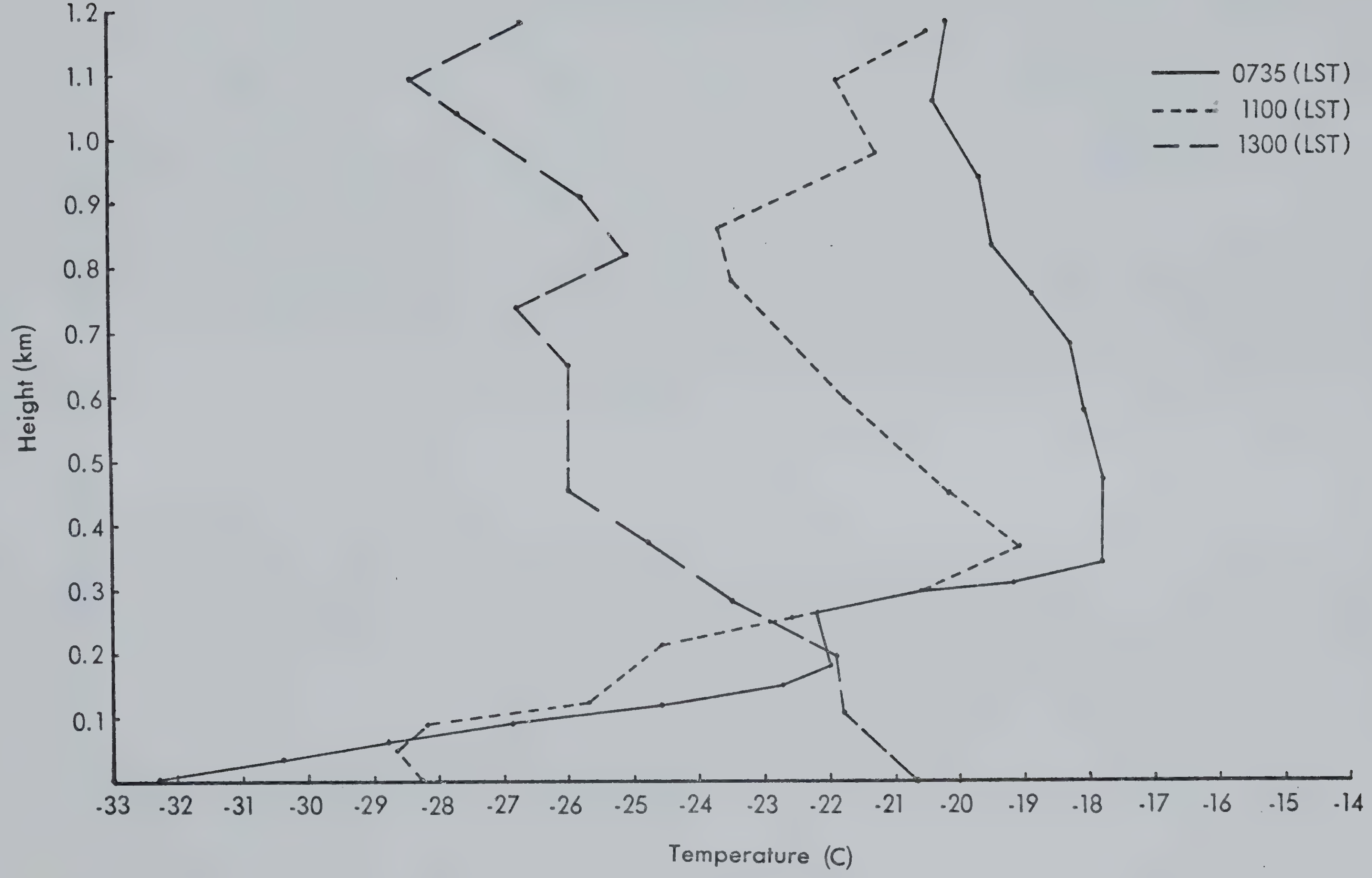

Fig. 3.2 Cold-Air Advection and Mixing Height
(Minisonde for March 4, 1976, Fort McMurray)

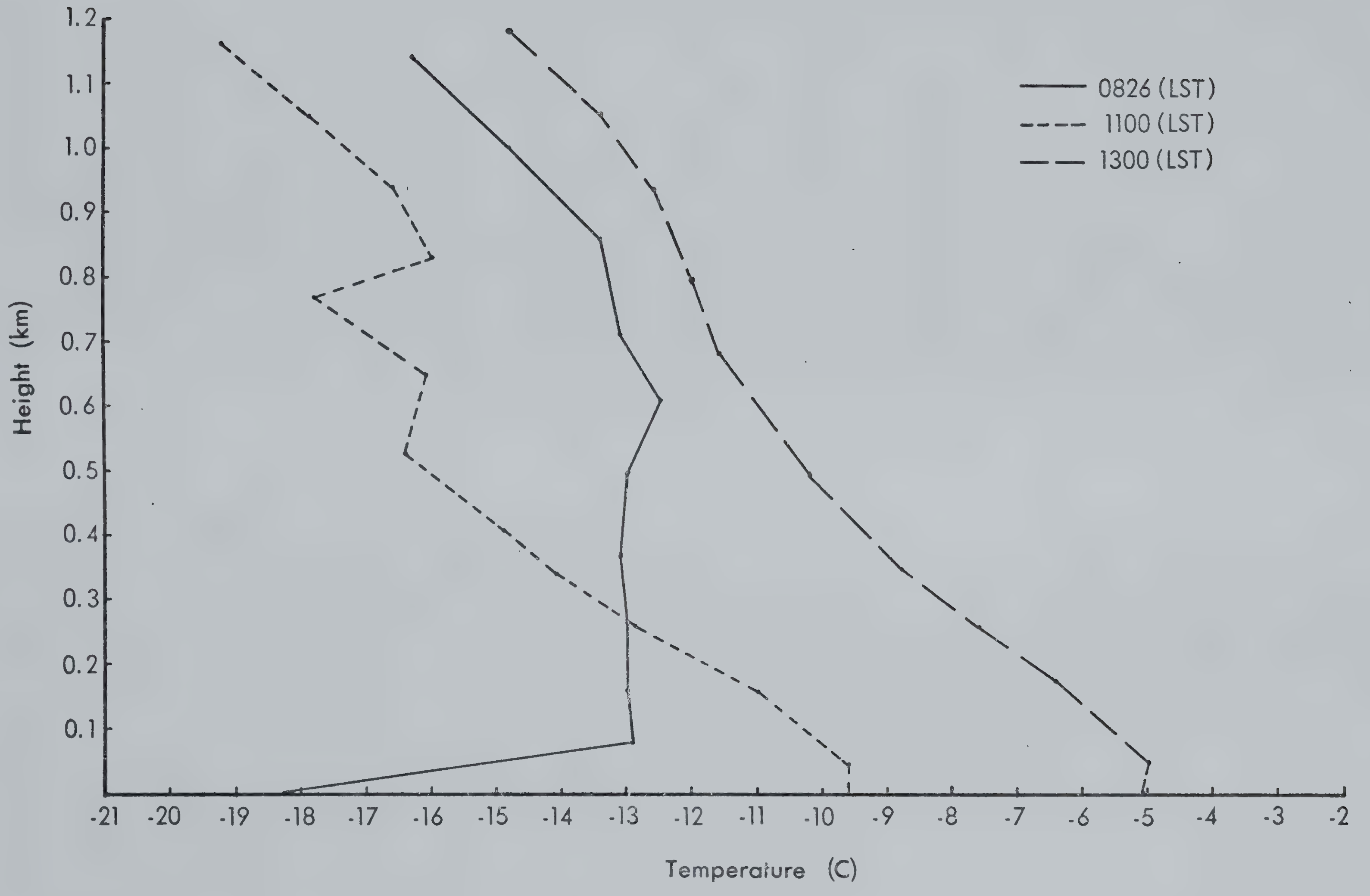

Fig. 3.3 Warm-Air Advection and Mixing Height
(Minisonde for March 11, 1976, Fort McMurray)

CHAPTER 4

ERROR ANALYSES AND RESULTS

4.1 Operation of the Model

In Chapter 3, development of the components of the model was discussed. The coupling of the various segments into a workable unit will now be considered. As the net radiation becomes positive (after sunrise), the model begins the calculation of mixing heights. The energy continues to be summed and transformed into an equivalent triangular area as described in Section 2.2. This transformation is explicated mathematically by;

$$A(t) = C \frac{Rg}{c_p \overline{P}} \int_{t_o}^{t} H(\tau)\,d\tau \qquad (4.1.1)$$

The sensible heat flux, $H(\tau)$, is integrated from the time of minimum temperature, t_o, to the time of interest, t. The value of $\overline{P}$ is defined in Section 2.2 and is calculated by assuming a hydrostatic atmosphere. The constant C transforms units from specific energy to area and has the magnitude 2.53×10^4 kg joule^{-1}.

The calculation of the mixing height, $h(t)$, is a problem in basic geometry. A simple formula relating the area to the base

and altitude of the triangle would be sufficient but this does not allow the required flexibility. Considering that the atmosphere is not always dry-adiabatic in the lower layers, it would be highly desirable to have the lapse rate used in the model depend only on the particular meteorological conditions present on the day of interest. This can be accomplished by specifying the angle on a thermodynamic diagram between the base level and the chosen lapse rate (see Fig. 4.1). Therefore, the formula used for calculating the mixing height, developed by the surface heat flux, is of the following form;

$$h(t) = \left[\left\{ \frac{2A(t)}{DT\sin\theta} \right\}^2 + DT^2 - \left\{ \frac{4A(t)}{DT\sin\theta} \right\} DT\cos\theta \right]^{\frac{1}{2}} \sin\phi \quad (4.1.2)$$

As illustrated in Fig. 4.1, the angle of interest is Θ. A value of $\Theta = 40$ degrees corresponds to the dry-adiabatic lapse rate. The value of mixing depth printed out by the model is given by (4.1.2) until the entire lower layer becomes unstable (see Section 3.5).

The program requires the input of basic meteorological parameters and geographical information for the location being analyzed (see Appendix B). With these values and the model components, a value of mixing height is calculated for each hour from sunrise until the surface heat flux diminishes to zero. The output includes a value for net radiation and solar radiation in joules per square meter per hour as well as the hourly mixing height in meters. Preliminary information in the printout includes the geographical location, date, albedo and the maximum and minimum temperatures for the location of interest (see Appendix A). The addition of these

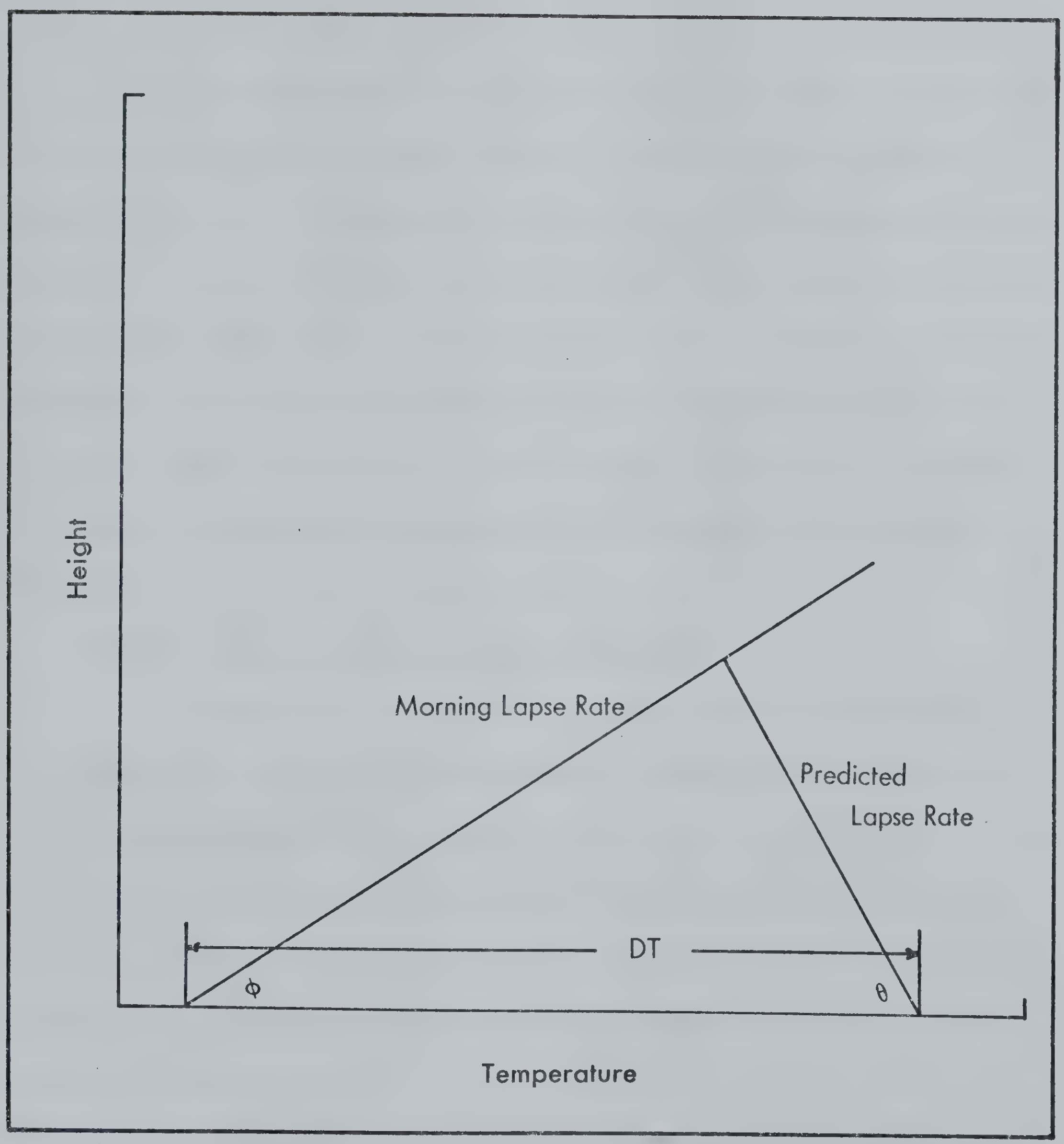

Fig. 4.1 Geometry for the Mixing Height Model

parameters in the printout will provide a check on the performance of the model.

4.2 Errors in the Model

In the development of the model, approximations of actual atmospheric processes created errors. Aside from developmental errors there are 'separation errors' introduced by using data from different locations within the same region. For example, the radiation values were taken from Stony Plain, Alberta, whereas cloud and temperature data were from Nisku, Alberta (Edmonton International Airport). The latter type of error is very difficult to estimate but must be considered when assessing the overall inaccuracies of the model.

4.2.1 Errors in the Shortwave Component

As described in Section 3.1, the shortwave component incorporates a forecast of cloud amount, derived turbidity values and a modelled solar flux. The errors could be rather large if care is not taken in the determination of these components. An error analysis was performed using observed cloud cover and temperature from Nisku, Alberta with radiation data from Stony Plain, Alberta used as a verification.

Assuming that the radiation values would be representative of conditions observed at Nisku, this analysis was a test of the accuracy of both the cloud model and the solar flux model (Section 3.1). The radiation model was used to analyze four randomly chosen days from each of six months. The months used encompassed each season

with an equal number of days in each. A graphical representation (see Fig. 4.2) gives the variation of the standard deviation versus local standard time (LST). Low error values in the morning and afternoon with a slight peak near maximum insolation, 1300 (LST), correlates well with the variation of the solar flux reaching the ground. The shape of the error curve is therefore considered to be the result of larger radiation values giving a higher probability of having greater errors. The mean value of the shortwave radiation calculated over this data set was found to be 100 x 10^4 joules m^{-2} hr^{-1} with a mean standard deviation of 24 x 10^4 joules $m^{-2}hr^{-1}$ (see Fig. 4.2).

4.2.2 Errors in the Net Longwave Component

The net longwave component was derived using a least-squares regression technique (see Section 3.2). By using the regression coefficients with their 95% confidence limits, as given in Table 3.3, upper and lower bounds were calculated using (3.2.4) for the net longwave radiation (see Table 4.1).

Table 4.1

Error Analysis of Net Longwave Radiation

Month	Net Longwave Radiation (Joules m^{-2} hr^{-1} x 10^4)
March	-6.9 ± 3.4
August	-24.5 ± 3.2
September	-27.8 ± 6.9
November	-28.9 ± 2.8

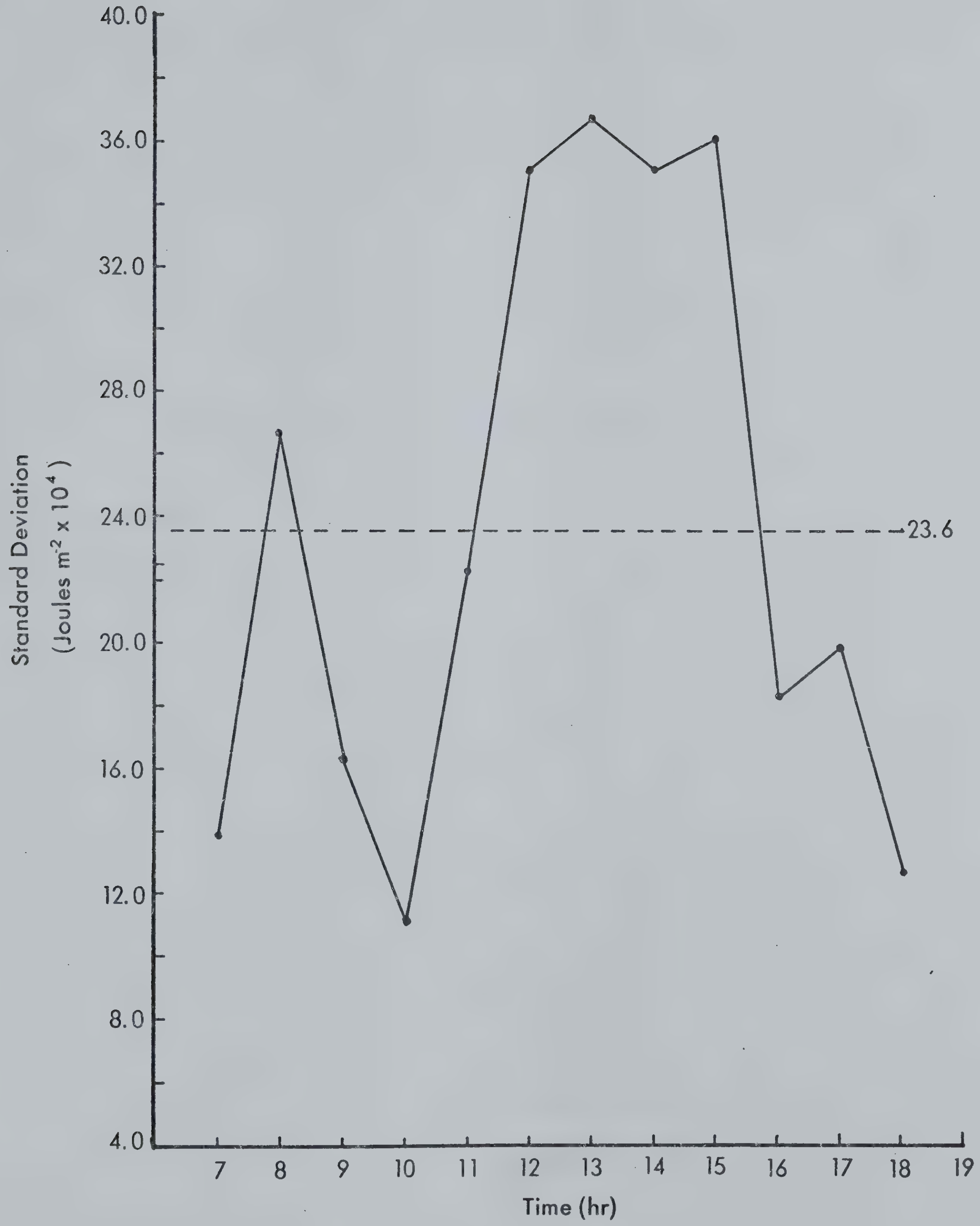

Fig. 4.2 Standard Deviation of Shortwave Radiation

A value of 10C was used in (3.2.4) to eliminate the effects of errors in the diurnal temperature-wave component of the model. From Table 4.1, the error analysis indicates relatively good results for all months except March. The larger percentage error indicated for the March calculation was caused by the rapidly varying albedo which entered into the original regression (see Section 3.2). Some of the problems that arise in deducing surface albedo during ablation periods have been discussed previously (Section 3.3).

4.2.3 Errors in the Net Radiation Component

In order to determine the error in this component, values of the net radiation calculated by the present model were compared with observed values recorded at Stony Plain, Alberta. Data used in this study excluded all days with snow cover in order to eliminate the problems with albedo values. The mean net radiation obtained using this data set was 34 x 10^4 joules $m^{-2}hr^{-1}$ with a mean standard deviation of 12 x 10^4 joules $m^{-2}hr^{-1}$ (see Fig. 4.3). The standard deviation of the net radiation did not exhibit a diurnal time-dependence. An error of this magnitude (12 x 10^4 joules $m^{-2}hr^{-1}$) was found to cause a 200 meter error in the mixing depth calculated in the early morning hours. The inaccuracy of the mixing-layer height drops sharply with time to approximately 20 meters by mid-day. It is interesting to note that the error in the net radiation is approximately one half that of the shortwave component. This demonstrates the effect of albedo as an 'error filter' in reducing the amount of variation originating in the shortwave component by exactly one minus the albedo value.

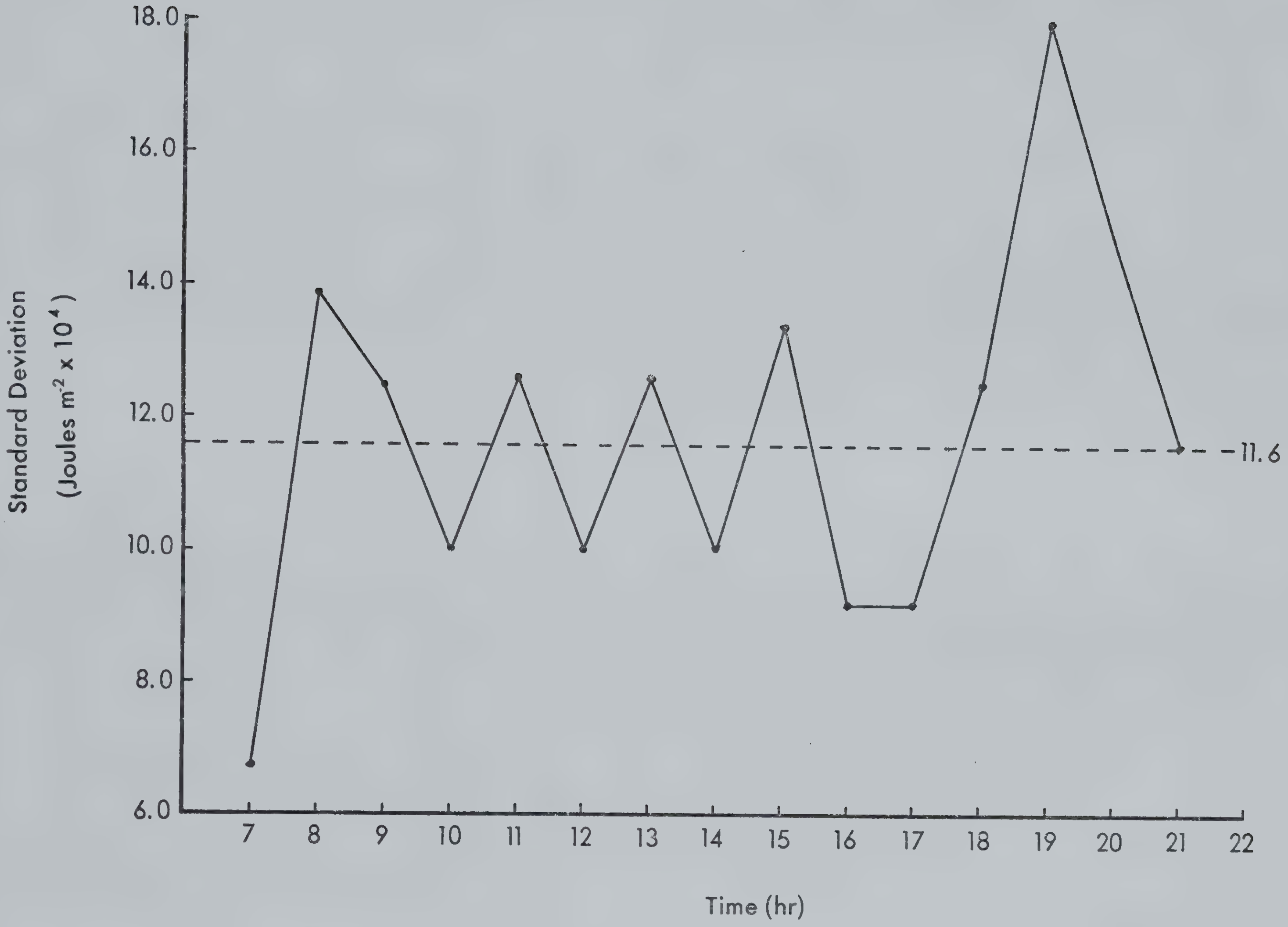

Fig. 4.3 Standard Deviation of Net Radiation

4.2.4 Albedo Errors

In the preceding discussion, albedo was held nearly constant. Unfortunately this constancy of albedo does not occur in actual practice. A rather thorough explanation of albedo and its variability was given in Section 3.3. It was evident that the required values ranged from 15 percent to nearly 90 percent. The error analysis, therefore, considers three representative albedo values and demonstrates the expected error in maximum mixing height that would be incurred by a predetermined error in albedo value. Albedoes in error by ten, fifteen and twenty percent were used to calculate mixing heights from the same data. By using the same data, errors from the other variables were eliminated. In Table 4.2, percentage errors are given for albedoes of twenty, forty-six and eighty-one percent.

Table 4.2

Analysis of the Effects of Errors in Surface Albedo

Albedo Value (%)	Error in Albedo Value (%)	Error in Maximum Mixing Height (%)
20	10	4
	15	6
	20	8
46	10	16
	15	23
	20	26
81	10	21
	15	34
	20	72

As indicated in Section 3.3, the value of the albedo used over snow cover (81% range in Table 4.2) is critical in attempting an

accurate solution of the mixing-height calculation. This is especially significant because an error of 72 percent will make the entire procedure futile when low mixing heights are considered. By determining albedo values, as discussed in Section 3.3, the inaccuracies discussed above can be reduced significantly.

4.2.5 Errors in the Diurnal Temperature-Wave Component

The diurnal temperature-wave component was verified at the same time as the shortwave component. Temperatures used were taken from four days in each of the six months chosen from the four different seasons. The standard deviation of temperature is plotted versus time in Figure 4.4. The peak in the error curve occurring in the mid-morning is due to the shape of the model curve (see Section 3.4). Although the peak appears rather pronounced, it represents a maximum error of only 2.4 C with the average error over the entire period being 1.4 C.

The errors in this component could be reduced by the use of a more complicated function to model the diurnal temperature-wave. However, these errors are considered small enough not to contribute significantly to the errors in the net longwave component or the model as a whole.

4.3 Performance of the Model in Northern Alberta

The performance of the model was assessed by comparing it with two simpler models. The simplest approach to forecasting mixing heights is to use the temperature profile produced by a numerical model such as the Primitive Equation Model (PE). A temperature profile from such a numerical model was simulated by using upper air data at

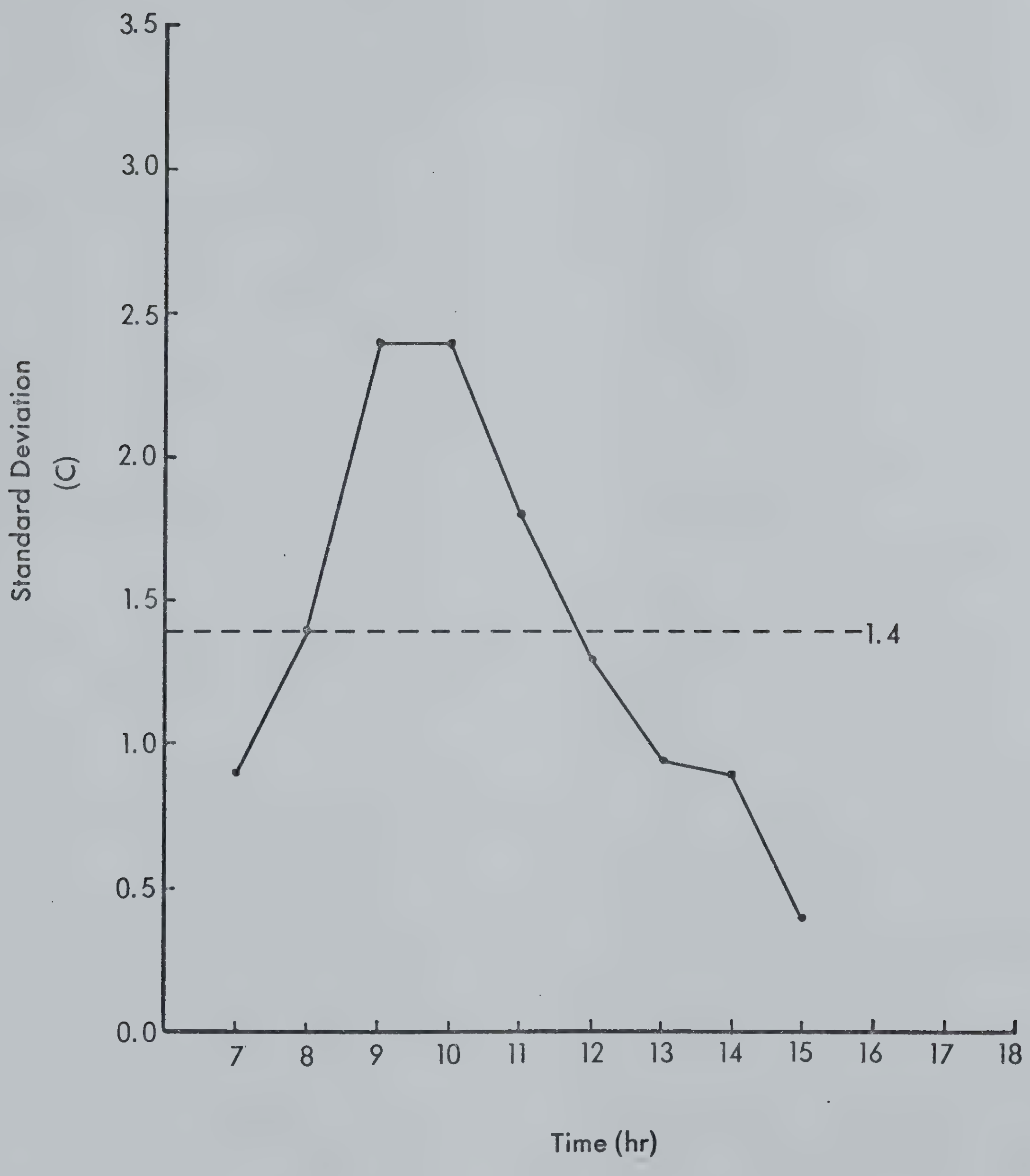

Fig. 4.4 Standard Deviation of the Diurnal Temperature-Wave

1200 (GMT) and 0000 (GMT) which is available from the Monthly Upper-Air Summary. Using these data, a five-level temperature profile was constructed for those periods required by the study. A second and slightly more sophisticated approach, Holzworth's (1964) technique, was used after being modified to give hourly mixing heights. The surface temperatures required for both models came from the diurnal temperature-wave component of the present model. It was hoped that this procedure would reduce the effect of errors in the prediction of surface temperatures from one of the models to the other. These two simpler models were chosen to help ascertain the improvement, if any, in forecasting mixing heights using the present model.

The absolute test of performance is to verify the model mixing heights with observed values. Minisonde data were used for this part of the study. The main criterion for establishing the height of the mixed layer is to determine the level at which the stratification changes from unstable to stable. In order to obtain a representative lapse rate, the temperature soundings were partitioned vertically in equal intervals (approximately 100 meters). This acted to smooth the profile. However sufficient detail remained for a realistic determination of the mixing depth. The present model was used to forecast mixing heights over Edmonton, Alberta for November, 1974 and over Fort McMurray, Alberta for March, August, and September, 1976.

When applying mixing-height models to pollution problems, the ability to forecast critical mixing heights is of utmost concern. For a mixing height to be critical, it must be within a few hundred

meters of the top of the pollution source, effectively trapping the effluent in the lower layers of the atmosphere. Under winter conditions, the mixing heights are often less than the average stack height (Portelli, 1975). In the spring and fall, however, mixing heights are slightly higher increasing the possibility of critical mixing heights.

The days used for verification purposes did not include periods in which continuous precipitation was falling. Precipitation is a problem when a dry-adiabatic lapse rate is being assumed as in Holzworth's (1964) technique. Advection days were included in the study in order to determine the effects that this fairly common phenomenon would have on the model being tested.

4.3.1 Fort McMurray Case Study

Minisonde data for this study were obtained from the Alberta Oil Sands Environmental Research Program (AOSERP) and from Syncrude Environmental Group (SEG). The AOSERP data (Appendix E) cover a period from the 4th to the 17th of March, 1976. From this data set, The Great Canadian Oil Sands (GCOS) site was chosen as the most representative location for the area. The GCOS minisonde was located on higher terrain, out of the actual valley and was, therefore, deemed better than sites in the valley. The SEG minisonde data (Appendix E) was recorded at Mildred Lake which is at approximately the same elevation as the GCOS site. The entire area in the vicinity of Fort McMurray is classified as Boreal forest with approximately forty percent tree cover.

The March analysis covers a period of snowmelt with its

inherent difficulties in determining albedo values. Forest cover added to this problem requiring that a weighted albedo value be determined using the percentages of tree and untreed land in the area. The values of mixing height obtained from the three models, for this period, can be found in Appendix D. A contingency table (Table 4.3 (a), (b), (c)) was prepared for each of the three models. From Table 4.3 (b), Holzworth's model produced 41 percent perfect forecasts which was superior to 29 percent by the present model. The numerical model produced 46 percent perfect forecasts, however the remainder of the predictions were very poor compared with the other two models (see Table 4.3 (c)). A rather strong bias toward under-prediction of mixing heights is shown in Table 4.3 (b) by Holzworth's model. The present model was free of bias. However, some scatter throughout the various classes is evident (see Table 4.3 (a)).

Table 4.3(a)

Contingency Table for the Present Model - March

Observed Mixing Heights (m)	Present Model Mixing Heights (m)						
	0-100	100-300	300-500	500-800	800-1200	above 1200	
0-100	3	5	2	1			11
100-300	1	7	3				11
300-500	1	1	1				3
500-800			2	1	1		4
800-1200	1			1			2
above 1200		2	3	2	3		10
	6	15	11	5	4	0	41

Table 4.3(b)

Contingency Table for Holzworth's Model - March

Observed Mixing Heights (m)	Holzworth's Model Mixing Heights(m)						
	0-100	100-300	300-500	500-800	800-1200	above 1200	
0-100	8	2		1			11
100-300	4	6	1				11
300-500	2			1			3
500-800		1	2	1			4
800-1200		1		1			2
above 1200			5	2	1	2	10
	14	10	8	6	1	2	41

Table 4.3(c)

Contingency Table for Numerical Model - March

Observed Mixing Heights (m)	Numerical Model Mixing Heights(m)						
	0-100	100-300	300-500	500-800	800-1200	above 1200	
0-100	7		1			3	11
100-300	8				1	2	11
300-500			1			2	3
500-800				1		3	4
800-1200						2	2
above 1200						10	10
	15		2	1	1	22	41

Strong surface heating and subsequent convective instability dominated the August data period (see Appendix E). As in the previous study a weighted albedo was determined but in this case remained constant throughout the period. Contingency tables (see Table 4.4 (a), (b), (c)) were constructed with the numerical model again being superior with 51 percent 'direct hits'. However, the numerical model performed very poorly in the remainder of the verification. Holzworth's model gave 49 percent correct forecasts which was slightly better than the 41 percent given by the present model. Bias to under-forecast mixing heights was again obvious in Holzworth's model (see Table 4.4 (b)). The numerical model demonstrated considerable bias to over-forecast heights (see Table 4.4 (c)). No comparable bias was observed in the present model (see Table 4.4 (a)).

Table 4.4(a)

Contingency Table for Present Model - August

Observed Mixing Heights(m)	Present Model Mixing Height(m)					
	0-300	300-600	600-900	900-1200	above 1200	
0-300	7	2	2			11
300-600	1					1
600-900	1	2	2	2		7
900-1200			1	5	1	7
above 1200				10	3	13
	9	4	5	17	4	39

Table 4.4(b)

Contingency Table for Holzworth's Model - August

Observed Mixing Heights(m)	Holzworth's Model Mixing Heights(m)					
	0-300	300-600	600-900	900-1200	above 1200	
0-300	11					11
300-600	1					1
600-900	3		3	1		7
900-1200	1	1	2	1	2	7
above 1200		1	3	5	4	13
	16	2	8	7	6	39

Table 4.4(c)

Contingency Table for Numerical Model - August

Observed Mixing Heights(m)	Numerical Model Mixing Heights(m)					
	0-300	300-600	600-900	900-1200	above 1200	
0-300	7				4	11
300-600					1	1
600-900					7	7
900-1200					7	7
above 1200					13	13
	7	0	0	0	22	39

The final set of S.E.G. data used contains the period from the 23rd to the 30th of September (see Appendix E). The surface heating remained strong enough to 'burn-off' the inversion but the number of hours of solar insolation was beginning to decrease. This created lower mixing heights than those observed in August. Fortunately, this period was free of measureable amounts of precipitation allowing a constant albedo value to be used. As in the other case studies over the Fort McMurray area, a weighted albedo value was used.

Contingency tables have been constructed (see Tables 4.5 (a), (b), (c)) using the September mixing depths calculated by the three models (see Appendix D). Holzworth's technique produced 41 percent correct forecasts, the numerical model gave 38 percent correct forecasts, and the present model gave 33 percent perfect forecasts.

Table 4.5(a)

Contingency Table for the Present Model - September

Observed Mixing Heights(m)	Present Model Mixing Heights(m)						
	0-100	100-300	300-500	500-800	800-1200	above 1200	
0-100	4	2					6
100-300	1		7	1	1		10
300-500				2			2
500-800	1		1	3			5
800-1200				1	6		7
above 1200					9		9
	6	2	8	7	16	0	39

Table 4.5(b)

Contingency Table for Holzworth'd Model - September

Observed Mixing Heights(m)	Holzworth's Model Mixing Heights(m)						
	0-100	100-300	300-500	500-800	800-1200	above 1200	
0-100	5				1		6
100-300	1	1	3	1	3	1	10
300-500				2			2
500-800	1		2	1	1		5
800-1200				2	1	4	7
above 1200				1		8	9
	7	1	5	7	6	13	39

Table 4.5(c)

Contingency Table for Numerical Model - September

Observed Mixing Heights(m)		Numerical Model Mixing Heights(m)					
	0-100	100-300	300-500	500-800	800-1200	above 1200	
0-100	5			1			6
100-300	1			2	3	4	10
300-500						2	2
500-800			1	1	1	2	5
800-1200						7	7
above 1200						9	9
	6	0	1	4	4	24	39

Only the numerical model demonstrated a noticeable bias by consistently over-forecasting the mixing-layer heights.

4.3.2 Edmonton Case Study

Minisonde data were available for a period from November 19th to December 2nd (see Appendix E) from the A.E.S. Ascents were taken at several locations in the vicinity of Edmonton, Alberta both in urban and rural sites. Only rural minisonde data were used in order to eliminate heat-island effects. The ground was frozen with trace amounts of snow. With no appreciable melting or precipitation in this period, the albedo value was taken to be constant. As discussed earlier, in Section 4.2, this is one of the seasons of the year when critical mixing heights can be expected and, in fact, this was observed (see Appendix D).

The contingency tables (see Table 4.6 (a), (b), (c)) indicate that Holzworth'd model is the best with 75 percent correct forecasts. However, the present model and the numerical model achieved 69 percent and 63 percent correct forecasts, respectively. It is the bias which separates the individual model performances. From Table 4.6(a), no bias is shown by the present model. However, Holzworth's model again demonstrated a tendency to under-forecast mixing heights (see Table 4.6(b)). The large values appearing in the lowest class are due to the correct prediction of zero mixing heights in the early morning hours.

4.4 Discussion of Verification

The four case studies covered all periods of the year

Table 4.6(a)

Contingency Table for the Present Model - November

Observed Mixing Heights(m)	Present Model Mixing Heights(m)				
	0-100	100-200	200-300	above 300	
0-100	15	3			18
100-200	1	3	5		9
200-300		1	3		4
above 300				1	1
	16	7	8	1	32

Table 4.6(b)

Contingency Table for Holzworth's Model - November

Observed Mixing Heights(m)	Holzworth's Model Mixing Heights(m)				
	0-100	100-200	200-300	above 300	
0-100	17	1			18
100-200	2	5	2		9
200-300	1	1	1	1	4
above 300				1	1
	20	7	3	2	32

Table 4.6(c)

Contingency Table for the Numerical Model - November

Observed Mixing Heights(m)	Numerical Model Mixing Heights(m)				
	0-100	100-200	200-300	above 300	
0-100	18				18
100-200	9				9
200-300	1		1	2	4
above 300			1		1
	28	0	2	2	32

except winter. Throughout the verification program very little difference was observed between the performance of Holzworth's technique and the proposed model. Both models did not perform well during the March study. This was caused by problems in determining albedo values and the high incidence of advection. The advection of cold or warm air effecting the mixing height was observed on 7 out of 11 days. The remaining studies were not affected significantly by either of the above problems and forecasts were slightly improved.

The use of contingency tables to display the model performances allows prompt assessment of accuracy. It must be remembered, however, that the classes chosen create arbitrary cut-offs which may produce incorrect conclusions in assessments of the model performances. By taking the diagonal elements plus the elements one class from the diagonal, an overall judgement can be made which may be more realistic.

Using a contingency table, the significance of the forecasts can be checked. For this purpose all of the data from the four studies were combined. A contingency table was constructed for the present model (see Table 4.7) and for Holzworth's technique (see Table 4.8). The significance test is based on the hypothesis that no skill is exhibited by the forecasts (the null hypothesis). A new contingency table is then developed using the above hypothesis to derive the number of forecasts that would appear in each cell if there was no skill. These are the values appearing in brackets in Tables 4.7 and 4.8. Assuming a chi-squared distribution (Panofsky and Brier, 1958), the difference between these tables of values can be tested. If the two sets of forecasts are independent the calculated chi-square value will be less than the tabulated value for the specified significance level and degrees of freedom. The chi-square value for Table 4.7 was found to be 133.3 whereas 115.3 was calculated for Table 4.8. The value of chi-square with 16 degrees of freedom at the 5 percent significance level was found from the appropriate table (Mendenhall and Schaeffer, 1973) to be 26.3. Therefore, both models exhibit skill. The degree of skill shown cannot be demonstrated by this test but can be inferred by considering the various diagonal elements.

The diagonal elements in Table 4.7, running from the top left to bottom right, indicate that the present model produced 56 percent 'direct hits'. The corresponding value from Table 4.8 was 62 percent perfect forecasts. If one cell on either side of this diagonal is included, values of 89 percent and 81 percent are obtained from Table 4.7 and 4.8, respectively. The last piece of information that can be gleaned from the tables is the percentage

Table 4.7

Contingency Table for the Present Model - All Data

Observed Mixing Heights(m)	Present Model Mixing Heights(m)					
	0-300	300-600	600-900	900-1200	above 1200	
0-300	61 (37.1)	14 (14.3)	5 (7.9)	(18.5)	(2.1)	80
300-600	3 (4.6)	7 (1.8)	(1.0)	(2.3)	(0.3)	10
600-900	3 (7.4)	3 (2.9)	5 (1.6)	5 (3.7)	(0.4)	16
900-1200	1 (6.0)	(2.3)	3 (1.3)	8 (3.0)	1 (0.3)	13
above 1200	2 (14.8)	3 (5.7)	2 (3.2)	22 (7.4)	3 (0.8)	32
	70	27	15	35	4	151

Table 4.8

Contingency Table for Holzworth's Model - All Data

Observed Mixing Heights(m)	Holzworth's Model Mixing Heights(m)					
	0-300	300-600	600-900	900-1200	above 1200	
0-300	68 (41.3)	7 (12.2)	1 (9.0)	4 (6.9)	(10.6)	80
300-600	3 (5.2)	4 (1.5)	2 (1.1)	(0.9)	1 (1.3)	10
600-900	5 (8.3)	2 (2.4)	7 (1.8)	1 (1.4)	1 (2.1)	16
900-1200	2 (6.7)	2 (2.0)	3 (1.5)	1 (1.1)	5 (1.7)	13
above 1200	(16.5)	8 (4.9)	4 (3.6)	7 (2.8)	13 (4.2)	32
	78	23	17	13	20	151

of unsatisfactory forecasts, more than one class from the diagonal. In Tables 4.7 and 4.8, 11 percent and 19 percent, respectively, are in this category. Both models gave accurate forecasts between 50 percent and 60 percent of the time, and gave acceptable forecasts more than 80 percent of the time.

Another aspect of this study is the use of the two previous models in pollution episode forecasting. It is the occurrence of the critical mixing height discussed earlier which is of greatest concern to pollution potential calculation. This critical height will usually be from 300 to 600 meters above ground when stacks are considered. Low mixing heights where a stack plume can penetrate the inversion and situations of unlimited mixing (mixing heights greater than 900 meters) are also of interest in the prediction of pollution episodes.

Table 4.9 has been constructed to demonstrate the performance of the present model and Holzworth's model in forecasting appropriate mixing heights for the three mixing-height categories. The

Table 4.9

Model Performances for Pollution Forecasting

Mixing Height (m)	Percent Correct Forecasts	
	Present Model	Holzworth's Model
<300	76	85
300-600	70	40
>900	76	58

present model performed acceptably in all ranges with Holzworth's model demonstrating success only in the first category. This test of the models was performed using a very small data sample hence firm conclusions regarding the demonstrated skill cannot be made with confidence.

CHAPTER 5

SUMMARY AND CONCLUSIONS

A time-dependent computer model was developed to calculate the height of the mixed layer without prior, detailed knowledge of the vertical temperature structure. In the development of this model three basic assumptions were required:

(1) the energy necessary to develop the mixed layer was derived solely from the surface net radiation and was transported upward by convective turbulence.

(2) the vertical temperature profile from the minimum temperature was linear with height.

(3) the vertical temperature gradient in the mixed layer remained constant throughout the forecast period.

Input for the model included the latitude, longitude and elevation of the site under consideration. Surface and cloud albedoes were required as were the minimum and maximum temperatures for the day. The time of minimum temperature was also necessary for the month from November to February. In the remaining months the time of minimum temperatures was assumed equal to that of sunrise and was calculated

by the model. In order to provide the vertical temperature structure aloft, values of the temperature and height of the 850 and 700 hectopascal levels were included for 0500(LST) and 1700(LST). With this information as input, the model generated hourly mixing heights for the location being studied.

The importance of the model parameters varied from one time of the year to the other. During periods when the ground was snow-covered, surface and cloud albedoes became the dominant variables in the calculation of mixing depths. In the seasons with no snow cover and low albedo values, the maximum temperature for the day was of the utmost importance.

The energy approach modelled the growth of the mixed layer quite closely through the summer and late fall. It was found that the detail afforded by the inclusion of upper-air data was needed to predict correctly the growth of the mixing layer in the spring and early fall. It was, therefore, deemed necessary to include the appropriate upper-air data in the model to ensure that the desired accuracy was obtained.

In order to determine the level of accuracy of the model, a comparison was drawn with other techniques. Predictions from two other models were verified along with those of the present model. The following information was obtained from the test comparisons:

(1) no significant difference was detected between the present model and Holzworth's technique.

(2) the numerical model gave the worst predictions and was strongly biased to over-forecast the mixing-layer

heights.

(3) Holzworth's technique exhibited bias to underforecast mixing heights in all of the case studies except September.

(4) the present model demonstrated no significant bias in any season.

The enhancement of the mixed layer due to cold-air advection and/or radiational cooling was found to be a problem in the spring and early fall. The inclusion of the 850 and 700 hectopascal heights and temperatures partially considered the effects of these processes. However, there was no improvement in the results when the cooling occurred entirely below the 850 hectopascal level without effecting that level. A more detailed vertical temperature profile would be required to eliminate this problem.

The energy approach used in this model has been incorporated in many other mixing-layer models. However, the present model does not require detailed knowledge of an initial temperature profile and is, therefore, more broadly applicable than a method such as Holzworth's technique. Approaches similar to Carson's model require the measurement of turbulent perturbations which are often impossible to obtain with acceptable accuracy. The present model is more easily applied to mixing height determination because it does not require such data. Therefore, the present model is looked upon as a first attempt to provide an operational model which is time-dependent and capable of producing useful forecasts of the mixing depth using input data that are readily available.

REFERENCE LIST

Arai, T., 1966: On the relationship between albedo and properties of snow cover. Japanese Prog. in Climat., pp. 88-95.

Agnew, T., and Jarvis, C., 1972: An air pollution prediction model. Internal Publication, Atmospheric Environment Service, Downsview, Ontario, 14 pp.

Barnum, D.C. and Rao, G.V., 1975: Role of advection and penetrative convection in affecting the mixing-height variations over an idealized metropolitan area. Bound.-Layer Meteor., Dordrecht, Holland, 8 (3/4), pp. 497-514.

Blackadar, A.K., 1962: The vertical distribution of wind and turbulent exchange in a neutral atmosphere. J. Geophys. Res., 67, pp. 3095-3101.

Brunt, D., 1932: Notes on radiation in the atmosphere. Quart. J. Roy. Meteor. Soc., 58, pp. 389-418.

Businger, J.A., 1973: Turbulent transfer in the atmospheric surface layer. In: Workshop on Micrometeorology, ed. D.A. Haugen, Amer. Meteor. Soc., Boston, Mass.

Carson, D.J., 1973: The development of a dry inversion-capped convectively unstable boundary layer. Quart. J. Roy. Meteor. Soc., 99, pp. 450-467.

__________ and Smith, F.B., 1974: Thermodynamic model for the development of a convectively unstable boundary layer. Bound.-Layer Meteor., Dordrecht, Holland, 8 (3/4), pp. 111-124.

Deardorff, J.W., 1972: Rate of growth of the nocturnal boundary layer. Proceedings of the Symposium on Air Pollution, Turbulence and Diffusion, December 1971, New Mexico, ed. H.W. Church and R.E. Luna, pp. 183-190.

__________, Willis, G.E. and Lilly, D.K., 1969: Laboratory investigation of non-steady penetrative convection. J. Fluid Mech., 35, pp. 7-31.

Fritz, S., 1951: Solar radiant energy and its modification by the earth and its atmosphere. Compendium of Meteor., Amer. Meteor. Soc., Boston, pp. 13-33.

Goddard, W.B., 1973: Description of a surface temperature equilibrium energy balance model with application to arctic pack ice in early spring. In: Alaska Science Conference, 24th, Univ. of Alaska, August 15-17, 1973, Climate of the Arctic: Proceedings, Alaska, Univ., Fairbanks, Geophysical Institute, 1975.

Godson, W.L., 1958: Atmospheric Thermodynamics, Canada, Dept. of Transport, Meteorological Branch, Lecture Notes.

Hage, K.D., 1972: Urban growth effects on low temperature fog in Edmonton. Bound.-Layer Meteor. Dordrecht, Holland, 2, pp. 334-347.

__________ and Longley, R.W., 1968: Ventilation and mixing in Alberta cities. In: Man and His Environment, Proceedings of the First Banff Conference on Pollution, Edited by M.A. Ward, Pergamon of Canada Ltd., Toronto, pp. 99-113.

Haltiner, G.J. and Martin, F.L., 1957: Dynamical and physical meteorology. McGraw-Hill Book Company, New York, 455 pp.

Hanna, S.R., 1969: The thickness of the planetary boundary layer. Atmospheric Environment, Oxford, England, 3 (5), pp. 519-536.

Holmgren, B., Spears, L., Wilson, C. and Benson, C.S., 1973: Acoustic soundings of the Fairbanks temperature inversions. In: Alaska Science Conference, 24th, Univ. of Alaska, August 15-17, 1973, Climate of the Arctic: Proceedings, Alaska, Univ., Fairbanks, Geophysical Institute, 1975, pp. 293-306.

Holzworth, G.C., 1964b: Estimates of mean maximum mixing depth in the continguous United States. Mon. Wea. Rev., 92, pp. 235-242.

______________, 1967: Mixing depths, wind speeds and air pollution potential for selected locations in the United States. J. Appl. Meteor., 6, pp. 1039-1044.

______________, 1972: Mixing heights, wind soeeds and potential for urban air pollution throughout the continguous United States. U.S. Environment Protection Agency, Office of Air Programs, Pub. No. AP-101, Research Triangle Park, North Carolina, pp. 32-35.

Hosler, C.R., 1961: Low-level inversion frequency in the contiguous United States. Mon. Wea. Rev., 89, pp. 319-339.

Kagawa, N.H., 1968: Design and evaluation of a tephigram overlay for predicting maximum temperatures. Dept. of Transport, Meteorological Branch, TEC-683, 22 pp.

Laikhtman, D.L., 1961: Physics of the boundary layer of the atmosphere. Available from the Office of Technical Services, U.S. Dept. of Commerce, Wash., D.C., 200 pp.

Latimar, J.R., 1974: Observation of direct solar radiation and atmospheric turbidity at Toronto-Scarborough from 1960 to 1970. Canadian Meteorological Research Reports, Environment Canada, Atmospheric Environment Service, Downsview, Ontario, 27 pp.

Leahey, D.M. and Friend J.P., 1971: A model for predicting the depth of the mixing layer over an urban heat island with application to New York city. J. Appl. Meteor., 6, pp. 1162-1173.

Liou, K.N., 1976: On the absorption, reflection and transmission of solar radiation in cloudy atmospheres. J. Atmos. Sci., 33, pp. 798-805.

Mendenhall, W., Scheaffer, R.L., 1973: Mathematical statistics with applications. Duxbury Press, North Scituate, Mass., 561 pp.

Miller, M.E., 1967: Forecasting afternoon mixing depths and transport wind speeds. Mon. Wea. Rev., 95, pp. 35-44.

Munn, R.E., 1975: Atmospheric transport and diffusion on the regional scale. Presented to the First Specialty Symposium on Atmospheric Contribution to the Chemistry of Lake Waters, 17 pp.

Neiburger, M., 1941: Insolation and the prediction of maximum temperatures. Bull. Amer. Meteor. Soc., 22, pp. 95-102.

Norton, C.L. and Hoidale, G.B., 1976: The diurnal variation of mixing height by season over White Sands Missile Range. Mon. Wea. Rev., 104, pp. 1317-1320.

Pandolfo, J.P., Cooley, D. and Newburg, E.A., 1963: Preliminary investigations of numerical models for the short-period prediction of wind, temperature, and moisture in the atmospheric boundary layer. U.S. Weather Bureau, Contract Cwb-10368, Final Report, The Travelers Research Center, Inc., Hartford, Conn., 82 pp.

Panofsky, H.A. and Brier, G.W., 1958: Some applications of statistics to meteorology. Mineral Industries Continuing Education, College of Mineral Industries, The Pennsylvania State University, University Park, Penn., 220 pp.

Petzold, D.E., 1974: Solar and net radiation over snow. McGill Univ., Montreal, Dept. of Geography, Climatological Research Series No. 9, Nov. 1974, 77 pp.

Portelli, R.V., 1976: Mixing height, wind speeds and air pollution potential for Canada. Unpublished manuscript, Atmospheric Environment Service, Downsview, Ontario, 21 pp.

Reynolds, D.W., Vonder Haar, T.N. and Cox, S.K., 1975: The effect of solar radiation absorption in the tropical troposhere. J. Appl. Meteor., 14, pp. 433-444.

Reuter, H., 1951: Forecasting minimum temperatures. Tellus, 3, pp. 141-147.

Rossby, C.G. and Montgomery, R.B., 1935: The layer of frictional influence in wind and ocean currents. Pap. Phys. Oceanog. Met., 3 (3), 101 pp.

Stagg, J.M., 1950: Solar radiation at Kew Observatory. Geophys. Mem., London, 11, No. 86, 37 pp.

Summers, P.W., 1965: An urban heat island model - Its role in air pollution problems, with applications to Montreal. Presented at the First Canadian Conference on Micrometeorology, Toronto, April 12-14, 22 pp.

Swinbank, W.C., 1963: Longwave radiation from clear skies. Quart. J. Roy. Meteor. Soc., 89, pp. 339-348.

Turner, J.S., 1973: Buoyancy effects in fluids. Cambridge University Press, London, England, 367 pp.

Wiscombe, W.J., 1973: Solar radiation calculations for arctic summer stratus conditions. In: Alaska Science Conference, 24th, Univ. of Alaska, August 15-17, 1973, Climate of the Arctic: Proceedings, Alaska, Univ., Fairbanks, Geophysical Institute, 1975.

APPENDIX A

SAMPLE OF MODEL OUTPUT

LOCATION 56.DEG. 65.MIN. 111.DEG. 22.MIN.
DATE 14/ 8
ALBEDO 0.18
MAX.TEMP.= 29. MIN.TEMP.= 15.

TIME (LST)	NET RADIATION ($J/M^2 X10^4$)	SOLAR RADIATION ($J/M^2 X10^4$)	MIXING HEIGHT (M)
4.84	-27.	0.	0.
5.00	-26.	2.	0.
6.00	-17.	12.	0.
7.00	8.	44.	56.
8.00	41.	85.	202.
9.00	89.	145.	388.
10.00	120.	184.	549.
11.00	141.	211.	690.
12.00	119.	184.	771.
13.00	117.	183.	1098.
14.00	105.	169.	1098.
15.00	86.	146.	1098.
16.00	59.	113.	1117.
17.00	27.	73.	1152.
18.00	-1.	40.	1151.
19.00	-24.	11.	1119.
20.00	-34.	0.	1098.

MAXIMUM MIXING HEIGHT 1152. (M) OCCURRED AT 17.00 (LST)

APPENDIX B

PREPARATION OF DATA FILE

File Line or Card Number	Column	Input Format	Description (all data entries are right justified)
1	1-2	I2	day of the month
	3-4	I2	month of the year (1 to 12)
	5-7	F3.2	surface albedo value
	8-9	F2.0	latitude with degrees and
	10-11	F3.0	minutes input separately
	12-14	F3.0	longitude with degrees and
	15-16	F2.0	minutes input separately
	17-20	F4.0	location elevation (A.S.L.) in meters
	21-22	F2.0	time of minimum temperature in hours
	23-25	F3.0	minimum temperature in degrees centigrade
	26-28	F3.0	maximum temperature in degrees centigrade
2	1-3	F3.2	cloud albedo for first layer-first 3 hours
	4-6	F3.2	cloud albedo for second layer-first 3 hours
	7-9	F3.2	cloud albedo for third layer-first 3 hours
3	1-3	F3.2	cloud albedo for first layer-second 3 hours
	4-6	F3.2	cloud albedo for second layer-second 3 hours
	7-9	F3.2	cloud albedo for third layer-second 3 hours
4			SAME AS ABOVE for third 3 hours
5			SAME AS ABOVE for fourth 3 hours
6			SAME AS ABOVE for fifth 3 hours
7	1-4	F4.1	850 hectopascal temperature in degrees centigrade at 1200(GMT)
	5-8	F4.0	850 hectopascal height (A.S.L.) in meters at 1200(GMT)

File Line or Card Number	Column	Input Format	Description (all data entries are right justified)
8	1-4	F4.1	850 hectopascal temperature in degrees centigrade at 0000(GMT)
	5-8	F4.0	850 hectopascal height (A.S.L.) in meters at 0000(GMT)
9	1-4	F4.1	700 hectopascal temperature in degrees centigrade at 1200(GMT)
	5-8	F4.0	700 hectopascal height (A.S.L.) in meters at 1200(GMT)
10	1-4	F4.1	700 hectopascal temperature in degrees centigrade at 0000(GMT)
	5-8	F4.0	700 hectopascal height (A.S.L.) in meters at 0000(GMT)

Example of prepared data file:

```
 1      14080185665111220371000015029
 2      011009003
 3      009000000
 4      006018003
 5      017009000
 6      009003000
 7      01621098
 8      01761098
 9      00402623
10      00522761
```

APPENDIX C

COMPUTER PROGRAM

```
C   LIST OF VARIABLES USED IN PART 1
C
C           D(I,J)=SOLAR DECLINATION
C           BA(I,K)=REGRESSION COEFFICIENTS
C           SD(I)=LOCATION PARAMETERS
C           AB(I,J)=CLOUD ALBEDO
C           UPT(I)=UPPER-AIR TEMP.
C           UPH(I)=UPPER-AIR HEIGHT
C
      DIMENSION D(12,31),SD(8),RD(12,31),TIME(18),H(18),R(18),TP(24),AB(
     *5,3),RIS(24),BA(12,14),UPT(4),UPH(4),AH(18)
      COMMON UPT,UPH,SD
      READ(1,1) ((D(I,J),I=1,12),J=1,31)
    1 FORMAT(12(F5.2))
      READ(1,2) ((BA(I,K),K=1,2),I=1,12)
    2 FORMAT(2F5.3)
      READ(2,3) NDAY,MONTH,ABO,(SD(L),L=1,8)
    3 FORMAT(2I2,F3.2,2F2.0,F3.0,F2.0,F4.0,F2.0,2F3.0)
      WRITE(6,4) (SD(I),I=1,4),NDAY,MONTH,ABO,SD(8),SD(7)
    4 FORMAT('1','LOCATION',2X,F3.0,'DEG.',1X,F3.0,'MIN.',3X,F4.0,'DEG.
     *',1X,F3.0,'MIN.'/' ','DATE',2X,I2,'/',I2/' ','ALBEDO ',2X,F4.2/' '
     *,'MAX.TEMP.= ',F3.0,2X,'MIN.TEMP.= ',F3.0)
      READ(2,5) ((AB(I,J),J=1,3),I=1,5)
    5 FORMAT(3F3.2)
      DO 7 I=1,4
      READ(2,6) UPT(I),UPH(I)
    6 FORMAT(F4.1,F4.0)
    7 CONTINUE
C
C   LIST OF VARIABLES USED IN PART 2
C
C           THETA=ANGLE BETWEEN LAPSE RATE AND SURFACE
C           S=SOLAR CONSTANT
C           Z=INITIALIZATION HEIGHT
C           W=EARTH'S ANGULAR VELOCITY
C           F1 AND F2=REGRESSION COEFICIENTS
C
      THETA=40.0*0.0174532
      INT=1
      H(1)=1.0
      HF=0.
      NUM=1
      ASUM=0.
      S=487.25
      Z=50.0
      W=.2625
      F1=BA(MONTH,1)
      F2=BA(MONTH,2)
      DO 8 IN=1,12
      DO 8 JN=1,31
      RD(IN,JN)=D(IN,JN)*0.0174532
    8 CONTINUE
C
C   LIST OF VARIABLES USED IN PART 3
C
```

```
C           S8=MAXIMUM TEMP IN DEG F.
C           S7=MINIMUM TEMP IN DEG F.
C           RLAT=LATITUDE OF LOCATION
C           ALOG=LONGITUDE OF LOCATION
C           HR=HOUR ANGLE OF SUN AT SUNRISE
C           TS=LOCAL APPARENT TIME
C           TSR=LOCAL STANDARD TIME AT SUNRISE
C           AMP=AMPLITUDE OF DIURNAL TEMP WAVE
C           AVG=AVERAGE VALUE OF TEMP WAVE
C
      S8=1.8*SD(8)+32.
      S7=1.8*SD(7)+32.
      RLAT=(SD(1)+SD(2)/60.)*0.0174532
      ALOG=SD(3)+SD(4)/60.
      SM=FLOAT((IFIX(ALOG/15.))*15)
      TCOR=(ALOG-SM)*4.
      HR=ARCOS(-TAN(RLAT)*TAN(RD(MONTH,NDAY)))
      TS=12.-57.3*HR*4./60.
      TSR=TS+TCOR/60.
      LT=IFIX(TSR+.999)
      IF((MONTH.LE.11).AND.(MONTH.GE.3)) GO TO 9
      TSR=SD(6)
      LT=IFIX(TSR+1.)
    9 AMP=S8-S7
      AVG=(S8+S7)/2.
      CONST=S8-.5*AMP*SIN(7.9)
C
C  LIST OF VARIABLES USED IN PART 4
C
C           Q=TRUBIDITY
C           TMAX=TIME OF MAXIMUM TEMP
C
      IF((MONTH.LE.2).OR.(MONTH.GE.11)) GO TO 10
      IF((MONTH.LE.5).OR.(MONTH.GE.9)) GO TO 11
      Q=.76
      TMAX=15.
      GO TO 12
   10 Q=.92
      TMAX=14.
      GO TO 12
   11 Q=.875
      TMAX=15.
   12 CONTINUE
C
C  LIST OF VARIABLES USED IN PART 5
C
C           APT=LOCAL APPARENT TIMR
C           CZ=COSINE OF SOLAR ZENITH ANGLE
C           TP(I)=TEMPERATURE
C           SEC=OPTICAL AIRMASS
C           RI=SOLAR RADIATION AT TOP OF ATMOS.
C           RC=SHORTWAVE RADIATION AT GROUND
C           R(NUM)=NET RADIATION AT GROUND
C           H(NUM)=MIXING HEIGHT
C           TMXH=TIME OF MAXIMUM MIXING HEIGHT
C           HMAX=MAXIMUM MIXING HEIGHT
C           A=ENERGY-AREA TRANSFORMATION
C           ASUM=SUMMATION OF AREA(A)
C           DT=TEMP DIFFERENCE (BASE OF ENERGY TRIANGLE)
C           AHMX=CORRECTED MIXING HEIGHT FROM UPPER-AIR TEST
C
C  **MAIN DO-LOOP OF THE MODEL BEGINS HERE**
C
```

```
      DO 32 I=1,18
      IF(NUM.EQ.1) GO TO 13
      HF=H(NUM-1)
13    IF(I.GT.1) GO TO 14
      T=TSR
      GO TO 15
14    T=FLOAT(LT+I-2)
15    APT=T-TCOR/60.
      CZ=(SIN(RLAT)*SIN(RD(MONTH,NDAY))-COS(RLAT)*COS(RD(MONTH,NDAY))*C
     *OS(W*APT))
      IF(T.GE.9.) GO TO 16
      IL=1
      GO TO 20
16    IF(T.GE.12.) GO TO 17
      IL=2
      GO TO 20
17    IF(T.GE.15.) GO TO 18
      IL=3
      GO TO 20
18    IF(T.GE.18.) GO TO 19
      IL=4
      GO TO 20
19    IL=5
20    CONTINUE
      IF(T.GE.TMAX) GO TO 22
      IF(I.GT.1) GO TO 21
      TP(I)=S7
      GO TO 23
21    JST=IFIX(TSR)
      ARG=4.7+3.2/(TMAX-FLOAT(JST))*FLOAT(I-1)
      TP(I)=CONST+.5*AMP*SIN(ARG)
      T16=TP(I)
      GO TO 23
22    TP(I)=S8
23    CONTINUE
      SEC=1./CZ
      IF(SEC.LE.5.76) GO TO 24
      SEC=5.76
24    RI=S*CZ*(Q**SEC)
      IF(RI.GT.0.) GO TO 25
      RI=0.
25    CONTINUE
      RC=(1.-AB(IL,1))*(1.-AB(IL,2))*(1.-AB(IL,3))*RI
      RIS(NUM)=RC
      TEMP=.56*(TP(I)-32.)
      R(NUM)=(1.-ABO)*RC+(F1*TEMP+F2)*4.186
      IF(R(NUM).GT.0.) GO TO 27
      IF(T.LT.TMAX) GO TO 27
      GO TO(26,27),INT
26    TMXH=T-1.
      HMAX=H(NUM-1)
      INT=INT+1
27    CONTINUE
      ZM=(Z+2.*SD(5))/2.
      PM=1013.25-.11*ZM
      A=7.09*R(NUM)/PM
      IF(A.GT.0.) GO TO 28
      IF(T.LT.12.) GO TO 29
28    ASUM=ASUM+A
      FTP=TP(I)
      FSD=S7
      DT=ABS(FTP-FSD)
      IF(DT.EQ.0.) GO TO 29
```

```
      SC=(2.*ASUM)/(DT*SIN(THETA))
      SA=SQRT(SC**2+DT**2-2.*SC*DT*COS(THETA))
      PHI=ARCOS(((SA**2)+(DT**2)-(SC**2))/(2.0*SA*DT))
      H(NUM)=2104.*SA*SIN(PHI)
      Z=H(NUM)
      IF(H(NUM).GE.0.) GO TO 30
      H(NUM)=0.
      Z=H(NUM)
      GO TO 30
   29 H(NUM)=HF
   30 TIME(NUM)=T
      HMX=H(NUM)
      CALL TEST(T,TEMP,HMX,AHMX)
      IF(AHMX.LE.0.0) GO TO 31
      H(NUM)=AHMX
   31 CONTINUE
      IF(T.GE.21.) GO TO 33
      NUM=NUM+1
   32 CONTINUE
C
C  **END OF THE MAIN DO-LOOP**
C
   33 WRITE(6,34)
   34 FORMAT('0',1X,'TIME ',4X,'NET RADIATION ',4X,'SOLAR RADIATION',4X,
     *'MIXING HEIGHT'/' ',1X,'(LST)',5X,'(J/M X10 )',9X,'(J/M X10 )',12X
     *,'(M)')
      JN=NUM-1
      NUM=JN
      DO 36 IT=1,NUM
      WRITE(6,35) TIME(IT),R(IT),RIS(IT),H(IT)
   35 FORMAT('0',1X,F5.2,6X,F6.0,14X,F5.0,14X,F5.0)
   36 CONTINUE
      WRITE(6,37) HMAX,TMXH
   37 FORMAT('-',' MAXIMUM MIXING HEIGHT  ',F5.0,'(M)','OCCURRED AT   ',
     *F5.2,'(LST)')
      STOP
      END
      SUBROUTINE TEST(T,TEMP,H,AH)
      DIMENSION UPT(4),UPH(4),SD(8)
      COMMON UPT,UPH,SD
      DLP=-0.0085
      AH=0.0
      RT8=(UPT(2)-UPT(1))/12.0
      RH8=(UPH(2)-UPH(1))/12.0
      RT7=(UPT(4)-UPT(3))/12.0
      RH7=(UPH(4)-UPH(3))/12.0
      TOP=TEMP-0.0098*H
      T85=UPT(1)+(RT8*(T-5.0))
      H85=(UPH(1)+(RH8*(T-5.0)))-SD(5)
      IF(H.GE.H85) GO TO 1
      UPLPS=(T85-TOP)/(H85-H)
      IF(UPLPS.GE.DLP) GO TO 2
      AH=H85
    1 T70=UPT(3)+(RT7*(T-5.0))
      H70=(UPH(3)+(RH7*(T-5.0)))-SD(5)
      IF(H.GE.H70) GO TO 2
      UPLPS=(T70-T85)/(H70-H85)
      IF(UPLPS.GE.DLP) GO TO 2
      AH=H70
    2 CONTINUE
      RETURN
      END
```

APPENDIX D

OBSERVED AND CALCULATED MIXING HEIGHTS

Values of observed and calculated mixing heights are given in Tables D1 - D4. Included in the tables are the results from the present model (model A), Holzworth's model (model B) and the numerical model (model C) at times corresponding to the observed mixing heights.

Table D-1. March Mixing Heights

Month: March			Location: Fort McMurray		
Date	Time(LST)	Observed Heights(m)	Model A Heights(m)	Model B Heights(m)	Model C Heights(m)
04	0735	0	0	0	0
	1100	50	260	100	0
	1300	740	311	280	1782
	1500	770	1150	310	1787
05	0830	0	68	0	0
	0930	0	181	50	1746
	1100	1280	279	310	1754
	1300	1600	1113	490	1765
	1500	1600	1126	900	2500
06	0930	1200	500	700	1832
	1100	1800	652	1200	2500
	1300	1800	743	1350	2500
09	0930	120	114	200	0
	1030	200	177	260	0
	1100	0	204	290	2500
	1345	400	310	590	2500
10	0930	100	200	0	0
	1100	200	310	160	1017
	1300	600	401	330	2500
11	0830	0	68	0	0
	0930	200	170	20	0
	1100	500	276	80	547
	1300	1600	378	530	2500

Table D-1. March Mixing Heights cont'd.

Date	Time(LST)	Observed Heights(m)	Model A Heights(m)	Model B Heights(m)	Model C Heights(m)
12	0830	110	0	0	0
	0930	400	20	0	2500
	1058	1100	72	200	2500
	1300	1240	380	380	2500
	1500	1600	1108	440	2500
14	0930	220	105	0	0
	1100	200	174	260	2500
	1300	220	248	375	2500
	1500	1600	282	700	2500
15	0930	90	200	0	0
	1100	140	309	150	0
	1300	1600	382	450	2500
16	0930	0	275	0	0
	1100	0	364	180	0
	1300	0	463	590	2500
17	0930	210	495	210	0
	1100	0	694	640	463
	1315	620	694	640	463

Table D-2. August Mixing Heights

Month: August Location: Fort McMurray

Date	Time (LST)	Observed Heights (m)	Model A Heights (m)	Model B Heights (m)	Model C Heights (m)
14	0605	0	0	50	0
	0936	297	454	250	>2600
	1304	807	1098	1060	>2600
	1435	935	1098	1250	>2600
	1802	>2550	1150	1330	>2600
15	0605	0	0	30	0
	0938	213	420	190	0
	1301	680	834	670	>2600
	1800	1700	1201	1020	>2600
16	0609	0	0	0	0
	0927	977	674	220	>2700
	1254	1105	1193	470	>2700
	1427	1600	1375	800	>2700
	1801	>2550	1545	960	>2700
17	0610	595	0	0	>2600
	0928	807	345	120	>2600
	1255	1105	997	700	>2600
	1425	>2550	1011	1040	>2600
	1806	1063	1127	1080	>2600
18	0601	680	0	0	>2600
	0928	638	367	150	>2600
	1258	680	879	730	>2600
	1425	1090	1061	790	>2600
	1759	2210	1172	810	>2600
19	0608	0	0	0	0
	0931	297	673	150	>2600
	1256	2040	1074	520	>2600
	1420	1190	1242	1350	>2600
	1811	1360	1424	1520	>2600
20	0613	0	0	0	0
	0943	127	291	120	>2600
	1313	>2550	1030	650	>2600
	1444	1402	1036	1150	>2600
	1805	>2550	1046	1520	>2600
21	0616	127	0	0	0
	0943	297	502	170	>2700
	1316	765	1118	690	>2700
	1441	>2550	1125	1030	>2700
	1801	>2550	1136	1550	>2700

Table D-3. September Mixing Heights

Month: September Location: Fort McMurray

Date	Time(LST)	Observed Heights(m)	Model A Heights(m)	Model B Heights(m)	Model C Heights(m)
23	0730	0	90	30	0
	1039	213	346	310	1129
	1342	297	450	870	1135
	1427	297	476	1010	1136
	1807	127	467	1060	>2700
24	0725	0	75	60	578
	1043	170	450	350	>2700
	1338	340	558	710	>2700
	1437	425	595	800	>2700
	1811	850	575	840	>2700
25	0728	0	190	0	0
	1050	255	718	200	576
	1350	722	800	500	578
	1431	1275	900	520	>2700
	1810	977	1024	520	>2700
26	0716	127	75	0	0
	1056	127	378	340	569
	1355	1275	1130	>1200	>2700
	1440	1063	1130	>1200	>2700
	1807	1317	1122	>1200	>2700
27	0748	0	75	0	0
	1057	510	318	360	0
	1330	722	738	870	>2700
	1430	850	1081	>1200	>2700
	1752	>2550	1081	>1200	>2700
28	0734	0	45	0	0
	1104	170	375	500	>2700
	1341	255	875	>1200	>2700
	1735	>2550	1080	>1200	>2700
	1812	>2550	1080	>1200	>2700
29	0754	765	0	0	>2600
	1109	807	1024	650	>2600
	1353	1530	1025	>1500	>2600
	1807	1105	1025	>1500	>2600
30	0756	0	153	1180	0
	1102	510	517	1820	>2600
	1354	1063	1054	>2000	>2600
	1445	1400	1055	>2000	>2600
	1808	>2550	1060	>2000	>2600

Table D-4. November Mixing Heights

Month: November Location: Edmonton

Date	Time(LST)	Observed Heights(m)	Model A Heights(m)	Model B Heights(m)	Model C Heights(m)
22	0700	0	0	0	0
	0800	0	0	30	0
	0930	36	51	40	0
	1100	84	174	68	0
23	0800	0	0	0	0
	0930	0	64	40	0
	1100	44	196	100	0
	1230	116	260	256	0
	1400	260	291	800	Undefined
26	0800	0	0	0	0
	0930	0	86	0	0
	1100	212	292	64	270
	1400	486	437	520	275
27	0800	0	0	0	0
	0930	20	13	0	0
	1100	160	68	60	0
	1230	152	127	144	0
	1400	264	147	220	Undefined
28	0800	0	0	0	0
	0930	28	45	0	0
	1100	80	147	32	0
	1230	140	187	108	0
	1400	220	205	176	0
29	0800	0	0	0	0
	0930	90	54	54	0
	1100	124	190	132	0
	1230	150	218	164	0
	1400	168	227	228	0
30	0810	0	0	0	0
	0930	88	68	0	0
	1100	132	247	20	0
	1230	120	232	108	0

APPENDIX E

MINISONDE DATA

Table E-1. March Data - Fort McMurray

DATE: March 04/76 Location: Lower Syncrude

Time(LST)	0735		1100		1300		1500	
Level	Height (M)	Temp (C)	Height (M)	Temp (C)	Height (M)	Temp (C)	Height (M)	Temp (C)
0	243	-32.3	244	-28.3	242	-20.7	242	-16.4
1	271	-30.4	286	-28.7	292	-21.2	286	-16.7
2	300	-23.8	328	-28.2	343	-21.8	330	-17.4
3	329	-26.9	369	-26.6	387	-21.6	383	-17.9
4	357	-24.6	411	-25.7	431	-21.9	436	-18.8
5	386	-22.7	451	-24.6	475	-22.5	489	-19.4
6	415	-22.0	491	-22.6	519	-23.5	541	-20.1
7	457	-22.1	531	-20.6	563	-24.1	584	-20.5
8	500	-22.2	571	-19.5	607	-24.8	628	-21.0
9	526	-21.5	601	-19.1	654	-25.3	672	-21.3
10	552	-18.4	630	-19.5	700	-26.0	715	-22.0
11	578	-17.8	687	-20.2	747	-25.8	759	-22.5
12	604	-17.8	743	-20.7	793	-26.0	803	-23.1
13	603	-17.7	789	-21.2	840	-26.1	844	-23.3
14	656	-17.6	835	-21.8	886	-26.8	885	-23.9
15	681	-17.7	880	-22.2	930	-27.4	926	-24.5
16	707	-17.8	925	-22.6	973	-27.8	968	-24.7
17	733	-17.7	972	-23.1	1017	-26.9	1009	-24.9
18	759	-17.8	1019	-23.5	1060	-26.1	1050	-24.7
19	785	-17.9	1058	-23.9	1104	-26.3	1091	-24.1
20	811	-18.1	1097	-23.7	1148	-26.8	1133	-24.5
21	837	-18.2	1136	-22.8	1193	-26.4	1174	-24.5
22	863	-18.2	1175	-21.9	1239	-27.2	1215	-24.7
23	889	-18.2	1213	-21.3	1285	-27.6	1253	-24.8
24	915	-18.3	1251	-21.6	1330	-28.4	1290	-25.0
25	941	-18.4	1289	-21.9	1374	-27.4	1328	-25.3
26	967	-18.7	1326	-21.9	1419	-26.7	1365	-25.5
27	993	-18.9	1364	-21.0	1463	-26.9	1408	-26.1
28	1019	-19.1	1402	-20.5	1507	-27.4	1450	-26.5
29	1045	-19.4	1440	-20.4	1553	-27.9	1503	-26.7
30	1071	-19.5	1477	-20.6	1599	-28.0	1555	-26.8
31	1097	-19.8	1513	-20.8	1647	-28.5	1613	-27.1
32	1123	-19.6	1548	-21.3	1694	-28.5	1672	-27.7
33	1149	-19.6	1583	-22.1	1742	-27.4	1733	-27.9

Table E-1. March Data - Fort McMurray cont'd.

Time(LST)	0735		1100		1300		1500	
Level	Height (M)	Temp (C)	Height (M)	Temp (C)	Height (M)	Temp (C)	Height (M)	Temp (C)
34	1175	-19.7	1618	-22.9	1789	-27.3	1793	-27.4
35	1204	-19.9	1661	-23.2	1837	-27.4	1828	-26.9
36	1234	-20.0	1704	-23.5	1884	-27.8	1863	-27.0
37	1264	-20.2	1768	-23.1	1928	-27.9	1898	-27.3
38	1294	-20.4	1832	-22.7	1972	-28.3	1934	-27.3
39	1324	-20.6	1896	-22.5	2026	-28.6	1969	-27.3
40	1353	-20.5	1960	-23.1	2080	-29.3	2004	-26.8
41	1383	-20.4						
42	1413	-20.2						
43	1443	-19.9						
44	1472	-19.8						

Table E-2. March Data - Fort McMurray

DATE: March 05/76 Location: Lower Syncrude

Time (LST)	0830		0930		1100		1300		1500	
Level	Hgt (M)	Temp (C)	Hgt (M)	Temp (C)	Hgt (M)	Temp (C)	Hgt (M)	Temp (C)	Hgt (M)	Temp (C)
0	242	- 7.0	237	- 5.1	239	- 2.6	237	- 0.5	237	- 1.2
1	306	- 6.0	286	- 4.7	301	- 2.9	286	- 0.6	287	- 1.5
2	371	- 5.9	334	- 4.8	363	- 3.3	335	- 1.1	336	- 2.1
3	428	- 6.2	422	- 4.8	420	- 3.8	389	- 1.6	393	- 3.3
4	486	- 6.5	510	- 5.3	477	- 4.5	442	- 2.3	450	- 3.9
5	560	- 7.0	575	- 5.7	525	- 4.8	492	- 2.9	514	- 4.7
6	635	- 7.3	641	- 6.3	573	- 5.3	543	- 3.4	578	- 5.6
7	670	- 7.2	707	- 7.0	621	- 5.7	592	- 3.9	645	- 6.4
8	705	- 6.2	773	- 7.8	668	- 6.2	642	- 4.5	712	- 7.5
9	752	- 5.7	829	- 8.1	714	- 6.4	692	- 5.0	761	- 8.0
10	799	- 6.1	886	- 8.6	761	- 6.8	742	- 5.6	810	- 8.4
11	846	- 6.6	942	- 9.2	805	- 7.2	791	- 6.1	861	- 9.1
12	893	- 7.1	999	- 9.6	849	- 7.7	841	- 6.6	912	- 9.8
13	940	- 7.5	1056	- 9.9	893	- 8.1	891	- 7.2	963	-10.4
14	987	- 7.9	1112	-10.4	937	- 8.5	941	- 7.9	1014	-10.9
15	1034	- 8.3	1162	-10.8	981	- 9.0	979	- 8.5	1065	-11.4
16	1081	- 8.7	1213	-11.2	1025	- 9.5	1017	- 9.0	1115	-11.9
17	1129	- 8.5	1263	-11.3	1069	-10.1	1055	- 9.4	1166	-12.4
18	1176	- 7.5	1313	-11.7	1113	-10.5	1093	- 9.9	1217	-12.7
19	1223	- 7.0	1363	-12.1	1157	-11.0	1131	-10.6	1268	-13.6
20	1270	- 6.4	1413	-12.5	1201	-11.5	1169	-11.1	1319	-14.3
21	1317	- 6.2	1464	-12.9	1245	-12.2	1210	-11.7	1370	-14.9
22	1364	- 6.6	1514	-13.1	1289	-12.7	1250	-12.3	1420	-15.0
23	1411	- 7.0	1573	-13.2	1333	-13.3	1290	-12.9	1471	-15.8
24	1458	- 7.6	1632	-13.7	1377	-13.7	1331	-13.5	1522	-16.6
25	1505	- 8.2	1691	-14.2	1421	-14.1	1353	-14.1	1573	-17.3
26	1553	- 8.6	1750	-14.6	1465	-14.6	1376	-14.7	1624	-17.8
27	1600	- 9.1	1809	-14.4	1509	-15.3	1399	-15.1	1675	-18.4
28	1647	- 9.7	1869	-14.5	1554	-15.0	1421	-15.7	1725	-18.4
29	1694	-10.2	1928	-14.6	1598	-14.6	1444	-15.9	1776	-18.8
30	1741	-10.8	1987	-14.1	1642	-14.3	1466	-16.7	1827	-19.3
31	1788	-11.1	2046	-14.2	1686	-14.4	1489	-17.1	1878	-19.1
32	1835	-11.7	2105	-14.8	1730	-14.5	1511	-17.7	1929	-18.6
33	1882	-12.1	2164	-15.3	1777	-14.7	1552	-18.3	1980	-18.7
34	1929	-12.7	2223	-15.4	1824	-15.1	1594	-18.7	2030	-18.3
35	1978	-13.6	2282	-14.7	1872	-15.7	1635	-19.1	2081	-18.1
36	2026	-14.2	2342	-13.5	1919	-16.1	1676	-19.2	2132	-18.3
37	2075	-14.6	2401	-13.3	1966	-16.7	1717	-19.5	2183	-18.7
38			2460	-13.6	2013	-17.1	1758	-19.8	2234	-19.3
39			2519	-13.9	2061	-17.6	1799	-19.9	2288	-19.7
40			2578	-14.1	2108	-18.1	1840	-20.5	2343	-20.3

Table E-2. March Data - Fort McMurray cont'd.

Time (LST)	0830		0930		1100		1300		1500	
Level	Hgt (M)	Temp (C)	Hgt (M)	Temp (C)	Hgt (M)	Temp (C)	Hgt (M)	Temp (C)	Hgt (M)	Temp (C)
41			2637	-14.1						
42			2696	-14.3						

Table E-3. March Data - Fort McMurray

DATE: March 06/76 Location: GCOS

Time(LST)	0930		1100		1300	
Level	Height (M)	Temp (C)	Height (M)	Temp (C)	Height (M)	Temp (C)
0	317	-12.3	307	- 7.8	318	- 5.0
1	351	-12.5	354	- 8.8	355	- 5.3
2	384	-12.9	401	- 9.0	391	- 5.6
3	433	-12.9	448	- 9.3	420	- 5.9
4	482	-13.3	496	- 9.7	450	- 6.4
5	523	-13.5	543	-10.1	488	- 6.6
6	563	-13.7	590	-10.7	526	- 6.9
7	584	-14.1	637	-11.1	564	- 7.2
8	605	-14.2	685	-11.6	602	- 7.5
9	635	-14.3	732	-11.9	641	- 7.7
10	665	-14.3	779	-12.3	680	- 8.1
11	695	-14.6	826	-12.5	725	- 8.6
12	725	-14.8	874	-12.8	771	- 8.9
13	755	-15.1	921	-13.0	824	- 9.4
14	785	-15.4	968	-13.4	877	- 9.8
15	815	-15.8	1015	-13.5	932	-10.3
16	845	-16.0	1062	-13.9	987	-10.8
17	875	-16.3	1110	-13.7	1042	-11.1
18	905	-16.6	1157	-13.9	1097	-11.8
19	935	-16.6	1204	-14.0	1153	-12.3
20	965	-16.7	1251	-14.0	1208	-12.6
21	995	-16.7	1299	-14.2	1263	-12.4
22	1025	-16.8	1346	-14.3	1318	-12.8
23	1055	-16.9	1393	-14.4	1373	-13.2
24	1085	-17.1	1440	-14.5	1429	-13.7
25	1115	-17.3	1483	-14.5	1484	-13.7
26	1145	-17.6	1535	-14.6	1539	-13.9
27	1175	-17.9	1582	-14.8	1587	-14.0
28	1205	-18.1	1629	-14.9	1683	-14.4
29	1235	-18.4	1677	-15.1	1731	-14.7
30	1265	-18.8	1724	-15.2	1769	-15.1
31	1295	-18.8	1771	-15.5	1806	-15.3
32	1325	-18.9	1818	-15.7	1844	-15.3
33	1355	-18.9	1866	-16.0	1881	-15.6
34	1385	-18.9	1913	-16.2	1919	-15.7
35	1415	-19.3	1960	-16.3	1956	-16.1
36	1445	-19.4	2007	-16.7	1994	-16.4
37	1475	-19.5	2055	-17.0	2032	-16.6
38	1505	-19.9	2102	-17.2	2069	-16.8
39	1535	-20.0			2107	-17.0
40	1565	-19.6			2152	-17.1

Table E-3. March Data - Fort McMurray cont'd.

Time(LST)	0930		1100		1300	
Level	Height (M)	Temp (C)	Height (M)	Temp (C)	Height (M)	Temp (C)
41	1595	-19.0			2197	-17.2
42	1625	-18.7			2243	-17.5
43	1665	-18.6			2288	-17.7
44	1685	-18.9			2333	-17.8
45	1717	-19.3			2379	-17.8
46	1750	-19.4			2424	-17.8
47	1782	-19.7			2469	-17.8
48	1814	-19.6			2515	-18.0
49	1847	-20.3			2560	-18.1
50	1879	-20.3			2649	-18.3
51	1911	-20.6			2738	-18.6
52	1943	-20.7			2827	-18.8
53	1976	-20.8			2916	-19.2
54	2008	-21.1			3006	-19.4
55	2040	-21.0			3095	-19.6
56	2073	-21.3			3184	-19.8

Table E-4. March Data - Fort McMurray

DATE: March 09/76 Location: GCOS

Time(LST)	0930		1030		1100		1345	
Level	Height (M)	Temp (C)	Height (M)	Temp (C)	Height (M)	Temp (C)	Height (M)	Temp (C)
0	320	-17.8	321	-14.8	324	-15.6	323	- 9.4
1	357	-18.9	365	-15.4	363	-14.7	355	- 9.2
2	394	-19.4	409	-16.1	402	-14.3	386	- 9.5
3	433	-19.4	446	-16.5	438	-14.6	418	- 9.5
4	472	-18.9	483	-16.7	474	-15.1	449	- 9.5
5	511	-18.0	515	-16.2	509	-15.4	481	- 9.5
6	551	-17.7	548	-16.1	544	-15.0	513	- 9.9
7	590	-16.0	581	-16.2	573	-14.7	545	-10.0
8	629	-13.1	614	-15.4	603	-14.7	577	-10.9
9	664	-12.1	647	-14.3	633	-14.9	610	-10.8
10	699	-11.6	680	-13.3	663	-14.9	643	-11.2
11	734	-11.8	717	-12.8	693	-14.8	680	-11.3
12	769	-11.9	753	-12.7	722	-14.3	717	-12.4
13	803	-12.4	794	-13.1	752	-13.4	754	-12.3
14	838	-12.9	835	-13.6	782	-13.1	791	-12.1
15	872	-12.8	876	-13.4	812	-13.0	828	-12.1
16	906	-11.4	917	-12.0	842	-13.1	864	-12.3
17	941	-10.9	958	-11.2	872	-13.2	901	-12.3
18	975	-10.4	999	-11.1	901	-12.0	938	-12.2
19	1009	- 9.8	1032	-11.1	931	-10.9	974	-12.0
20	1043	- 9.6	1066	-11.2	961	-10.5	1011	-11.6
21	1078	- 9.8	1099	-11.5	991	-10.2	1047	-11.6
22	1112	- 9.8	1131	-11.8	1021	-10.5	1084	-12.1
23	1146	-10.2	1162	-12.1	1050	-10.7	1120	-12.2
24	1181	-10.6	1192	-12.6	1080	-11.1	1157	-12.7
25	1215	-11.0	1222	-13.1	1110	-11.5	1191	-13.1
26	1249	-11.6	1252	-13.5	1140	-12.0	1225	-13.7
27	1284	-12.2	1282	-13.8	1170	-12.3	1254	-14.1
28	1318	-12.9	1311	-14.1	1199	-12.7	1282	-14.8
29	1352	-13.2	1341	-14.5	1229	-13.1	1329	-14.9
30	1387	-13.8	1371	-14.8	1259	-13.5	1375	-16.0
31	1421	-14.3	1397	-15.0	1289	-13.9	1422	-16.1
32	1455	-14.8	1424	-15.2	1319	-14.4	1469	-16.9
33	1490	-15.3	1451	-15.5	1348	-14.9	1516	-17.1
34	1524	-15.8	1477	-15.9	1370	-15.3	1563	-17.9
35	1558	-16.0	1504	-16.3	1408	-15.9	1616	-18.2
36	1592	-16.6	1530	-16.6	1438	-16.4	1668	-19.1
37	1626	-17.2	1557	-17.1	1468	-16.8	1721	-19.4
38	1660	-17.9	1584	-17.5	1497	-17.2		
39	1693	-18.1	1610	-17.9	1527	-17.4		
40	1727	-18.8	1637	-18.4	1557	-18.2		

Table E-4. March Data - Fort McMurray cont'd.

Time(LST)	0930		1030		1100		1345	
Level	Height (M)	Temp (C)	Height (M)	Temp (C)	Height (M)	Temp (C)	Height (M)	Temp (C)
41	1761	-19.3			1588	-18.8		
42	1795	-19.8			1620	-19.4		
43	1829	-20.4			1651	-19.8		
44	1863	-21.1			1683	-20.7		
45					1714	-20.8		
46					1746	-21.4		
47					1777	-21.9		
48					1808	-22.4		
49					1840	-23.1		
50					1871	-23.7		
51					1903	-24.1		
52					1934	-24.7		

Table E-5. March Data - Fort McMurray

DATE: March 10/76 Location: GCOS

Time(LST)	0934		1100		1300	
Level	Height (M)	Temp (C)	Height (M)	Temp (C)	Height (M)	Temp (C)
0	368	-17.7	322	-14.9	320	- 9.4
1	380	-18.2	353	-16.2	349	-10.8
2	393	-18.8	384	-15.6	379	-11.4
3	425	-18.8	415	-15.1	410	-11.6
4	456	-17.9	447	-15.1	441	-11.9
5	487	-17.1	474	-15.5	473	-12.0
6	519	-16.4	501	-15.8	505	-12.4
7	549	-15.5	528	-15.6	538	-12.6
8	580	-15.4	554	-15.1	570	-12.7
9	610	-15.6	587	-14.3	602	-13.2
10	640	-14.6	619	-14.5	633	-13.5
11	670	-13.3	651	-13.9	665	-14.0
12	700	-13.2	683	-14.2	697	-14.5
13	731	-13.7	716	-14.6	724	-14.7
14	763	-14.7	748	-15.1	751	-14.9
15	795	-15.4	778	-15.7	778	-15.1
16	826	-15.8	808	-16.1	806	-15.2
17			838	-16.5	833	-15.7
18			869	-16.6	860	-16.0
19			899	-16.6	887	-16.0
20			930	-16.6	914	-16.2
21			960	-16.6	943	-15.9
22			990	-16.7	973	-15.3
23			1021	-16.7	1004	-15.1
24			1051	-16.4	1036	-15.0
25			1082	-15.3	1068	-15.2
26			1112	-14.4	1099	-15.5
27			1142	-14.5	1131	-15.6
28			1173	-14.5	1163	-15.9
29			1203	-14.4	1194	-15.8
30			1234	-14.3	1226	-16.2
31			1264	-14.5	1258	-15.8
32			1294	-14.3	1289	-16.1
33			1325	-15.0	1321	-16.3
34			1355	-15.1	1353	-16.7
35			1386	-15.1	1384	-17.0
36			1416	-15.5	1416	-17.4
37			1446	-15.9	1448	-17.7
38			1477	-16.2	1480	-17.6
39			1507	-16.5	1511	-18.3
40			1538	-16.9	1543	-18.3

Table E-5. March Data - Fort McMurray cont'd.

Time(LST)	0934		1100		1300	
Level	Height (M)	Temp (C)	Height (M)	Temp (C)	Height (M)	Temp (C)
41					1575	-18.6
42					1606	-18.8
43					1638	-18.9
44					1670	-19.4

Table E-6. March Data - Fort McMurray

DATE: March 11/76 Location: GCOS

Time(LST)	0826		0931		1100		1300	
Level	Height (M)	Temp (C)	Height (M)	Temp (C)	Height (M)	Temp (C)	Height (M)	Temp (C)
0	322	-18.2	319	-11.6	321	- 9.6	320	- 5.1
1	360	-14.0	362	-12.2	360	- 9.6	363	- 5.0
2	397	-12.9	404	-12.9	399	-10.2	405	- 5.4
3	435	-12.9	431	-13.0	438	-10.5	448	- 5.9
4	473	-13.0	457	-13.3	477	-11.0	491	- 6.4
5	510	-12.8	487	-13.4	489	-11.4	534	- 6.8
6	548	-13.1	516	-13.6	502	-11.8	578	- 7.6
7	581	-13.0	545	-13.8	540	-12.1	622	- 8.2
8	615	-13.2	575	-13.7	578	-12.9	665	- 8.8
9	648	-13.7	604	-13.7	616	-13.3	702	- 9.2
10	682	-13.1	634	-13.6	654	-14.1	738	- 9.6
11	715	-12.8	663	-13.7	689	-14.4	774	-10.0
12	749	-12.8	692	-13.7	725	-14.9	810	-10.2
13	783	-13.1	722	-13.8	755	-15.5	844	-10.3
14	816	-13.0	751	-14.2	786	-16.1	877	-10.9
15	852	-12.5	781	-14.4	816	-16.5	908	-10.9
16	887	-12.6	810	-14.7	847	-16.4	939	-11.2
17	923	-12.5	840	-14.6	877	-15.8	970	-11.2
18	959	-12.8	869	-14.8	908	-15.9	1001	-11.6
19	995	-12.7	898	-14.6	938	-15.8	1029	-11.7
20	1030	-13.1	928	-14.8	969	-16.1	1058	-11.8
21	1066	-13.2	957	-15.1	998	-16.4	1079	-11.9
22	1102	-13.1	986	-15.4	1027	-16.6	1100	-12.0
23	1137	-13.1	1015	-15.3	1057	-16.8	1121	-12.2
24	1173	-13.4	1044	-15.4	1086	-17.0	1142	-12.6
25	1209	-13.7	1073	-15.1	1115	-17.0	1170	-12.6
26	1244	-14.0	1102	-14.8	1145	-16.0	1199	-12.8
27	1280	-14.4	1131	-14.7	1172	-16.1	1228	-12.8
28	1316	-14.8	1160	-14.4	1200	-16.2	1256	-12.6
29	1351	-15.2	1189	-14.1	1227	-16.1	1285	-12.7
30	1387	-15.5	1218	-14.2	1255	-16.6	1313	-12.9
31	1423	-15.9	1247	-14.2	1283	-16.7	1342	-13.1
32	1459	-16.3	1276	-14.5	1310	-17.2	1371	-13.4
33	1494	-16.6	1305	-14.8	1338	-17.5	1399	-13.8
34	1530	-17.1	1334	-15.0	1365	-17.9	1428	-14.1
35	1566	-17.5	1363	-15.3	1393	-17.9	1461	-14.5
36	1601	-17.9	1392	-15.6	1421	-18.5	1495	-14.8
37	1637	-18.3	1421	-15.9	1448	-18.8	1529	-15.2
38	1673	-18.7	1450	-16.4	1476	-19.2	1562	-15.6
39	1708	-19.0	1479	-16.6	1503	-19.6	1596	-16.1
40	1744	-19.7	1508	-16.9	1531	-20.1	1630	-16.6

Table E-6. March Data - Fort McMurray cont'd.

Time(LST)	0826		0931		1100		1300	
Level	Height (M)	Temp (C)	Height (M)	Temp (C)	Height (M)	Temp (C)	Height (M)	Temp (C)
41			1537	-17.2			1663	-17.1
42			1566	-17.7			1697	-17.6
43							1731	-18.1
44							1764	-18.8
45							1798	-18.2
46							1832	-19.7

Table E-7. March Data - Fort McMurray

DATE: March 12/76						Location: GCOS				
Time (LST)	0830		0930		1058		1300		1500	
Level	Hgt (M)	Temp (C)	Hgt (M)	Temp (C)	Hgt (M)	Temp (C)	Hgt (M)	Temp (C)	Hgt (M)	Temp (C)
0	324	- 6.6	320	- 6.3	319	- 2.6	321	- 2.6	321	- 1.5
1	376	- 7.1	363	- 6.9	364	- 3.5	349	- 2.6	359	- 1.9
2	428	- 7.3	407	- 7.2	410	- 4.3	376	- 2.3	396	- 2.1
3	468	- 7.3	440	- 7.5	472	- 5.0	401	- 3.4	434	- 2.6
4	509	- 7.2	472	- 7.2	534	- 5.6	427	- 3.8	471	- 2.9
5	549	- 7.3	503	- 7.3	596	- 6.4	452	- 4.1	509	- 3.3
6	589	- 7.5	534	- 7.6	659	- 7.3	477	- 4.5	548	- 3.8
7	629	- 7.7	564	- 7.6	708	- 7.8	514	- 4.8	582	- 4.2
8	669	- 7.3	595	- 7.7	757	- 8.4	550	- 5.3	617	- 4.7
9	709	- 6.9	626	- 7.9	807	- 8.8	591	- 5.8	652	- 5.1
10	749	- 6.4	657	- 8.1	856	- 9.3	633	- 6.3	687	- 5.4
11	795	- 6.4	687	- 8.2	903	- 9.6	670	- 6.8	722	- 5.8
12	842	- 6.5	718	- 8.2	951	-10.0	707	- 7.1	757	- 6.1
13	888	- 6.8	749	- 7.9	984	-10.2	745	- 7.5	792	- 6.6
14	934	- 7.1	779	- 7.7	1018	-10.0	782	- 7.9	827	- 6.9
15	980	- 7.5	810	- 7.8	1051	-10.0	819	- 8.2	862	- 7.2
16	1026	- 7.9	841	- 8.1	1085	-10.1	856	- 8.6	897	- 7.5
17	1072	- 8.3	871	- 8.6	1107	-10.3	893	- 9.1	930	- 7.9
18	1118	- 8.6	902	- 8.9	1128	-10.2	931	- 9.6	962	- 8.3
19	1165	- 8.8	929	- 9.2	1150	-10.2	968	- 9.8	994	- 8.7
20	1211	- 9.2	956	- 9.4	1171	-10.3	1005	-10.2	1026	- 9.0
21	1257	- 8.8	983	- 9.5	1204	-10.5	1042	-10.5	1058	- 9.4
22	1303	- 9.2			1237	-10.8	1080	-10.9	1090	- 9.8
23	1349	-10.1			1270	-11.1	1117	-11.1	1122	-10.1
24	1395	-10.5			1303	-11.4	1154	-11.3	1154	-10.5
25	1441	-10.8			1337	-11.7	1191	-11.6	1183	-10.8
26	1483	-11.1			1370	-11.8	1228	-12.1	1212	-11.2
27	1534	-11.4			1403	-11.8	1269	-13.0	1241	-11.5
28	1580	-11.5			1436	-12.0	1310	-13.2	1269	-11.8
29	1626	-11.7			1469	-12.1	1351	-13.1	1298	-12.2
30	1672	-12.0			1502	-11.9	1392	-13.3	1327	-12.4
31	1718	-12.3			1535	-11.7	1432	-13.3	1356	-12.8
32	1764	-12.5			1568	-11.7	1473	-13.4	1385	-13.2
33	1811	-12.6			1601	-11.8	1514	-13.5	1423	-13.5
34	1856	-12.9			1634	-11.6	1555	-13.5	1460	-13.8
35	1903	-13.1			1667	-11.8	1596	-13.5	1498	-14.3
36	1949	-13.1			1700	-12.3	1637	-13.5	1535	-14.7
37	1995	-13.1			1734	-12.7	1677	-13.8	1573	-15.8
38	2041	-13.3			1767	-13.2	1718	-13.9	1610	-15.4
39	2088	-13.5			1800	-13.7	1759	-14.0	1648	-15.5
40	2134	-13.6			1833	-14.2	1800	-14.1	1686	-15.3

Table E-7. March Data - Fort McMurray cont'd.

Time (LST)	0830		0930		1058		1300		1500	
Level	Hgt (M)	Temp (C)	Hgt (M)	Temp (C)	Hgt (M)	Temp (C)	Hgt (M)	Temp (C)	Hgt (M)	Temp (C)
41							1841	-14.2		
42							1882	-14.2		
43							1922	-14.4		
44							1963	-14.8		

Table E-8. March Data - Fort McMurray

DATE: March 14/76 Location: GCOS

Time(LST)	0930		1100		1300		1500	
Level	Height (M)	Temp (C)	Height (M)	Temp (C)	Height (M)	Temp (C)	Height (M)	Temp (C)
0	324	-16.0	324	-12.3	324	- 8.6	309	- 6.8
1	363	-16.0	352	-13.0	369	- 9.5	427	- 7.0
2	402	-16.4	379	-13.2	414	-10.3	545	- 7.4
3	441	-16.4	401	-13.7	454	-10.8	577	- 8.0
4	480	-16.5	423	-13.8	494	-11.4	608	- 8.6
5	508	-16.6	449	-14.1	534	-11.5	638	- 8.9
6	535	-16.5	475	-14.3	573	-11.2	667	- 9.1
7	568	-16.1	508	-14.3	606	-11.0	697	- 9.6
8	601	-15.3	542	-13.9	639	-10.7	726	- 9.8
9	633	-14.2	568	-12.6	672	-10.8	756	-10.1
10	666	-12.5	595	-11.6	705	-11.2	785	-10.1
11	698	-11.6	623	-13.0	738	-11.3	815	-10.3
12	703	-11.0	652	-13.4	771	-11.3	844	-10.6
13	761	-11.1	685	-13.6	799	-11.7	873	-10.7
14	792	-11.3	719	-14.0	826	-12.0	902	-10.9
15	824	-11.5	755	-14.3	866	-12.2	930	-11.1
16	855	-11.8	791	-14.6	906	-12.4	959	-11.4
17	886	-11.9	813	-14.8	941	-12.6	987	-11.6
18	917	-12.1	835	-15.0	976	-12.8	1016	-11.5
19	949	-12.4	864	-15.4	1010	-12.7	1045	-11.8
20	980	-12.5	893	-15.4	1045	-12.7	1073	-12.1
21	1011	-12.5	922	-15.5	1079	-13.0	1104	-12.4
22	1043	-12.2	952	-15.4	1114	-13.4	1135	-12.6
23	1073	-12.0	981	-15.7	1157	-13.7	1165	-12.8
24	1104	-11.7	1011	-16.1	1201	-14.1	1196	-13.0
25	1135	-11.9	1041	-16.4	1231	-14.4	1227	-13.1
26	1165	-11.8	1070	-16.7	1262	-14.7		
27	1188	-11.8	1098	-16.9	1293	-15.1		
28	1211	-12.0	1126	-16.8	1323	-15.3		
29	1255	-12.4	1154	-17.0	1354	-15.4		
30	1299	-12.9	1182	-17.2	1385	-15.6		
31	1334	-13.1	1210	-17.5	1423	-16.0		
32	1370	-13.5	1238	-17.9	1462	-16.3		
33	1417	-13.9	1266	-18.1	1500	-16.6		
34	1463	-14.3	1294	-18.4	1539	-16.5		
35	1509	-14.6	1322	-18.8	1577	-16.7		
36	1556	-15.1	1350	-19.2	1616	-16.9		
37	1602	-15.4	1378	-19.6	1654	-17.2		
38	1648	-15.8	1406	-19.9	1693	-17.5		
39	1695	-16.2	1434	-20.3	1731	-17.8		
40	1741	-16.5	1462	-20.7	1769	-18.0		

Table E-8. March Data - Fort McMurray cont'd.

Time(LST)	0930		1100		1300		1500	
Level	Height (M)	Temp (C)	Height (M)	Temp (C)	Height (M)	Temp (C)	Height (M)	Temp (C)
41			1490	-21.0				
42			1518	-21.2				
43			1546	-21.4				
44			1575	-21.8				

Table E-9. March Data - Fort McMurray

DATE: March 15/76				Location: GCOS		
Time(LST)	0930		1100		1300	
Level	Height (M)	Temp (C)	Height (M)	Temp (C)	Height (M)	Temp (C)
0	320	-15.0	320	-11.2	322	- 7.0
1	360	-15.3	353	-11.0	365	- 7.6
2	400	-15.6	387	-11.3	409	- 7.8
3	440	-14.1	421	-11.5	452	- 8.2
4	480	-12.8	454	-11.7	496	- 8.0
5	519	-12.6	488	-11.6	539	- 8.0
6	559	-12.7	521	-11.3	582	- 8.2
7	580	-12.8	555	-10.6	626	- 8.6
8	602	-12.5	589	-10.4	669	- 8.3
9	633	-12.4	622	-10.3	713	- 8.5
10	663	-12.3			756	- 8.6
11	694	-12.1			800	- 8.7
12	725	-11.7			843	- 8.8
13	755	-10.0			887	- 8.9
14	786	-10.2			930	- 9.2
15	817	-10.2			974	- 9.3
16	848	-10.3			1017	- 9.5
17	876	-10.4			1061	- 9.7
18	904	-10.6			1104	-10.1
19	923	-10.7			1148	-10.4
20	941	-10.9			1191	-10.7
21	990	-11.2			1235	-10.9
22	1040	-11.4			1278	-11.0
23	1062	-11.7			1322	-11.1
24	1085	-12.0			1365	-11.4
25	1129	-12.3			1409	-11.5
26	1173	-12.4			1452	-11.7
27	1205	-12.7			1496	-11.9
28	1236	-12.8			1539	-12.0
29	1268	-13.2			1583	-12.3
30	1300	-13.4			1626	-12.6
31	1331	-13.7			1670	-12.9
32	1363	-13.9			1713	-13.1
33	1395	-14.2			1757	-13.4
34	1426	-14.4			1800	-13.5
35	1458	-14.7			1844	-13.7
36	1490	-14.8			1887	-14.0
37	1521	-15.0			1930	-14.3
38	1553	-15.4			1974	-14.7
39	1587	-15.6			2017	-14.9
40	1620	-15.8			2061	-14.8

Table E-9. March Data - Fort McMurray cont'd.

Time(LST)	0930		1100		1300	
Level	Height (M)	Temp (C)	Height (M)	Temp (C)	Height (M)	Temp (C)
41	1654	-16.0			2104	-14.9
42	1688	-16.2			2148	-15.0
43	1722	-15.5			2191	-15.1
44	1755	-15.5			2235	-15.6
45	1789	-16.6			2278	-15.9
46	1823	-16.7			2322	-16.3
47	1856	-16.9			2365	-16.4
48	1890	-17.0			2409	-16.7
49	1924	-17.3			2452	-16.9
50	1958	-17.6			2496	-17.2
51	1991	-17.8			2539	-17.4
52	2025	-17.9			2583	-17.4
53	2059	-18.1			2626	-17.8
54	2092	-18.2			2670	-17.9
55	2126	-18.6			2713	-18.1
56	2160	-18.8			2757	-18.3
57	2194	-19.0			2800	-18.6
58	2227	-19.2			2844	-18.8
59	2261	-19.4			2887	-19.0
60	2295	-19.6			2931	-19.2

Table E-10. March Data - Fort McMurray

DATE: March 16/76				Location: GCOS		
Time(LST)	0930		1100		1300	
Level	Height (M)	Temp (C)	Height (M)	Temp (C)	Height (M)	Temp (C)
0	321	- 7.8	318	- 4.6	318	0.0
1	371	- 7.6	361	- 4.8	358	- 0.2
2	421	- 7.5	403	- 4.3	397	- 0.1
3	458	- 7.7	445	- 4.0	433	- 0.1
4	494	- 6.8	487	- 3.7	469	- 0.1
5	524	- 4.8	530	- 3.8	499	0.0
6	553	- 4.3	572	- 3.4	529	0.0
7	589	- 4.2	614	- 3.5	565	- 0.1
8	626	- 4.3	656	- 3.6	601	- 0.4
9	662	- 4.6	699	- 3.7	637	- 0.6
10	699	- 4.8	741	- 3.4	673	- 1.0
11	735	- 4.6	783	- 3.3	709	- 1.3
12	772	- 4.5	825	- 3.4	745	- 1.8
13	805	- 4.6	866	- 3.6	782	- 2.0
14	838	- 4.8	907	- 4.0	819	- 2.2
15	871	- 4.7	949	- 4.2	855	- 2.6
16	905	- 5.2	990	- 4.4	892	- 2.9
17	938	- 5.4	1028	- 4.6	930	- 3.2
18	971	- 5.5	1066	- 4.8	967	- 3.4
19	1004	- 5.7	1105	- 5.0	1005	- 3.6
20	1037	- 5.8	1143	- 5.1	1043	- 3.8
21	1071	- 6.0	1181	- 5.4	1080	- 3.9
22	1104	- 6.4	1220	- 5.7	1118	- 3.8
23	1137	- 6.5	1258	- 5.8	1156	- 3.8
24	1170	- 6.7	1296	- 5.8	1193	- 4.1
25	1204	- 7.0	1334	- 6.0	1230	- 4.1
26	1237	- 7.2	1373	- 6.1	1268	- 4.4
27	1275	- 7.4	1411	- 6.4	1305	- 4.9
28	1313	- 7.6	1449	- 6.6	1343	- 4.9
29	1351	- 7.6	1488	- 6.8	1382	- 5.2
30	1390	- 7.8	1526	- 7.0	1421	- 5.4
31	1428	- 8.0	1564	- 7.2	1446	- 5.6
32	1466	- 8.3	1603	- 7.3	1470	- 5.7
33	1504	- 8.6	1641	- 7.4	1499	- 6.0
34	1543	- 8.9	1679	- 7.6	1528	- 6.1
35	1581	- 9.0	1717	- 7.9	1557	- 6.3
36	1619	- 9.2	1756	- 8.0	1586	- 6.3
37	1658	- 9.4	1794	- 8.2	1615	- 6.6
38	1697	- 9.7	1832	- 8.5	1644	- 6.7
39	1736	- 9.9	1871	- 8.8	1672	- 7.0
40	1775	-10.2	1909	- 9.2	1699	- 7.2

Table E-10. March Data - Fort McMurray cont'd.

Time(LST)	0930		1100		1300	
Level	Height (M)	Temp (C)	Height (M)	Temp (C)	Height (M)	Temp (C)
41	1814	-10.4	1947	- 9.4	1727	- 7.4
42	1853	-10.5	1986	- 9.6	1755	- 7.4
43	1893	-10.7	2019	- 9.8	1784	- 7.8
44	1932	-10.8	2053	-10.1	1814	- 7.9
45	1971	-10.8	2087	-10.3	1844	- 8.2
46	2010	-10.8	2121	-10.6	1873	- 8.3
47	2049	-11.0	2155	-10.8	1903	- 8.4
48	2088	-11.2	2188	-10.9	1933	- 8.7
49	2127	-11.4	2222	-11.1	1966	- 9.1
50	2166	-11.8	2256	-11.3	2000	- 9.2
51	2205	-12.1	2290	-11.5	2033	- 9.4
52	2244	-12.2	2324	-11.6	2067	- 9.6
53	2283	-12.5	2357	-11.8	2101	- 9.8
54	2323	-12.8	2391	-12.0	2134	- 9.9
55	2362	-13.0	2425	-12.3	2168	-10.0
56	2401	-13.2	2459	-12.6	2202	-10.2
57	2440	-13.4	2497	-12.7	2235	-10.3
58	2479	-13.7	2535	-13.3	2269	-10.4
59	2518	-13.8	2574	-13.6	2302	-10.7
60	2557	-14.0	2612	-13.9	2334	-11.0

Table E-11. March Data - Fort McMurray

DATE: March 17/76 Location: GCOS

Time(LST)	0930		1100		1315	
Level	Height (M)	Temp (C)	Height (M)	Temp (C)	Height (M)	Temp (C)
0	320	0.0	320	1.5	318	5.2
1	355	- 0.6	353	1.3	355	5.3
2	389	- 0.8	387	1.5	393	4.9
3	423	- 1.0	421	1.4	425	4.6
4	457	- 1.1	454	1.1	458	4.2
5	491	- 1.3	488	1.1	495	4.0
6	525	- 1.3	522	1.0	531	3.6
7	559	- 0.9	555	0.8	568	3.4
8	593	- 0,1	589	1.9	605	3.2
9	628	0.9	622	1.9	638	3.0
10	662	0.9	656	1.7	671	2.7
11	696	0.8	690	1.5	705	2.4
12	730	0.4	723	1.2	738	2.1
13	764	0.6	757	1.2	770	1.9
14	798	0.8	790	1.1	803	1.7
15	832	0.9	823	1.0	835	1.5
16	866	- 0.1	857	0.8	868	1.2
17	900	- 0.2	890	0.8	900	1.1
18	934	- 0.2	923	0.6	933	0.9
19	968	- 0.1	957	0.6	965	0.9
20	1002	0.0	990	0.8	997	1.6
21	1038	0.0	1024	1.1	1032	2.0
22	1074	0.2	1057	1.5	1066	2.4
23	1110	0.2	1093	1.6	1100	2.4
24	1146	0.1	1130	1.5	1134	2.7
25	1182	- 0.1	1167	1.4	1169	3.6
26	1218	0.0	1205	1.3	1204	3.9
27	1254	- 0.1	1243	1.2	1240	4.0
28	1290	0.1	1281	1.2	1276	3.9
29	1332	0.2	1325	1.3	1311	3.8
30	1375	0.2	1370	1.5	1346	3.6
31	1417	0.0	1410	1.4	1386	3.4
32	1460	- 0.2	1451	1.3	1426	3.0
33	1504	- 0.3	1491	1.2	1466	2.8
34	1549	- 0.2	1531	1.0	1506	2.6
35	1594	- 0.2	1584	0.8	1546	2.3
36	1638	- 0.4	1637	0.7	1585	2.0
37	1683	- 0.4	1669	0.6	1631	1.7
38	1728	- 0.4	1700	0.5	1677	1.4
39	1773	- 0.6	1732	0.3	1722	1.2
40	1817	- 0.7	1764	0.1	1768	0.8

Table E-11. March Data - Fort McMurray cont'd.

Time(LST)	0930		1100		1315	
Level	Height (M)	Temp (C)	Height (M)	Temp (C)	Height (M)	Temp (C)
41	1868	- 0.9	1797	- 0.2	1814	0.6
42	1919	- 1.2	1830	- 0.6	1860	0.3
43	1970	- 1.4	1863	- 0.8	1911	0.2
44	2021	- 1.7	1897	- 1.2	1963	0.0
45	2055	- 1.9	1930	- 1.5	2021	- 0.2
46	2089	- 2.1	1963	- 1.6	2079	- 0.4
47	2123	- 1.9	1996	- 1.4	2137	- 0.5
48	2157	- 1.7	2029	- 1.6	2194	- 0.8
49	2191	- 1.7	2067	- 1.6	2258	- 1.0
50	2225	- 1.8	2106	- 1.8	2322	- 1.1
51	2259	- 1.8	2163	- 2.0	2386	- 1.1
52	2294	- 2.1	2221	- 2.2	2449	- 1.1
53	2328	- 2.2	2262	- 2.4	2513	- 1.3
54	2362	- 2.5	2304	- 2.7	2577	- 1.4
55	2396	- 2.7	2388	- 2.8	2641	- 1.5
56	2430	- 3.1	2472	- 3.1	2704	- 1.7
57	2464	- 3.3	2579	- 3.3	2762	- 1.9
58	2498	- 3.5	2687	- 3.5	2820	- 2.1
59	2532	- 3.7	2726	- 3.7	2865	- 2.1
60	2566	- 4.1	2764	- 3.9	2910	- 2.2

Table E-12. August Data - Fort McMurray

DATE: August 14/76			Location: Mildred Lake		
Time(LST)	0605	0936	1304	1435	1802
Height (M)	Temp (C)	Temp (C)	Temp (C)	Temp (C)	Temp (C)
0	15.3	20.0	26.1	27.8	26.3
43	15.5	19.1	24.9	27.1	25.8
85	15.8	18.6	24.5	26.8	25.3
127	15.9	18.2	24.2	26.6	24.9
170	15.9	17.8	23.9	26.3	24.5
213	16.2	17.6	23.5	25.9	24.2
255	16.6	17.5	23.3	25.5	23.9
297	16.5	17.2	23.0	25.1	23.6
340	16.4	17.8	22.6	24.7	23.4
382	16.4	17.8	22.5	24.4	23.0
425	16.4	17.6	22.1	23.9	22.7
467	16.3	17.6	21.7	23.5	22.4
510	16.3	18.1	21.3	23.1	22.1
552	16.3	18.1	21.0	22.7	21.6
595	16.3	18.0	20.5	22.4	21.3
638	16.2	17.5	20.0	22.1	21.1
680	16.0	17.3	19.6	21.8	20.6
722	15.7	17.0	19.2	21.6	20.3
765	15.5	16.2	19.2	21.6	20.1
807	15.7	15.8	19.3	21.5	19.8
850	16.2	15.4	19.6	21.1	19.4
892	16.2	15.4	19.4	20.6	19.1
935	16.3	15.5	19.2	20.9	18.9
977	16.3	15.9	19.1	21.0	18.7
1020	16.2	15.9	18.9	20.9	18.1
1063	16.2	15.7	18.8	20.7	17.9
1105	16.2	15.7	18.6	20.6	17.6
1147	15.9	15.7	18.2	20.3	17.3
1190	15.6	15.7	18.1	19.9	16.8
1232	15.5	15.6	18.0	19.3	16.6
1275	15.7	15.7	17.9	18.9	16.3
1317	15.9	15.9	17.6	18.5	15.9
1360	15.8	15.9	17.4	18.1	15.6
1402	15.5	15.7	17.4	17.5	15.2
1445	15.1	15.3	17.6	17.2	14.9
1487	14.7	15.0	17.4	16.7	14.7
1530	14.4	14.8	17.1	16.2	14.4
1572	14.0	14.6	16.4	15.8	14.0
1615	14.0	14.5	16.2	15.3	13.7
1657		14.0	15.8	14.9	13.4
1700	13.4	13.7	15.5	14.6	13.2
1742		13.5		14.3	12.9

Table E-12. August Data - Fort McMurray cont'd.

Time(LST)	0603	0936	1304	1435	1802
Height (M)	Temp (C)	Temp (C)	Temp (C)	Temp (C)	Temp (C)
1785	12.7	12.9	15.0	13.9	12.6
1827		12.4			
1870	12.1	12.2	14.2	13.4	12.2
1912		11.7			
1955	11.4	11.4	13.2	12.7	11.8
1997		11.0			
2040	10.8	10.7	12.3	11.9	11.4
2082		10.2			
2125	10.2	9.7	11.4	11.6	10.8
2167		9.5			
2210	9.4	8.8	10.8	10.7	10.3
2252		8.4			
2295	8.9	8.1	10.2	10.2	9.6
2337		7.9			
2380	8.2	7.2	9.1	9.6	8.8
2422		7.0			
2465	7.4	6.7	8.6	9.4	8.0
2507		6.5			
2550	6.9	6.2	7.6	8.3	7.1

Table E-13. August Data - Fort McMurray

DATE: August 15/76 Location: Mildred Lake

Time(LST)	0605	0938	1301	1800
Height (M)	Temp (C)	Temp (C)	Temp (C)	Temp (C)
0	17.0	23.3	27.2	29.7
43	18.5	22.9	26.6	29.2
85	19.5	22.3	26.1	28.7
127	19.5	21.6	25.3	28.3
170	19.4	21.4	24.8	27.7
213	19.3	21.5	24.3	27.3
255	19.2	22.6	23.8	27.0
297	19.8	23.4	23.7	26.7
340	20.1	23.6	23.3	26.2
382	20.4	23.5	22.8	25.8
425	20.3	23.1	22.5	25.3
467	20.2	23.0	22.0	25.1
510	19.9	22.9	21.9	24.9
552	19.9	22.7	21.7	24.5
595	20.2	22.3	21.2	24.2
638	20.6	22.0	20.9	23.8
680	20.4	21.7	20.5	23.5
722	20.1	21.4	20.4	23.1
765	19.8	21.2	20.4	22.7
807	19.4	20.8	20.4	22.3
850	19.1	20.4	20.1	21.8
892	18.7	20.4	19.8	21.3
935	18.4	20.3	19.5	20.9
977	18.6	20.1	19.1	20.5
1020	18.9	19.5	18.8	20.2
1063	18.8	19.2	18.5	19.6
1105	18.7	18.6	18.1	19.3
1147	18.6	18.3	17.7	18.9
1190	18.4	17.8	17.3	18.6
1232	18.1	17.6	16.6	18.3
1275	18.0	17.1	16.1	18.1
1317	17.7	16.8	15.6	17.7
1360	17.6	16.5	15.1	17.3
1402	17.5	16.5	14.9	17.0
1445	17.3	16.4	14.9	16.6
1487	17.1	15.9	14.7	16.4
1530	16.6	15.7	14.6	16.1
1572	16.4	15.5	14.2	15.7
1615	16.0	15.0	14.2	15.6
1657	15.7	14.7	14.2	15.3
1700	15.4	14.4	13.8	14.9
1742			13.5	

Table E-13. August Data - Fort McMurray cont'd.

Time(LST)	0605	0938	1301	1800
Height (M)	Temp (C)	Temp (C)	Temp (C)	Temp (C)
1785	14.8	13.9	13.1	14.9
1827			13.0	
1870	13.8	13.0	13.0	15.5
1912			13.2	
1955	13.1	12.4	13.1	15.6
1997			13.0	
2040	12.1	12.0	12.7	15.4
2082			12.3	
2120	11.3	11.2	12.1	15.2
2167			11.9	
2210	10.6	10.9	11.7	14.4
2252			11.5	
2295	9.9	10.6	11.3	13.5
2337			10.6	
2380	9.3	10.0	10.4	12.4
2422			9.9	
2465	8.5	9.6	9.7	11.8
2507			9.1	
2550	7.7	9.6	8.7	10.6

Table E-14. August Data - Fort McMurray

DATE: August 16/76 Location: Mildred Lake

Time(LST)	0609	0927	1254	1427	1801
Height (M)	Temp (C)	Temp (C)	Temp (C)	Temp (C)	Temp (C)
0	17.8	22.2	28.1	28.5	28.3
43	18.2	21.1	27.3	27.6	27.7
85	18.4	20.7	26.7	27.0	27.0
127	18.5	20.0	26.5	26.2	26.6
170	18.5	19.1	25.9	25.8	26.1
213	18.8	18.5	25.6	25.2	25.8
255	19.3	17.8	25.2	25.2	25.5
297	19.7	17.6	25.0	24.4	25.1
340	19.7	17.4	24.6	23.7	24.8
382	19.8	17.0	24.4	22.8	24.4
425	20.5	16.4	24.0	22.3	24.2
467	21.0	16.0	23.5	21.8	23.7
510	21.0	15.6	22.9	21.5	23.1
552	20.9	15.1	22.0	20.8	22.7
595	20.6	14.8	21.3	20.3	22.2
638	20.1	14.7	20.9	20.0	22.0
680	19.8	14.6	20.3	19.4	21.5
722	19.4	14.7	19.5	19.1	21.0
765	19.0	14.4	19.1	18.7	20.6
807	18.7	14.0	18.6	18.3	20.3
850	18.3	13.9	17.8	17.9	19.8
892	18.1	13.5	17.1	17.4	19.5
935	18.1	13.4	16.2	17.1	18.9
977	18.0	13.9	16.1	16.8	18.6
1020	18.0	14.2	16.0	16.4	18.0
1063	17.9	14.2	16.7	15.9	17.4
1105	17.8	14.3	16.8	15.7	17.0
1147	17.8	14.4	17.1	15.3	16.8
1190	17.5	14.3	17.2	15.0	16.3
1232	17.4	14.2	17.2	14.6	15.9
1275	17.4	14.4	17.0	14.1	15.6
1317	17.2				
1360	17.1	14.4	16.2	13.5	14.6
1402	16.7				
1445	16.5	14.2	15.2	13.4	14.1
1487	16.2				
1530	15.9	13.8	14.7	12.5	13.5
1572	15.6				
1615	15.3	13.8	14.3	12.8	13.0
1657	15.0				
1700	14.7	13.8	13.4	13.0	12.1
1742					

Table E-14. August Data - Fort McMurray cont'd.

Time(LST)	0609	0927	1254	1427	1801
Height (M)	Temp (C)	Temp (C)	Temp (C)	Temp (C)	Temp (C)
1785	14.0	13.2	12.7	12.9	11.9
1827					
1870	13.2	12.7	11.9	12.8	11.4
1912					
1955	12.5	11.8	11.4	12.4	11.5
1997					
2040	11.9	11.3	11.5	11.9	11.7
2082					
2120	11.2	10.6	11.1	11.7	11.1
2167					
2210	10.9	9.8	10.9	11.0	10.7
2252					
2295	10.4	9.3	10.4	10.5	10.5
2337					
2380	9.7	8.8	9.8	9.9	9.5
2422					
2465	9.0	8.2	9.3	9.4	9.3
2507					
2550	8.4	7.4	8.6	8.5	8.7

Table E-15. August Data - Fort McMurray

DATE: August 17/76 Location: Mildred Lake

Time(LST)	0610	0928	1255	1425	1806
Height (M)	Temp (C)	Temp (C)	Temp (C)	Temp (C)	Temp (C)
0	14.1	13.9	13.9	15.3	17.2
43	14.0	13.4	12.5	14.4	16.3
85	13.7	12.7	11.6	13.8	15.5
127	13.4	12.0	11.1	13.3	15.0
170	13.1	11.6	10.7	12.3	14.8
213	12.6	11.2	10.3	11.8	14.4
255	12.4	10.9	10.0	11.4	14.0
297	12.2	10.6	9.6	11.0	13.9
340	12.0	10.0	9.0	10.2	13.0
382	11.7	9.7	8.8	9.4	12.7
425	11.4	9.2	8.6	9.2	12.2
467	11.3	8.8	8.3	9.0	11.6
510	11.0	8.4	8.1	8.5	11.2
552	11.0	8.0	7.9	8.4	10.6
595	11.2	7.7	8.0	8.3	10.1
638	11.3	7.4	8.0	8.0	9.5
680	11.1	7.3	7.9	7.7	9.1
722	10.9	7.0	7.7	7.6	9.0
765	10.6	7.0	7.5	7.5	8.5
807	10.3	6.9	7.3	7.3	7.9
850	10.0	7.0	7.0	7.1	7.9
892	9.9	7.2	6.8	7.0	7.6
935	9.5	7.2	6.5	6.7	7.3
977	9.1	7.0	6.4	6.6	6.6
1020	8.8	6.9	6.2	6.5	5.8
1063	8.6	6.6	5.9	6.3	5.1
1105	8.6	6.3	6.0	5.8	5.7
1147	8.3	6.1	5.9	5.3	6.1
1190	7.9	5.9	5.9	5.1	6.4
1232	7.6	5.7	5.7	5.0	6.4
1275	7.1	5.7	5.6	4.8	6.5
1317			5.3		6.4
1360	6.8	5.3	5.3	3.8	6.0
1402			4.9		
1445	6.0	4.9	4.8	3.4	5.3
1487			4.5		
1530	6.1	4.6	4.1	2.6	4.9
1572			3.9		
1615	6.1	4.3	3.7	1.7	4.3
1657			3.3		
1700	6.0	4.2	2.9	1.5	3.8
1742			2.7		

Table E-15. August Data - Fort McMurray cont'd.

Time(LST)	0610	0928	1255	1425	1806
Height (M)	Temp (C)	Temp (C)	Temp (C)	Temp (C)	Temp (C)
1785	5.5	3.9	2.6	1.2	3.3
1827			2.6		
1870	5.3	3.9	2.4	1.0	2.3
1912			1.9		
1955	4.9	3.3	1.5	.6	2.4
1997			1.2		
2040	4.6	2.8	.7	- .1	2.0
2082			.3		
2125	4.0	2.3	- .2	- .8	1.7
2167			- .5		
2210	3.1	1.8	-1.0	- .6	.9
2252			-1.4		
2295	2.4	1.0	-1.5	-1.0	.6
2337			-1.1		
2380	1.9	.7	- .7	-1.4	
2422			- .5		
2465	1.4	.1	- .4	-1.8	
2507			- .4		- .2
2550	.9	- .2	- .5	-2.0	- .3

Table E-16. August Data - Fort McMurray

DATE: August 18/76 Location: Mildred Lake

Time(LST)	0601	0928	1258	1425	1759
Height (M)	Temp (C)	Temp (C)	Temp (C)	Temp (C)	Temp (C)
0	14.4	16.7	18.3	18.6	17.7
43	14.1	16.0	17.4	17.5	17.1
85	13.7	15.3	15.9	16.6	16.6
127	13.5	14.6	15.3	16.1	16.0
170	13.6	14.3	14.8	15.7	15.6
213	13.4	13.9	14.2	15.5	15.2
255	13.0	13.3	13.9	15.0	14.6
297	12.7	13.0	13.4	14.8	14.2
340	12.2	12.5	13.0	14.7	14.0
382	11.7	12.2	12.6	14.2	13.7
425	11.2	12.0	12.2	14.1	13.2
467	10.8	11.7	11.6	13.9	13.1
510	10.3	11.5	11.1	13.6	12.2
552	9.9	11.4	10.5	13.4	11.7
595	9.5	11.0	9.9	13.3	11.5
638	9.2	10.9	9.3	13.0	11.2
680	9.1	11.4	9.1	12.6	10.8
722	9.1	11.6	9.5	12.3	10.5
765	9.7	11.3	9.5	12.0	10.2
807	10.3	10.8	9.4	11.6	10.1
850	10.9	10.3	9.1	11.2	9.7
892	11.0	9.9	8.9	10.9	9.6
935	10.7	9.3	8.5	10.5	9.4
977	10.3	9.1	8.2	10.2	9.0
1020	10.2	8.7	7.9	9.9	8.9
1063	10.0	8.2	7.3	9.7	8.8
1105	9.9	7.8	7.1	9.6	8.5
1147	9.6	7.9	6.9	9.1	8.3
1190	9.2	8.5	7.0	8.6	8.0
1232	8.8	9.0	7.0	8.9	7.7
1275	8.6	9.1	6.9	8.9	7.5
1317			6.9	8.3	
1360	7.9	8.6	6.6	8.2	6.8
1402					
1445	7.4	8.1	6.0	8.1	6.0
1487					
1530	6.9	7.6	5.5	8.1	6.0
1572					
1615	6.1	7.6	4.7	7.2	5.9
1657					
1700	5.6	6.8	4.8	6.8	5.6
1742					

Table E-16. August Data - Fort McMurray cont'd.

Time(LST)	0601	0928	1258	1425	1759
Height (M)	Temp (C)	Temp (C)	Temp (C)	Temp (C)	Temp (C)
1785	4.6	5.9	4.6	6.7	5.2
1827					
1870	4.1	5.3	4.0	5.9	4.5
1912					
1955	3.1	4.4	4.0	5.0	3.9
1997					
2040	2.7	3.9	3.6	4.2	2.7
2082					
2125	1.9	3.2	2.8	3.5	2.6
2167					
2210	1.3	2.5	2.3	2.7	1.9
2252				2.6	
2295	.4	1.8	1.5		2.2
2337				2.2	
2380	- .3	1.4	.8	2.0	2.1
2422					
2465	- .8	.8	- .1	1.6	2.0
2507					
2550	-1.2	.5	- .4	1.5	1.8

Table E-17. August Data - Fort McMurray

DATE: August 19/76 Location: Mildred Lake

Time(LST)	0608	0931	1256	1420	1811
Height (M)	Temp (C)	Temp (C)	Temp (C)	Temp (C)	Temp (C)
0	11.7	15.2	20.0	20.5	21.7
43	12.2	14.3	18.9	18.9	21.2
85	12.3	13.8	18.0	17.7	20.5
127	12.2	13.2	17.2	17.1	20.0
170	12.5	12.5	16.7	16.9	19.5
213	14.1	12.0	16.4	16.1	18.8
255	14.4	11.3	16.0	15.3	18.1
297	14.5	11.0	15.8	14.7	17.4
340	14.6	11.8	15.5	14.1	16.6
382	14.4	11.9	15.2	13.4	15.8
425	14.3	12.0	14.9	12.7	14.8
467	14.2	12.0	14.7	12.2	14.2
510	14.0	11.7	14.5	11.7	13.4
552	13.6	11.4	14.2	10.9	12.8
595	13.3	11.1	13.9	10.1	12.2
638	13.1	10.7	13.5	9.3	11.6
680	12.7	10.4	13.4	8.7	11.2
722	12.5	10.0	13.1	7.6	10.6
765	12.1	9.6	12.8	7.2	10.0
807	11.8	9.3	12.4	6.3	9.4
850	11.5	9.0	12.0	5.2	8.5
892	11.2	8.7	11.5	5.1	7.9
935	10.9	8.4	11.3	5.0	7.4
977	10.6	8.1	10.8	4.4	6.6
1020	10.3	7.8	10.4	3.8	6.2
1063	9.9	7.5	10.0	3.2	5.2
1105	9.5	7.2	9.4	3.1	4.3
1147	9.1	6.8	9.0	2.9	3.8
1190	8.7	6.6	8.7	2.1	3.2
1232	8.2	6.3	8.4	2.8	2.5
1275	7.7	6.1	8.2	2.8	2.0
1317		5.7		2.9	1.5
1360	7.2	5.6	7.8	2.6	1.2
1402					1.2
1445	7.0	4.8	6.8	1.6	1.2
1487					1.1
1530	6.5	4.3	5.8	1.1	1.0
1572					1.1
1615	5.8	3.5	5.1	.6	1.1
1657					1.0
1700	5.2	3.0	4.8	.3	.9
1742		2.6			.6

Table E- 17. August Data - Fort McMurray cont'd.

Time(LST)	0608	0931	1256	1420	1811
Height (M)	Temp (C)	Temp (C)	Temp (C)	Temp (C)	Temp (C)
1785	4.3	2.2	4.3	- .1	.4
1827		2.1			.2
1870	3.6	1.8	3.8	-1.1	- .4
1912		1.6			- .7
1955	2.8	1.1	3.3	-1.8	-1.2
1997		1.1			-1.7
2040	1.9	1.0	2.3		-2.1
2082		.6		-2.0	-2.1
2125	1.4	.2	2.3	-2.7	-2.2
2167		- .3		-3.4	-2.8
2210	.6	- .5	2.3		-2.9
2252		- .7		-3.9	-3.2
2295	- .1	- .9	2.2	-2.7	-3.0
2337				-2.9	
2380	- .9	-1.3	2.0		-3.4
2422					
2465	-2.0	-1.8		-4.5	-3.9
2507			1.6		
2550	-2.3	-1.9	.9	-6.1	-4.6

Table E-18. August Data - Fort McMurray

DATE: August 20/76 Location: Mildred Lake

Time(LST)	0613	0943	1313	1444	1805
Height (M)	Temp (C)	Temp (C)	Temp (C)	Temp (C)	Temp (C)
0	9.4	12.6	17.0	18.5	19.4
43	9.3	11.6	16.4	17.3	18.7
85	9.4	11.1	16.2	16.5	18.4
127	10.5	10.7	15.8	16.0	18.0
170	11.4	11.5	15.4	15.4	17.5
213	11.7	11.5	15.2	14.8	17.1
255	11.8	11.5	15.0	14.4	16.6
297	11.8	11.1	15.0	14.1	16.0
340	11.6	10.9	14.9	13.8	15.8
382	11.4	10.7	14.5	13.4	14.8
425	11.2	10.5	13.6	13.0	14.3
467	10.8	10.3	13.2	12.6	13.6
510	10.6	10.0	13.1	12.2	12.9
552	10.4	9.4	12.7	11.8	12.2
595	10.1	9.1	12.2	11.6	11.6
638	9.9	8.7	12.1	11.2	11.0
680	9.6	8.4	12.0	10.9	10.3
722	9.3	8.1	11.5	10.8	9.6
765	9.0	7.5	11.2	10.2	9.0
807	8.7	7.3	11.0	10.0	8.9
850	8.5	6.9	10.5	9.6	
892	8.2	6.5	10.3	9.3	7.9
935	7.9	6.2	10.0	8.9	7.9
977	7.6	5.8	9.7	8.8	7.8
1020	7.4	5.5	9.3	8.2	7.1
1063	7.1	5.2	9.1	7.7	6.5
1105	6.6	4.9	8.7	7.5	6.5
1147	6.3	4.7	8.3	7.0	6.4
1190	6.0	4.4	7.9	6.8	6.2
1232	5.5	4.0	7.8	6.1	5.7
1275	5.2	3.7	7.1	6.1	5.5
1317				5.4	
1360	4.6	3.1	6.6	4.9	4.8
1402				4.7	
1445	4.0	2.4	6.1	4.7	4.7
1487				4.7	
1530	3.0	1.8	5.7	4.6	3.9
1572					
1615	2.9	1.2	4.9	3.9	3.0
1657					
1700	2.4	.7	4.6	3.3	2.8
1742					

Table E-18. August Data - Fort McMurray cont'd.

Time(LST)	0613	0943	1313	1444	1805
Height (M)	Temp (C)	Temp (C)	Temp (C)	Temp (C)	Temp (C)
1785	1.8	.3	4.0	2.9	2.1
1827					
1870	1.0	.0	3.4	2.1	1.3
1912					
1955	.6	- .4	3.1	1.7	.7
1997					
2040	.2	-1.0	2.6	1.1	.1
2082					
2125	.0	-1.2	2.2	.5	- .4
2167					
2210	- .6	-1.5	1.9	.1	-1.4
2252					
2295	-1.4	-2.0	1.6	- .4	-1.7
2337					
2380	-2.0	-2.4	1.0	-1.0	-1.6
2422					
2465	-2.3	-2.6	.5	-1.4	-2.6
2507					
2550	-2.9	-3.3	- .1	-2.2	-2.3

Table E- 20. August Data - Fort McMurray

DATE: August 21/76			Location: Mildred Lake		
Time(LST)	0616	0943	1316	1441	1801
Height (M)	Temp (C)	Temp (C)	Temp (C)	Temp (C)	Temp (C)
0	9.7	15.5	18.5	19.4	18.3
43	10.2	14.6	16.4	18.8	17.8
85	10.1	14.1	15.8	18.0	
127	9.9	13.5	16.1	17.2	
170	10.9	13.1	14.1	17.0	16.5
213	11.6	12.8	13.7	16.7	16.0
255	11.8	12.7	13.2	16.3	15.5
297	11.6	12.3	12.5	16.1	15.0
340	11.4	12.3	12.0	15.8	14.2
382	11.9	12.3	11.4	15.5	13.2
425	11.9	12.6	10.8	15.1	12.3
467	11.7	12.5	10.6	14.9	11.6
510	11.2	12.2	9.4	14.1	10.8
552	11.0	12.0	9.1	13.9	10.1
595	10.8	11.8	8.5	13.5	9.1
638	10.6	11.4	7.9	13.0	8.8
680	10.6	11.1	7.6	12.8	8.0
722	10.5	10.6	6.8	12.3	7.6
765	10.2	10.6	6.1	11.5	6.8
807	9.9	10.5	6.3	10.8	6.3
850	9.6	10.3	7.3		5.8
892	9.4	10.1	9.2	10.2	5.6
935	9.0	9.0	11.0	9.8	4.5
977	8.7	9.4	13.2	9.3	3.9
1020	8.5	9.2	14.6	8.6	2.2
1063	8.2	8.9	16.7	8.0	
1105	7.8	8.6			
1147	7.5	8.3		6.9	
1190	7.3	8.0		6.6	
1232	6.8	7.5		6.1	
1275	6.6	7.1		5.4	
1317				5.2	
1360	5.9	6.5		4.9	
1402				4.5	
1445	5.3	6.2		4.2	
1487				4.2	
1530	4.6	5.8		3.9	
1572				3.7	
1615	3.9	5.0		3.7	
1657				3.3	
1700	3.2	4.8		3.2	
1742					

Table E-20. August Data - Fort McMurray cont'd.

Time(LST)	0616	0943	1316	1441	1801
Height (M)	Temp (C)	Temp (C)	Temp (C)	Temp (C)	Temp (C)
1785	2.3	3.9		3.0	
1827					
1870	1.8	3.4		2.2	
1912					
1955	1.0	3.3		2.0	
1997					
2040	.4	2.2		1.1	
2082					
2125	- .1	1.2		.3	
2167					
2210	- .6	.6		.1	
2252					
2295	-1.5	- .1		- .5	
2337					
2380	-1.8	- .7		- .7	
2422					
2465	-2.2	-1.7		-1.7	
2507					
2550	-2,4	-2.5		-2.5	

Table E-21. September Data - Fort McMurray

DATE: September 23/76				Location: Mildred Lake	
Time(LST)	0730	1039	1342	1427	1807
Height (M)	Temp (C)	Temp (C)	Temp (C)	Temp (C)	Temp (C)
0	0.6	7.4	12.2	13.3	19.8
43	2.1	5.4	11.5	12.2	19.3
85	2.8	4.9	11.0	11.5	19.0
127	3.6	4.7	10.7	11.0	19.9
170	3.7	4.1	10.3	10.7	19.3
213	3.8	3.8	9.8	10.2	19.5
255	5.1	4.4	9.5	9.9	19.2
297	6.2	5.0	9.3	10.0	18.9
340	7.8	7.3	9.3	9.9	18.4
382	9.2	7.9	9.5	9.7	18.0
425	10.5	8.6	9.5	9.7	17.5
467	10.7	9.3	9.8	9.6	17.1
510	10.4	9.1	10.5	9.6	16.7
552	10.2	9.1	10.8	10.1	16.5
595	10.1	9.2	10.7	10.1	16.1
638	10.0	9.3	10.3	10.0	15.9
680	9.8	9.3	10.1	9.7	15.6
722	9.5	9.1	10.0	9.4	15.6
765	9.4	9.2	9.6	9.1	15.2
807	9.3	9.1	9.4	8.8	14.8
850	9.2	9.0	9.3	8.5	14.4
892	9.1	8.9	8.9	8.1	14.1
935	8.8	8.6	8.7	7.9	13.8
977	8.7	8.3	9.2	7.6	13.7
1020	8.5	8.0	9.2	7.5	13.5
1063	8.5	7.8	9.1	7.3	13.1
1105	8.3	7.3	8.8	7.4	13.0
1147	8.1	7.1	7.8		12.8
1190	7.8	6.8	7.4	6.8	12.6
1232	7.3	6.6	7.2	6.4	12.4
1275	6.9	6.6	7.2	6.3	12.2
1317	6.6	6.5	7.3		12.1
1360	6.4	6.6	7.3	6.3	11.7
1402	6.0	6.0	7.1	6.2	11.4
1445	5.6	5.7		6.1	10.9
1487	5.6	5.2		5.8	10.6
1530	5.5	5.4	6.5	5.7	10.3
1572	5.4	5.2	6.1	5.2	10.1
1615	5.3	5.1	5.9	5.1	9.9
1657	5.0	4.5	5.5	4.6	9.8
1700	4.8	4.4	5.4	4.4	9.7
1742	4.6	4.5	5.1	4.2	9.7

Table E-21. September Data - Fort McMurray cont'd.

Time(LST)	0730	1039	1342	1427	1807
Height (M)	Temp (C)	Temp (C)	Temp (C)	Temp (C)	Temp (C)
1785	4.2	4.7	4.8	4.0	9.7
1827		4.7	4.6	3.9	9.4
1870	4.1	4.7	4.6		9.3
1912	3.9	4.3	4.7		8.9
1955	3.8	3.9	4.6		8.7
1997	3.6	3.6	4.5	3.3	8.4
2040	3.5	3.5	4.0	2.8	8.0
2082	3.4	3.3	3.6		7.9
2125	3.5		3.5	2.7	7.7
2167	3.5		2.8	2.8	7.3
2210	3.4	2.2			7.0
2252	3.1	2.0	2.4	2.2	6.6
2295	3.0	1.8	2.3	1.8	6.5
2337	3.0	1.5	2.2		6.4
2380	2.6	1.0	2.0		6.2
2422	2.2	.7	1.6	0.8	6.0
2465	1.9	0.5	1.1	0.7	5.6
2507	1.4	0.2	0.8	0.5	5.2
2550	1.1	0.0	0.6	0.3	5.0

Table E-22. September Data - Fort McMurray

DATE: September 24/76			Location: Mildred Lake		
Time(LST)	0725	1043	1338	1437	1811
Height (M)	Temp (C)	Temp (C)	Temp (C)	Temp (C)	Temp (C)
0	5.5	10.3	15.6	16.7	18.9
43	5.8	9.0	12.9	14.7	17.9
85	6.3	8.3	12.0	14.1	17.5
127	6.4	7.6	11.4	13.6	17.3
170	6.4	6.9	10.9	12.6	16.9
213	6.4	9.3	10.5	11.9	16.7
255	7.1	9.8	10.3	11.5	16.3
297	8.3	10.4	9.6	11.1	16.0
340	9.2	10.5	9.2	10.8	15.6
382	10.1	10.5	9.3	10.2	15.4
425	10.3	10.4	9.5	9.9	15.2
467	10.7	10.3	9.8	10.2	15.2
510	11.1	10.2	10.3	10.5	15.1
552	11.2	11.4	10.5	11.2	14.9
595	11.1	12.1	11.1	11.1	14.5
638	11.2	12.2	11.2	11.0	14.3
680	11.3	12.3	11.2	11.1	13.9
722	11.6	12.3	10.9	11.0	13.6
765	11.5	12.2	10.6	10.9	13.5
807	11.3	11.9	10.4	10.7	13.0
850	11.2	11.7	10.4	10.3	12.7
892	11.0	11.4	10.2	10.1	12.6
935	10.7	11.1	10.2	9.7	12.6
977	10.6	10.8	9.5	9.1	12.7
1020	10.2	10.4	9.4	8.8	11.9
1063	10.0	10.2	9.3	8.7	11.6
1105	9.7	9.8	8.9	8.4	11.4
1147	9.4	9.5	8.7	7.8	11.0
1190	9.0	9.1	8.3	7.5	10.8
1232	8.7	9.0	8.0	7.4	10.7
1275	8.3	8.9	7.4	7.1	10.0
1317	7.8	8.5	7.2	6.7	9.7
1360	7.7	8.3	6.9	6.2	9.4
1402	7.5	7.8	6.4		9.0
1445	7.2	7.6	6.3		8.5
1487	7.0	7.1		5.6	8.4
1530	6.6	6.6	5.7	5.4	7.9
1572	6.4	6.4	5.5	4.8	7.4
1615	6.1	6.1	5.2	4.6	7.0
1657	5.7	5.7	5.0	4.2	6.8
1700	5.4	5.4	4.5	4.0	6.4
1742	5.0		4.0	3.9	6.2

Table E-22. September Data - Fort McMurray cont'd.

Time(LST)	0725	1043	1338	1437	1811
Height (M)	Temp (C)	Temp (C)	Temp (C)	Temp (C)	Temp (C)
1785	5.3	4.5	3.9		5.8
1827	4.3	4.4	3.6	3.0	5.5
1870	3.9	3.9	3.3	3.0	5.3
1912	3.6	3.7	2.9	2.7	5.0
1955	3.3	3.5	2.7	2.6	5.0
1997	3.1	3.2	2.5	2.0	
2040	3.2	2.8	2.0	1.4	4.5
2082	2.6	2.6	1.7	1.0	4.3
2125	2.2	2.3	1.4	.9	4.2
2167	1.8	1.9	1.3	1.6	4.2
2210	1.4	1.6	0.9	1.2	4.0
2252	1.3	1.4	0.5	1.0	3.9
2295	1.1	1.0	0.4		3.4
2337	0.8	0.7	-0.1	0.8	3.3
2380	0.4	0.3	-0.4	0.5	3.1
2422	0.2	0.0	-0.7	0.1	2.9
2465	-0.2	-0.4	-1.1		2.9
2507	-0.6	-0.7	-1.3	-0.5	2.7
2550	-1.0	-1.0	-1.6	-0.8	2.6

Table E-23. September Data - Fort McMurray

DATE: September 25/76			Location: Mildred Lake		
Time(LST)	0728	1050	1350	1431	1810
Height (M)	Temp (C)	Temp (C)	Temp (C)	Temp (C)	Temp (C)
0	6.1	10.8	12.6	12.8	13.3
43	6.9	9.3	10.7	10.3	11.7
85	8.0	8.6	10.3	9.6	11.0
127	8.0	7.9	9.7	9.3	10.5
170	7.9	7.5	9.0	9.0	10.0
213	7-9	7.1	8.5	8.8	9.7
255	8.1	6.6	7.9	8.4	9.3
297	8.4	6.6	7.4	8.2	9.0
340	8.3	6.8	6.6	7.9	8.6
382	8.0	6.6	6.0	7.5	8.3
425	7.9	6.3	5.5	7.2	7.9
467	7.6	6.0	4.9	6.7	7.5
510	7.6	5.6	4.6	6.3	7.1
552	7.6	5.6	4.2	5.9	6.6
595	7.7	5.5	3.8	5.5	6.2
638	7.8	5.6	3.4	5.3	5.9
680	7.3	5.6	3.2	4.9	5.5
722	7.1	5.5	3.1	4.5	4.9
765	6.7	5.4	3.2	4.2	4.6
807	6.5	5.6	3.3	3.9	4.3
850	6.3	5.7	3.1	3.6	4.1
892	6.2	5.6	3.0	3.4	4.0
935	5.9	5.6	3.5	3.2	4.0
977	5.8	5.5	4.2	3.1	3.8
1020	5.6	5.4	4.4	8.0	3.8
1063	6.1	5.3	4.4	2.8	3.8
1105	6.4	5.3	4.5	2.7	3.8
1147	6.6	5.3	4.4	2.4	3.9
1190	6.6	5.3	4.3	2.1	3.8
1232	6.5	5.4	4.2	2.0	3.5
1275	6.5	5.4	3.8	1.9	3.3
1317	6.1	5.2	3.3	3.5	3.2
1360	6.0	5.2	3.0	4.4	3.0
1402	6.0	5.0	2.7	4.6	2.8
1445	6.0	4.8	2.3	4.4	2.8
1487	5.7	4.4	2.2	4.4	2.9
1530	5.4	4.4	2.0	4.2	3.1
1572	5.1	4.4	1.9	3.9	3.3
1615	4.5	4.1	1.7	3.4	3.2
1657	4.1	4.0	1.6	3.1	3.2
1700	3.9	3.7	1.3	2.9	3.1
1742	3.6	3.4	1.1	2.7	3.0
1785	3.4	3.1	.8	2.4	3.0

Table E-23. September Data - Fort McMurray cont'd.

Time(LST)	0728	1050	1350	1431	1810
Height (M)	Temp (C)	Temp (C)	Temp (C)	Temp (C)	Temp (C)
1827	3.3	2.8	.5		2.5
1870	3.1	2.4	0.0	2.0	2.6
1912	2.8	2.1	0.0	1.7	2.5
1955	2.4	1.6	0.0	1.6	2.2
1997	2.2	1.5		1.3	2.2
2040	1.7	1.0		1.2	2.0
2082	1.4	0.8	-0.4	1.1	1.8
2125	0.9	0.4	-0.4	1.0	1.8
2167	0.9	0.1	-0.6	0.8	1.8
2210	0.6	-0.1	-0.7	0.5	1.8
2252	0.3	-0.4	-0.6	0.1	1.7
2295	-0.3	-0.7	-0.5	-0.1	1.5
2337	-0.3	-1.0	-0.6	-0.1	1.5
2380	-0.4	-1.3	-0.7	-0.1	1.5
2422	-0.4	-1.6	-0.8	-0.3	1.4
2465	-0.6	-1.7	-1.1	-0.4	1.2
2507	-0.6	-1.7	-1.4	-0.4	1.1
2550	-0.4	-1.8	-1.6	-0.3	0.7

Table E-24. September Data - Fort McMurray

DATE: September 26/76			Location: Mildred Lake		
Time(LST)	0716	1056	1355	1440	1807
Height (M)	Temp (C)	Temp (C)	Temp (C)	Temp (C)	Temp (C)
0	6.1	8.9	18.3	21.1	21.7
43	3.8	4.0	15.2	19.9	21.1
85	3.3	3.5	14.7	19.2	20.6
127	4.1	3.2	14.2	18.8	20.4
170	5.5	4.2	14.0	18.2	20.1
213	6.0	5.1	13.2	17.7	20.0
255	6.5	5.4	13.5	17.2	19.3
297	8.9	5.9	13.6	16.8	18.8
340	10.1	6.5	13.0	16.3	18.3
382	10.1	7.2	12.6	15.6	18.2
425	9.8	7.5	12.5	14.9	17.6
467	9.5	7.2	12.1	14.6	17.2
510	9.2	7.1	12.0	14.1	16.9
552	9.1	6.8	11.8	13.4	16.4
595	8.9	6.7	11.6	13.0	16.6
638	8.7	6.7	11.3	12.7	15.3
680	8.4	6.5	10.8	12.1	14.8
722	8.1	6.2	10.8	11.6	14.1
765	7.7	6.0	10.6	11.4	13.8
807	7.3	5.8	10.6	11.0	12.9
850	6.9	5.8	10.5	10.4	12.4
892	6.6	5.8	10.4	9.9	11.7
935	6.4	5.7	10.4	10.0	11.4
977	6.1	5.7	10.3	9.9	11.2
1020	6.0	5.6	9.9	9.6	10.4
1063	5.9	5.3	9.8	10.0	10.2
1105	6.0	5.1	9.7	10.0	9.7
1147	6.0	4.8	9.2	10.1	9.5
1190	5.7	4.7	9.1	10.1	9.0
1232	5.4	4.2	8.9	10.0	9.0
1275	5.1	4.0	8.5	9.9	8.9
1317	4.8	3.7	8.8	9.7	8.8
1360	4.6	3.3	8.9	9.7	8.9
1402	4.3	3.2	8.9	9.5	9.1
1445	4.3	2.7	8.6	9.5	9.2
1487	4.2	2.6	8.4	9.4	9.6
1530	4.3	2.3	8.1	9.1	9.7
1572	4.3	2.0	8.1	9.1	8.9
1615	4.1	2.1	7.8	9.4	8.8
1657	4.0	2.1	7.8	9.1	8.7
1700	4.2	2.2	8.0	8.9	8.7
1742	4.3	2.3	7.5	8.4	8.2

Table E-24. September Data - Fort McMurray cont'd.

Time(LST)	0716	1056	1355	1440	1807
Height (M)	Temp (C)	Temp (C)	Temp (C)	Temp (C)	Temp (C)
1785	4.3	2.4	7.4	8.0	8.2
1827	4.4	2.4	6.9	7.9	7.9
1870	4.3	2.5	7.0	7.9	7.8
1912	4.0	2.3	6.8	7.9	7.4
1955	3.8	2.1	6.0	7.8	7.3
1997	3.4	2.0	5.8	7.8	7.1
2040	3.3	1.9	6.0	6.8	6.8
2082	3.1	1.7	5.4		6.5
2125	2.9	1.6	5.8	6.3	6.4
2167	2.7	1.4	6.1		5.9
2210	2.2	1.2	5.8	5.5	5.7
2252	1.8	1.0	5.4	5.4	5.5
2295	1.7	0.8	5.3	5.1	5.2
2337	1.4	0.4	4.9	4.6	5.1
2380	1.2	0.4	4.6	4.4	4.7
2422	0.9	0.2	4.9	4.2	4.5
2465	0.6	0.1	4.8	3.8	4.1
2507	0.5	-0.3	4.7	3.8	4.1
2550	0.0	-0.4	4.8	3.4	4.1

Table E-25. September Data - Fort McMurray

DATE: September 27/76 Location: Mildred Lake

Time(LST)	0748	1057	1330	1430	1752
Height (M)	Temp (C)	Temp (C)	Temp (C)	Temp (C)	Temp (C)
0	6.1	17.5	23.3	25.3	26.7
43	7.5	17.2	22.4	24.5	26.7
85	9.1	17.0	21.8	23.8	26.6
127	9.7	16.5	21.1	23.4	26.3
170	10.1	16.3	20.6	23.0	25.9
213	10.1	16.1	20.2	22.6	25.6
255	10.4	15.6	20.0	22.2	25.0
297	11.8	15.2	19.6	21.6	24.7
340	13.3	15.1	19.1	21.2	24.1
382	14.4	15.1	18.7	20.7	23.8
425	15.1	15.1	18.6	20.0	23.4
467	15.1	14.9	18.4	19.6	23.0
510	15.2	17.5	17.9		22.6
552	15.2	18.2	17.7		22.1
595	15.2	19.1	17.3		21.7
638	15.3	19.2	17.0		21.3
680	15.9	18.4	16.9	16.7	20.7
722	16.2	18.7	16.9	16.6	20.4
765	16.3	18.5	17.0	16.1	19.8
807	16.3	18.2	17.0		19.2
850	16.2	17.9	17.5	15.8	18.7
892	16.0	17.8	17.7	16.2	18.3
935	15.8	17.5	17.9	17.3	18.0
977	15.6	16.9	17.9	17.9	17.5
1020	15.1	17.3	17.3	17.9	17.0
1063	14.9	17.0	16.8	17.9	16.6
1105	14.7	17.3	16.7	17.7	16.2
1147	14.5	16.8	16.8	17.7	15.8
1190	14.3	16.5	16.8	17.6	15.4
1232	13.9		16.4	17.6	14.9
1275	13.8	16.1	16.3	16.8	14.3
1317	13.6	16.0	16.0	16.3	14.2
1360	13.4	15.3	15.5	15.9	13.8
1402	13.3	15.3	15.3	15.7	13.3
1445	13.2	15.0	15.0	15.9	13.0
1487	13.0	14.9	14.8		12.6
1530	12.9	15.1	14.0		12.2
1572	12.7	14.8	14.0	14.5	11.9
1615	12.6	14.2	13.9	14.2	11.8
1657	12.5	13.9	13.5	13.5	11.2
1700	12.3	13.6	13.1	13.4	11.5
1742	12.2		13.0	12.8	11.0

Table E-25. September Data - Fort McMurray cont'd.

Time(LST)	0748	1057	1330	1430	1752
Height (M)	Temp (C)	Temp (C)	Temp (C)	Temp (C)	Temp (C)
1785	12.1	14.0	12.8	12.4	10.8
1827	12.0	13.9	12.7	12.3	10.4
1870	11.9	13.2	12.5	12.2	10.6
1912	11.8	12.7	12.1	12.1	10.3
1955	11.8	12.5	12.0	11.6	10.0
1997	11.7	12.8	11.6	11.0	9.9
2040	11.6	11.8	11.4		9.8
2082	11.5	11.8	10.8		9.7
2125	11.4	12.0	10.8		9.6
2167	11.4	11.6	10.3		9.6
2210	11.5	11.4	10.4		9.5
2252	11.7	11.2	10.0		9.3
2295	11.8	10.9	9.7		8.6
2337	11.8	10.0	9.7	8.5	8.6
2380	12.0	10.0	9.6	8.3	8.6
2422	12.1	10.0	9.4	8.3	8.3
2465		9.6	9.1	8.3	7.9
2507	12.5	9.8	9.1	8.1	7.5
2550	12.5	9.1	9.6	7.8	7.4

Table E-26. September Data - Fort McMurray

DATE: September 28/76			Location: Mildred Lake		
Time(LST)	0734	1104	1341	1735	1812
Height (M)	Temp (C)	Temp (C)	Temp (C)	Temp (C)	Temp (C)
0	5.6	15.5	21.7	23.9	26.4
43	8.4	14.2	19.7	24.3	26.1
85	9.7	13.6	19.2	24.5	25.7
127	10.1	12.9	18.8	24.1	25.3
170	10.1	12.7	18.5	23.6	25.2
213	10.5	12.9	18.2	23.3	24.7
255	10.9	13.6	17.9	23.3	24.5
297	11.0	13.9	17.9	22.9	24.2
340	11.2	14.2	17.9	22.5	23.9
382	11.5	14.6	17.9	22.1	23.6
425	12.1	15.0	18.1	21.7	23.5
467	12.7	15.0	17.9	21.2	23.2
510	13.2	15.2	17.7	20.6	22.9
552	13.3	15.7	17.7	20.1	22.6
595	13.3	15.9	17.4	19.6	22.4
638	13.4	16.2	17.1	19.2	22.0
680	13.5	16.2	17.2	18.7	21.6
722	13.8	16.0	17.3	18.3	21.3
765	13.7	15.9	17.5	18.0	21.0
807	13.7	15.6	17.3	17.8	20.7
850	13.5	15.4	17.3	17.7	19.9
892	13.4	15.1	17.2	17.4	19.4
935	13.2	14.8	16.8	17.2	18.7
977	13.0	14.4	16.6	16.9	18.1
1020	12.7	14.2	16.4	16.8	17.6
1063	12.5	13.9	15.9	16.8	17.2
1105	12.4	13.7	15.9	16.6	16.5
1147	12.0	13.5	15.7	16.4	16.1
1190	11.7	13.4	15.5	15.9	15.8
1232	11.5	13.0	15.2	15.8	15.5
1275	11.2	12.8	14.8	15.5	15.1
1317	11.0	12.5	14.6	15.3	14.7
1360	10.8	12.3	14.3	14.9	14.3
1402	10.6	12.0	13.7	14.5	13.8
1445	10.2	11.8	13.6	14.2	13.2
1487	9.9	11.5	13.3	14.0	12.9
1530	9.4	11.1	13.1	13.5	12.6
1572	8.8	10.7	13.0	13.1	12.6
1675	8.5	10.4	12.7	12.7	12.3
1657	8.2	10.2	11.9	12.5	12.3
1700	7.8	9.9	11.9	12.4	12.2
1742	7.3	9.4	11.7	12.2	11.8

Table E-26. September Data - Fort McMurray cont'd.

Time(LST)	0734	1104	1341	1735	1812
Height (M)	Temp (C)	Temp (C)	Temp (C)	Temp (C)	Temp (C)
1785	7.0	9.2	11.5	11.6	11.4
1827	6.8		11.4	11.2	11.4
1870	6.6	8.5	11.3	10.8	11.2
1912	6.4		11.0	10.4	10.9
1955	6.1	7.9	10.6	10.0	10.5
1997	6.1		10.4	9.4	10.4
2040	5.9	7.2	10.1	8.8	10.2
2082	6.0		9.6	8.4	10.2
2125	6.1	6.6	9.3	8.2	10.0
2167	6.5		8.8	7.6	9.9
2210	6.6	6.0	8.7	7.5	9.5
2252	6.8		8.2	6.8	9.3
2295	6.7	5.6		6.4	9.0
2337	6.6		8.0	6.1	8.7
2380	6.3	5.3	6.9	5.6	8.4
2422	5.9		6.8	5.1	8.2
2465	5.5	4.8	6.4	5.2	8.2
2507	5.1		6.0	5.3	7.8
2550	4.8	4.0	5.7	5.0	7.2

Table E-26. September Data - Fort McMurray

DATE: September 29/76			Location: Mildred Lake	
Time(LST)	0754	1109	1353	1807
Height (M)	Temp (C)	Temp (C)	Temp (C)	Temp (C)
0	15.6	16.7	16.0	18.7
43	15.6	16.1	14.6	17.5
85	15.3	15.6	14.1	17.0
127	15.1	15.2	13.7	16.5
170	14.9	14.9	12.9	15.6
213	14.7	14.5	12.3	15.3
255	14.6	14.2	11.5	14.1
297	14.3	13.8	10.8	13.7
340	13.9	13.5	10.0	13.0
382	13.7	13.0	9.0	12.7
425	13.4	12.6	8.1	11.9
467	13.0	12.1	7.3	10.9
510	12.9	11.6	7.0	9.6
552	12.7	11.1	6.5	9.5
595	12.4	10.5	5.7	9.2
638	12.2	10.0	4.9	8.8
680	12.0	9.6	4.0	6.9
722	11.8	9.2	3.5	5.6
765	11.8	9.1	3.0	4.4
807	12.0	8.8	2.5	3.8
850	11.9	9.7	2.2	3.6
892	11.8	9.8	2.1	2.8
935	11.4	9.8	1.0	2.0
977	11.1	9.6	0.3	1.6
1020	10.8	9.4	-0.3	1.2
1063	10.5	9.1	-0.8	0.8
1105	10.0	8.7		0.9
1147	9.5	8.5		1.2
1190	9.4	8.2	-2.2	1.2
1232	9.2	7.9		0.5
1275	8.7	7.6		0.2
1317	8.3	7.2	-3.6	0.1
1360	8.0	6.8	-4.1	-0.3
1402	7.7	6.4	-3.9	-0.4
1445	7.1	6.0	-4.7	-0.5
1487	7.0	5.7	-4.5	-1.0
1530	6.6	5.3	-4.8	-1.1
1572	6.2	4.7	-4.8	-1.2
1615	5.8	4.4	-4.6	-1.6
1657		4.1		-1.6
1700	9.1	3.7		-1.7
1742	4.8	3.5	-5.1	-2.6

Table E-26. September Data - Fort McMurray cont'd.

Time(LST)	0754	1109	1353	1807
Height (M)	Temp (C)	Temp (C)	Temp (C)	Temp (C)
1785	4.4	3.3	-4.7	-2.9
1827	4.0	3.3	-4.6	-3.2
1870	3.8	3.2	-3.9	-3.7
1912	3.5	2.9	-4.5	-4.0
1955	3.3	2.8	-4.7	-3.9
1997	3.3		-4.8	-4.0
2040	3.1	2.5	-5.3	-4.1
2082	3.0	2.0	-5.6	-4.4
2125	2.8	1.5	-6.0	-4.4
2167	2.7	1.2	-6.1	-4.8
2210	2.3	1.0	-6.2	-4.8
2252	2.2	0.7	-6.2	-5.0
2295	2.4	0.5	-6.2	-5.1
2337	1.7	0.2	-6.2	-5.1
2380		0.0	-6.0	-5.0
2422		-0.4	-6.1	-5.0
2465		-0.8	-6.4	-5.2
2507		-0.9	-6.5	-5.2
2550		-1.0	-6.5	-5.2

Table E-27. September Data - Fort McMurray

DATE: September 30/76 Location: Mildred Lake

Time(LST)	0756	1102	1354	1445	1808
Height (M)	Temp (C)	Temp (C)	Temp (C)	Temp (C)	Temp (C)
0	5.3	11.4	16.1	15.5	15.1
43	5.0	10.3	15.0	14.5	14.4
85	5.0	9.8	13.6	14.1	13.6
127	5.3	9.3	12.3	13.6	12.7
170	6.1	9.0	11.5	13.5	12.1
213	6.7	8.4	10.3	12.1	11.8
255	6.9	8.1	9.7	11.5	11.4
297	6.9	7.7	9.0	11.0	11.0
340	6.9	7.3	8.8	10.7	10.7
382	6.7	6.4	8.2	9.9	10.2
425	6.7	5.9	7.4	9.3	9.6
467	6.6	5.5	6.5	8.6	9.2
510	6.5	5.4	5.9	8.2	8.9
552	6.2	6.5	5.1	7.7	8.3
595	6.1	7.0	4.2	7.6	8.1
638	6.1	6.9	3.3	6.9	7.9
680	5.8	6.6	2.7	6.3	7.7
722	5.6	6.7	1.8	5.7	7.3
765	5.2	6.6	0.9	5.5	6.6
807	4.8	6.3	-0.1	5.1	6.2
850	4.8	6.0	-1.0	4.6	5.6
892	4.4	6.0	-1.5	3.9	5.1
935	4.2	5.8	-2.1	3.3	4.7
977	3.9	5.5	-2.5	3.1	4.2
1020	3.6	5.2	-2.6	3.0	3.5
1063	3.4	4.8	-2.7	1.6	3.1
1105	3.0	4.6	-2.2	1.1	2.6
1147		4.2	-2.0	0.6	2.1
1190	2.8	4.1	-2.2	0.3	1.9
1232	2.4	4.0	-2.2	-0.3	1.3
1275	2.1	3.7	-2.6	-0.6	1.0
1317	1.9	3.4	-3.0	-0.5	0.5
1360	1.6	3.2	-3.3	-1.0	0.1
1402	12.	3.0	-3.7	-0.5	-0.3
1445	0.9	2.5	-4.1	-1.1	-0.4
1487	0.6	2.3	-4.5	-1.1	-0.9
1530	0.3	2.0	-4.9	-1.3	-1.3
1572	-0.2	1.6	-5.7	-0.9	-1.7
1615	-0.4	1.2	-5.5	-1.8	-2.0
1657	-0.6	0.9	-6.1	-1.7	-2.1
1700	-0.7	0.8	-6.2	-2.3	-2.2
1742	-0.4	0.7	-6.7	-2.7	-2.7

Table E-27. September Data - Fort McMurray cont'd.

Time(LST)	0756	1102	1354	1445	1808
Height (M)	Temp (C)	Temp (C)	Temp (C)	Temp (C)	Temp (C)
1785	0.0	0.4	-7.6	-2.6	-2.7
1827	-0.2	-0.1	-7.7	-3.8	-3.0
1870	-0.4	-0.2	-8.0	-4.2	-3.6
1912	-0.9	-0.6	-8.6	-4.5	-3.6
1955	-1.3		-9.0	-5.8	-4.2
1997	-16.	-1.4	-9.3	-5.7	-4.8
2040	-2.0	-1.4	-9.6	-6.4	
2082		-1.7	-10.1	-6.7	
2125	-2.6	-2.1		-6.9	-5.4
2167	-3.1	-2.5	-10.5	-7.0	-5.8
2210	-3.9	-2.8	-11.0	-7.1	-6.4
2252	-4.0	-3.0	-11.4	-9.1	-6.9
2295	-4.2	-2.8	-11.7	-8.9	-7.2
2337	-4.8	-3.8	-11.9	-9.2	-7.4
2380	-5.3	-4.1	-12.1	-9.8	-7.8
2422	-5.8	-4.3	-12.1	-10.6	-8.1
2465	-6.1	-4.7	-12.3	-11.1	-8.4
2507		-5.1		-11.5	-8.5
2550	-6.7	-5.3		-11.9	-9.1

Table E-28. November Data - Edmonton.

DATE: November 22/74 Location: Edmonton

Time(LST)	0715		0828		0955		1100	
Level	Height (M)	Temp (C)	Height (M)	Temp (C)	Height (M)	Temp (C)	Height (M)	Temp (C)
0	0	-15.5	0	-15.1	0	-12.7	0	-10.4
1	40	-12.7	39	-12.6	57	-12.7	64	-10.8
2	124	- 8.4	133	- 6.9	154	- 7.2	167	- 7.1
3	236	- 7.2	236	- 5.4	242	- 6.1	257	- 6.1
4	300	- 6.1	324	- 4.5	328	- 4.9	347	- 4.6
5			414	- 4.0	416	- 4.9	434	- 6.2
6			502	- 4.9	501	- 5.5	521	- 6.7
7			588	- 5.4	602	- 6.0	606	- 7.2
8			676	- 5.4	689	- 6.8	697	- 7.6
9			765	- 4.8	759	- 7.4	780	- 8.1
10			854	- 6.7	847	- 7.7	860	- 9.0
11			944	- 7.8	935	- 8.4	948	- 9.5
12			1033	- 9.5	1020	- 8.9	1028	-10.0
13			1122	-10.5	1109	- 8.4	1119	-10.1
14			1212	-11.0	1199	- 8.6	1214	- 9.3
15			1301	-12.7	1290	- 9.1	1299	- 8.8
16			1390	-12.9	1377	- 9.2	1383	- 9.2
17			1479	-11.4	1459	-10.0	1472	-10.0
18			1569	-11.5	1542	-10.4	1575	-10.4
19			1658	-12.4	1628	-10.6	1608	-10.5
20			1747	-13.0	1715	-11.1	1757	-10.9

Table E-29. November Data - Edmonton

DATE: November 23/74 Location: Edmonton

Time (LST)	0800		0930		1100		1230		1400	
Level	Hgt (M)	Temp (C)	Hgt (M)	Temp (C)	Hgt (M)	Temp (C)	Hgt (M)	Temp (C)	Hgt (M)	Temp (C)
0	0	-11.4	0	-11.2	0	- 5.6	0	- 1.8	0	0.9
1	46	- 9.4	47	-10.2	56	- 6.0	64	- 3.0	66	- 1.0
2	138	- 6.9	135	- 7.0	152	- 5.0	170	- 2.7	187	- 2.3
3	232	- 5.7	222	- 5.3	235	- 3.5	262	- 2.7	307	- 1.5
4	325	- 3.9	311	- 4.0	274	- 0.3	352	- 0.7	428	- 0.9
5	413	- 2.5	397	- 2.9	398	- 0.6	441	- 0.4	548	- 1.2
6	501	- 2.8	485	- 3.7	484	- 1.2	528	- 0.7	669	- 1.0
7	591	- 3.1	581	- 3.8	567	- 1.1	616	- 1.5	790	- 1.7
8	675	- 3.5	680	- 4.4	653	- 1.5	702	- 2.1	911	- 2.4
9	758	- 4.2	782	- 4.5	741	- 2.0	789	- 2.8	1032	- 3.1
10	849	- 4.7	883	- 5.0	829	- 2.8	874	- 3.1	1153	- 3.6
11	931	- 5.2	970	- 5.4	926	- 3.2	963	- 3.8	1274	- 4.2
12	1007	- 5.2	1054	- 6.2	1014	- 4.0	1054	- 4.3	1395	- 4.8
13	1104	- 5.8	1148	- 6.9	1101	- 4.6	1134	- 5.0	1516	- 5.5
14	1189	- 6.5	1232	- 7.3	1192	- 5.0	1217	- 5.8	1637	- 6.2
15	1263	- 7.3	1327	- 7.9	1279	- 5.7	1311	- 6.5	1758	- 7.0
16	1360	- 7.8	1430	- 8.4	1376	- 6.3	1401	- 7.5	1879	- 7.8
17	1461	- 8.4	1505	- 8.9	1457	- 7.1	1491	- 8.2	2000	- 8.3
18	1577	- 9.3	1570	- 9.5	1543	- 8.0	1592	- 9.0	2121	- 9.0
19	1636	- 9.9	1680	- 9.9	1640	- 8.5	1685	- 9.9	2241	- 9.6
20	1721	-10.1	1717	-10.5	1729	- 8.9	1776	-10.4	2362	-10.3

Table E-30. November Data - Edmonton

DATE: November 26/74 Location: Edmonton

Time(LST)	0800		0930		1100		1400	
Level	Height (M)	Temp (C)	Height (M)	Temp (C)	Height (M)	Temp (C)	Height (M)	Temp (C)
0	0	- 5.4	0	- 4.1	0	- 1.5	0	1.1
1	69	- 4.2	65	- 4.2	65	- 2.6	65	0.5
2	187	- 3.5	187	- 3.8	184	- 3.8	195	- 0.8
3	290	- 4.2	309	- 4.2	302	- 4.5	343	- 2.2
4	402	- 4.5	431	- 4.8	420	- 5.2	486	- 3.6
5	512	- 5.5	553	- 5.4	538	- 5.2	596	- 4.2
6	615	- 6.2	674	- 6.0	656	- 5.5	685	- 4.6
7	703	- 6.2	796	- 6.4	774	- 5.6	766	- 4.9
8	788	- 6.9	918	- 7.0	893	- 6.0	846	- 5.1
9	874	- 7.6	1040	- 7.6	1011	- 6.4	913	- 5.2
10	963	- 8.3	1162	- 7.9	1129	- 6.0	980	- 5.4
11	1058	- 9.0	1284	- 8.4	1247	- 6.5	1054	- 5.3
12	1152	- 9.7	1405	- 9.2	1365	- 6.4	1127	- 5.7
13	1241	-10.4			1484	- 6.7	1212	- 5.3
14	1325	-11.2			1602	- 7.1	1303	- 5.1
15	1451	-11.9			1720	- 7.4	1372	- 5.8
16	1569	-12.4			1833	- 7.3	1440	- 6.4
17	1639	-12.9			1956	- 7.6	1497	- 6.8
18	1715	-13.1			2074	- 8.0	1574	- 7.1
19	1821	-13.5			2193	- 8.3	1636	- 7.4
20	1920	-14.2			2311	- 8.8	1723	- 7.6

Table E-31. November Data - Edmonton

DATE: November 27/74						Location: Edmonton				
Time (LST)	0800		0930		1100		1230		1400	
Level	Hgt (M)	Temp (C)	Hgt (M)	Temp (C)	Hgt (M)	Temp (C)	Hgt (M)	Temp (C)	Hgt (M)	Temp (C)
0	0	-6.3	0	-4.8	0	-2.4	0	-0.2	0	1.2
1	53	-6.3	68	-4.9	64	-3.3	54	-1.1	57	0.4
2	142	-2.9	173	-0.3	167	-3.3	144	-1.8	160	-0.7
3	223	-0.6	261	0.7	260	-0.5	233	-0.1	257	-1.7
4	300	-0.4	349	0.4	350	-0.9	321	-0.2	346	-1.0
5	381	-0.3	436	-0.2	437	-0.7	408	-0.3	435	-1.1
6	461	-0.4	521	0.3	525	-0.9	496	-0.7	521	-1.5
7	542	-0.1	604	0.9	616	-1.1	584	-1.2	602	-1.5
8	624	-0.5	688	0.9	705	-0.3	670	-1.7	686	-1.8
9	707	-0.1	773	0.7	796	-0.2	761	-1.6	769	-1.9
10	789	-0.3	864	-0.1	887	-0.5	848	-1.2	854	-1.6
11	871	-0.7	955	-0.8	979	-0.5	936	-1.7	950	-2.0
12	953	-1.1	1040	-0.9	1070	-1.4	1032	-2.1	1044	-2.4
13	1035	-1.2	1123	-1.5	1156	-2.2	1121	-2.6	1138	-3.0
14	1117	-1.3	1215	-2.4	1239	-3.0	1211	-3.3	1230	-3.7
15	1200	-2.0	1319	-3.1	1340	-3.5	1306	-3.5	1317	-4.3
16	1282	-2.7	1363	-3.9	1432	-4.3	1390	-4.0	1403	-4.9
17	1364	-3.4	1444	-4.6	1517	-5.1	1478	-4.7	1492	-5.7
18	1446	-4.0	1586	-5.4	1608	-5.9	1573	-5.6	1587	-6.5
19	1528	-4.7	1694	-6.1	1686	-6.6	1655	-6.5	1669	-7.0
20	1610	-5.4	1785	-7.0	1777	-7.3	1744	-7.1	1759	-7.7

Table E-32. November Data - Edmonton

DATE: November 28/74 Location: Edmonton

Time (LST)	0800		0930		1100		1230		1400	
Level	Hgt (M)	Temp (C)	Hgt (M)	Temp (C)	Hgt (M)	Temp (C)	Hgt (M)	Temp (C)	Hgt (M)	Temp (C)
0	0	-10.8	0	-9.6	0	-7.9	0	-1.7	0	0.7
1	64	-7.6	57	-7.6	68	-6.1	81	-2.2	57	0.6
2	159	-2.2	149	-1.7	168	-0.7	195	0.6	150	-0.3
3	236	-0.8	234	0.2	251	1.5	280	3.3	238	1.1
4	313	1.7	320	3.0	338	3.4	364	4.7	325	4.4
5	388	3.2	403	4.1	425	3.8	449	5.4	410	4.5
6	463	3.3	488	3.9	5.4	3.9	532	5.1	494	4.7
7	540	2.8	575	3.4	602	3.2	608	4.7	577	4.5
8	619	2.7	659	2.8	687	2.4	690	4.0	664	4.3
9	696	2.3	742	2.4	776	2.1	772	3.7	751	4.1
10	771	1.7	823	1.9	865	1.6	855	3.3	835	3.5
11	847	1.1	909	1.5	952	0.9	938	2.9	921	3.0
12	922	0.6	1002	1.2	1047	0.4	1012	2.4	1005	2.5
13	999	0.2	1085	0.7	1146	-0.1	1092	1.9	1094	1.7
14	1079	0.0	1162	0.2	1237	-0.7	1168	1.2	1179	1.2
15	1156	-0.4	1247	-0.1	1322	-1.4	1245	0.7	1257	0.6
16	1224	-0.9	1331	-0.8	1408	-1.7	1338	0.0	1337	0.3
17	1303	-1.5	1406	-1.2	1487	-2.4	1419	-0.6	1426	-0.2
18	1394	-2.0	1487	-2.0	1568	-3.0	1505	-0.8	1521	-0.8
19	1474	-2.6	1572	-2.3	1666	-3.6	1595	-1.5	1612	-1.3
20	1553	-3.2	1656	-2.9	1756	-4.0	1681	-2.4	1699	-1.9

Table E-33. November Data - Edmonton

DATE: November 29/74 Location: Edmonton

Time (LST)	0800		0930		1100		1230		1400	
Level	Hgt (M)	Temp (C)	Hgt (M)	Temp (C)	Hgt (M)	Temp (C)	Hgt (M)	Temp (C)	Hgt (M)	Temp (C)
0	0	-8.9	0	-7.2	0	-3.3	0	-1.5	0	0.1
1	68	-8.2	65	-7.4	56	-4.9	55	-2.3	60	-0.6
2	179	-3.0	181	-3.7	152	-2.1	150	-3.1	165	-1.7
3	268	-0.3	279	-0.9	241	1.2	235	1.3	263	-0.1
4	347	2.9	363	1.3	330	2.5	320	2.7	351	3.9
5	425	4.3	443	5.0	422	4.5	411	4.6	436	4.5
6	505	5.7	525	5.6	510	5.8	499	4.8	520	4.2
7	581	6.3	612	5.7	596	6.1	582	5.5	605	4.7
8	661	6.4	699	6.1	683	6.2	666	5.5	692	5.1
9	743	5.9	788	5.7	765	5.7	749	5.3	780	5.0
10	824	5.9	874	5.3	848	5.2	840	5.0	866	4.8
11	910	5.5	963	5.2	937	4.7	930	4.6	951	4.3
12	996	4.9	1050	5.1	1023	4.1	1013	4.2	1038	4.3
13	1076	4.3	1125	4.7	1109	3.7	1097	3.8	1128	3.9
14	1153	3.7	1206	4.3	1200	3.2	1181	3.4	1218	3.8
15	1237	3.1	1295	4.1	1291	2.9	1264	3.1	1307	3.5
16	1333	2.4	1382	3.8	1376	2.7	1345	2.7	1442	2.9
17	1415	2.1	1467	3.3	1460	2.2	1431	1.8	1523	2.0
18	1486	2.0	1556	2.7	1548	1.8	1513	1.3	1554	1.4
19	1563	1.5	1646	2.0	1629	1.3	1594	0.9	1644	1.1
20	1647	1.1	1735	1.5	1716	0.5	1680	0.5	1733	0.9

Table E-34. November Data - Edmonton

DATE: November 30/74 Location: Edmonton

Time(LST)	0810		0930		1100		1230	
Level	Height (M)	Temp (C)	Height (M)	Temp (C)	Height (M)	Temp (C)	Height (M)	Temp (C)
0	0	-9.9	0	-9.2	0	-6.9	0	-6.0
1	48	-8.7	59	-9.5	53	-7.3	55	-6.4
2	132	-7.5	154	-7.3	148	-7.7	145	-5.9
3	211	-2.2	234	-2.9	229	-2.6	228	-2.5
4	286	1.1	311	1.2	300	-0.6	315	1.0
5	360	2.7	391	3.4	374	1.5	399	2.6
6	433	3.9	471	4.0	452	3.1	481	3.4
7	507	4.7	548	4.7	533	4.0	566	3.9
8	582	5.3	629	5.0	614	4.5	652	3.4
9	657	5.7	706	5.0	694	4.7	734	3.4
10	732	5.5	782	4.8	773	4.5	810	3.1
11	807	5.2	843	4.5	850	4.5	885	2.7
12	883	4.9	924	4.5	934	4.5	962	2.5
13	961	4.8	1026	4.0	1017	4.0	1035	2.5
14	1041	4.5	1109	3.6	1097	3.8	1108	2.4
15	1113	4.2	1186	3.0	1180	3.6	1186	2.0
16	1185	3.6	1268	2.4	1257	3.1	1265	1.7
17	1264	3.1	1368	2.1	1335	2.9	1350	1.8
18	1341	2.4	1444	1.9	1426	2.4	1436	2.2
19	1419	2.3	1507	1.4	1504	2.4	1516	1.8
20	1496	1.8	1588	1.0	1584	1.9	1598	1.1